AD_____

Award Number: DAMD17-03-1-0701

TITLE: Application of Nanoparticles/Nanowires and Carbon Nanotubes for Breast Cancer Research

PRINCIPAL INVESTIGATOR: Balaji Panchapakesan, Ph.D.

CONTRACTING ORGANIZATION: University of Delaware
Newark, DE 19716

REPORT DATE: September 2005

TYPE OF REPORT: Final

PREPARED FOR: U.S. Army Medical Research and Materiel Command
Fort Detrick, Maryland 21702-5012

REPORT DOCUMENTATION PAGE

Form Approved
OMB No. 0704-0188

1. REPORT DATE	2. REPORT TYPE	3. DATES COVERED
01-09-2005	Final	1 Sep 2003 – 31 Aug 2005

4. TITLE AND SUBTITLE
Application of Nanoparticles/Nanowires and Carbon Nanotubes for Breast Cancer Research

5a. CONTRACT NUMBER

5b. GRANT NUMBER
DAMD17-03-1-0701

5c. PROGRAM ELEMENT NUMBER

6. AUTHOR(S)
Balaji Panchapakesan, Ph.D.

5d. PROJECT NUMBER

5e. TASK NUMBER

5f. WORK UNIT NUMBER

7. PERFORMING ORGANIZATION NAME(S) AND ADDRESS(ES)
University of Delaware
Newark, DE 19716

8. PERFORMING ORGANIZATION REPORT NUMBER

9. SPONSORING / MONITORING AGENCY NAME(S) AND ADDRESS(ES)
U.S. Army Medical Research and Materiel Command
Fort Detrick, Maryland 21702-5012

10. SPONSOR/MONITOR'S ACRONYM(S)

11. SPONSOR/MONITOR'S REPORT NUMBER(S)

12. DISTRIBUTION / AVAILABILITY STATEMENT
Approved for Public Release; Distribution Unlimited

13. SUPPLEMENTARY NOTES

14. ABSTRACT

The purpose of this research is to develop a new and cost effective technique of monitoring cancer cells at an early stage. Molecular targeting of cancer cells using nanotube electronic device and cell killing using nanotubes has been demonstrated. Variety of techniques such as fabrication of single wall carbon nanotubes, functionalization of nanotubes with antibodies, interaction of cells with antibodies on nanotube surfaces, and finally cell killing using nano-bombs has been successfully achieved with impressive results. These results show that cost effective diagnostic techniques can be developed for monitoring breast cancer cells at an early stage. Further, potent nano-bombs can be developed as therapeutic agents in the and can potentially outperform most nanotechnology techniques for killing cancer cells

15. SUBJECT TERMS
Carbon Nanotubes, antibodies, Confocal Microscopy, Nanobombs, Cancer Cell detection, Drug Delivery

16. SECURITY CLASSIFICATION OF:			17. LIMITATION OF ABSTRACT	18. NUMBER OF PAGES	19a. NAME OF RESPONSIBLE PERSON
a. REPORT	b. ABSTRACT	c. THIS PAGE			USAMRMC
U	U	U	UU	68	19b. TELEPHONE NUMBER *(include area code)*

Table of Contents

I. Introduction

In 2004, invasive breast cancer will attack approximately 190,000 US women, and this malignancy will take the lives of approximately 41,000 patients. Breast cancer is the leading cause of cancer in US women (excluding skin cancers). Diagnostic systems that can detect cancer at an early stage can be a priceless gift to patients suffering from this disease. With progress in the area of nanotechnology, it is now possible to synthesize nanotubes and nanowires approaching the size of proteins or DNA or other functional biological molecules (1.5 nm to 10 nm). Keeping these rapid advances in mind, this research presents a revolutionary approach of developing a nano-biohybrid system where, nanowires and nanotubes are used as probes for detecting and killing cancer cells by assembling specific anti-oncogene antibodies on nanowire/nanotube surfaces for detecting over expressed cell surface receptors called Her2 in cancer cells. The hypothesis used is that assembling antibodies on the nanowire/nanotube surfaces will change the surface electronic and optical properties of the material that can be detected using tunneling, confocal microscopic and field effect modulation techniques. This hypothesis will work as most of the atoms in the nanotubes and nanowires are surface atoms. Hence modulation of surface electronic charge density by functionalizing antibodies can change the electronic and optical properties dramatically, which can be used to develop highly sensitive sensors for detecting breast cancer cells approaching the limits of being able to detect single cancer cells. This would be a significant step in the area of biomedical nanotechnology and could revolutionize cancer diagnostic systems as we will be able to nanoelectronically detect a single cancer cell. Further, the success of this technology can result in cancer diagnostic systems for various other types of cancer based on similar principles that can be used in a clinical set up for early detection of cancer.

II. Body

II. A. Carbon Nanotube Synthesis:

In this research, the first task was to fabricate nanoparticles, nanowires and carbon nanotubes. To this, we started fabricating carbon nanotubes using a methane based chemical vapor deposition approach. We found that nanotubes were much more suited for our research for coating antibodies due to the inert nature of carbon nanotubes and their biological compatibility.

Carbon nanotubes are first grown in-house using methane based thermo chemical vapor deposition technique at 900 °C at atmospheric pressure using 10 nm iron nanoparticles as catalyst metal. The growth is set in the reaction rate limited regime with high temperatures facilitating high kinetic energy of the gas molecules and with low supply of carbon, allowing the formation of single wall carbon nanotubes. The grown nanotubes are purified by first heating in dry air at 400 °C for removing the soot and an acid reflux (3 M HCL for 10 hrs) to remove the catalyst particles. Following growth, the nanotubes were characterized using scanning electron and transmission electron microscopes. Figure 1(a), (b) & (c) is the SEM and TEM image of the nanotube grown

using this approach about 1.5 nm in diameter and 1 micron in length. The PIs group at University of Delaware has grown nanotubes about 0.9 nm to 10 nm in diameter and 1 μm in length.

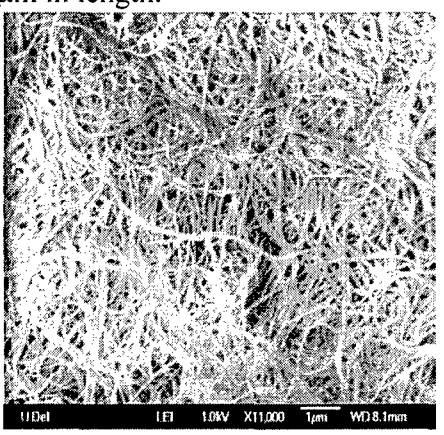

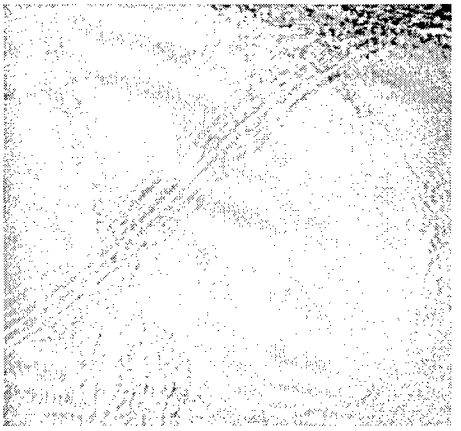

Figure 1. (a) Scanning electron microscope image of bundles of single wall carbon nanotubes, (b) Transmission electron microscopic image of single wall carbon nanotubes of 1.5-1.6 nm in diameter.

II.B Characterization of Nanotubes for their Quantum Electronic Properties:

In this task the quantum conductance of the nanotubes and nanowires were measured and the differential conductance as a function of voltage was measured using nanoprobes. We used atomic force microscope tips and connected it with the regular probes tips to measure the conductance which is the most direct way of measuring conductance in carbon nanotubes directly. Atomic force microscope tips have a tip radius of 17 nm which is quite close to carbon nanotubes (1.5 nm to 10 nm). Using these tips the nanotube conductance can be measured directly using probe stations that is conducted to a semiconductor parameter analyzer. The probe tips were initially welded to the base of the AFM tip and the tip was positioned on the substrate consisting of separated carbon nanotubes. Figure 3 is the micrograph of the differential conductance measured for carbon nanotubes and platinum nanowires. The gap is the conductance across V=0 gives the energy or conductance gap. The step like behavior is associated with the non-linear current voltage characteristics of carbon nanotubes. These nanotubes are semiconducting in nature and this characterization allows for measuring the base-line conductance of carbon nanotubes.

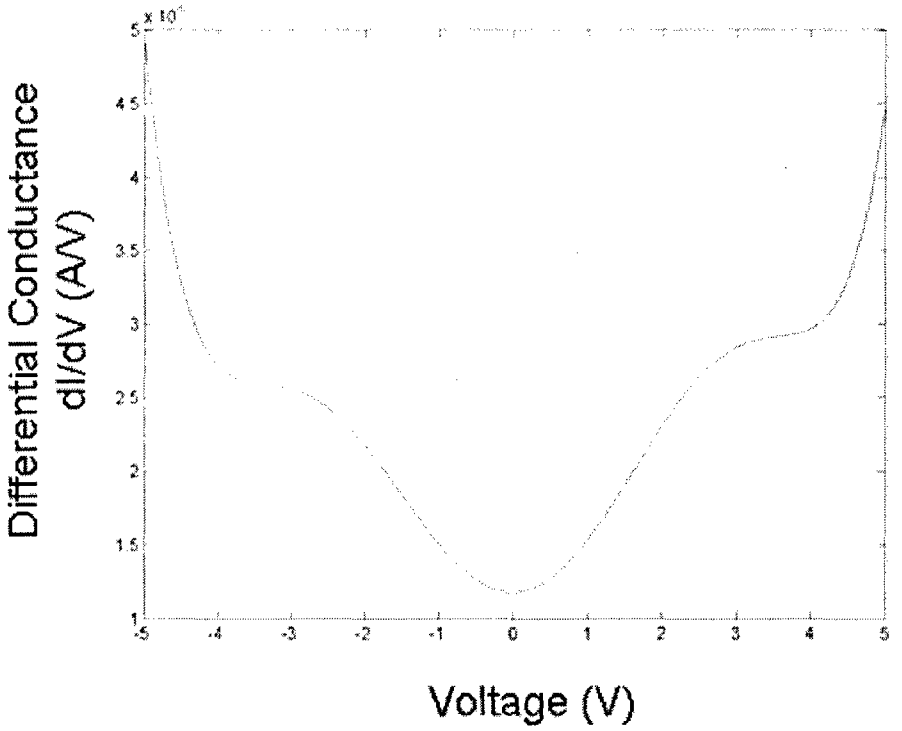

Figure 2. Differential conductance as a function of voltage for carbon nanotubes between -5 to +5 V. Note that the gap at V=0 gives the conductance or energy gap.

II C. Antibody Functionalization of Carbon Nanotubes:

In order for nanotubes and nanowires to be used for biomolecular recognition, it is important to first separate the nanotubes and nanowires, measure the conductance, functionalize antibodies on nanotube and nanowire surfaces and measure the conductance of the antibody coated nanotubes and nanowires. Confocal microscopy was used to characterize the functionalization of nanotubes and nanowires with antibodies. This is also the first time to visualize carbon nanotubes directly using confocal microscopes as they are very small to be observed. For observing in confocal microscopes, the nanotubes have to be first separated and labeled using flourophores. The first step was the separation of nanotube bundles into individual nanotubes.

II.C.1. Separation of Nanotube Bundles into Individual Nanotubes:

Most applications employing the unique electronic, thermal, optical and mechanical properties of individual nanotubes will require large scale manipulation of stable suspensions at high weight fraction. Nanotube solubilization provides access to solution-phase separation methodologies, facilitates chemical derivatization and controlled dispersion which is critical for antibody functionalization.

For controlled dispersion and solubilization, the CNTs were prepared in a solution of distilled water at a density of approximately 0.33mg/ml and solubilized in sodium dodecylbenzene sulphonate (ICN Biomedicals Inc.), a surfactant that ensured their separation in aqueous environment at a ratio of 1:20 of CNT: surfactant by weight [1]. The entire mixture was gently agitated for 24 hours in a sonicator that resulted in non-

specific adsorption of surfactant on the sidewalls of the carbon nanotube and separation of the nanotube bundles into individual nanotubes. To view in an SEM, a drop of the nanotube-surfactant mixture was placed on a silicon wafer and the sample was viewed after evaporation of the solvents. Figure 4 (a) is the SEM image of carbon nanotube bundles, and Figure 4 (b) is the SEM image of separated nanotubes. These results are in very good agreement with the results reported previously in the literature. We have found that NaDDBS is the most effective for our nanotubes grown in our laboratory. The superior dispersing capability of NaDDBS can be explained in terms of graphite-surfactant interactions, alkyl chain length, head group size and charge as pertains to the molecules that lie along the surface, parallel to the central tube axis. Figure 3 (c) is the schematic illustration of how a surfactant may adsorb on to the nanotubes. It is because of the π-like stacking of the benzene rings onto the surface of the graphite that causes the surfactant to bind to the surface of the nanotube. Previous studies have reported the lack of adsorption of other surfactant molecules such as SDS on nanotube surfaces [2]. This is attributed due to the absence of benzene rings on the surfactant molecules and our study shows the effectiveness of using NADDBS as surfactant for this study.

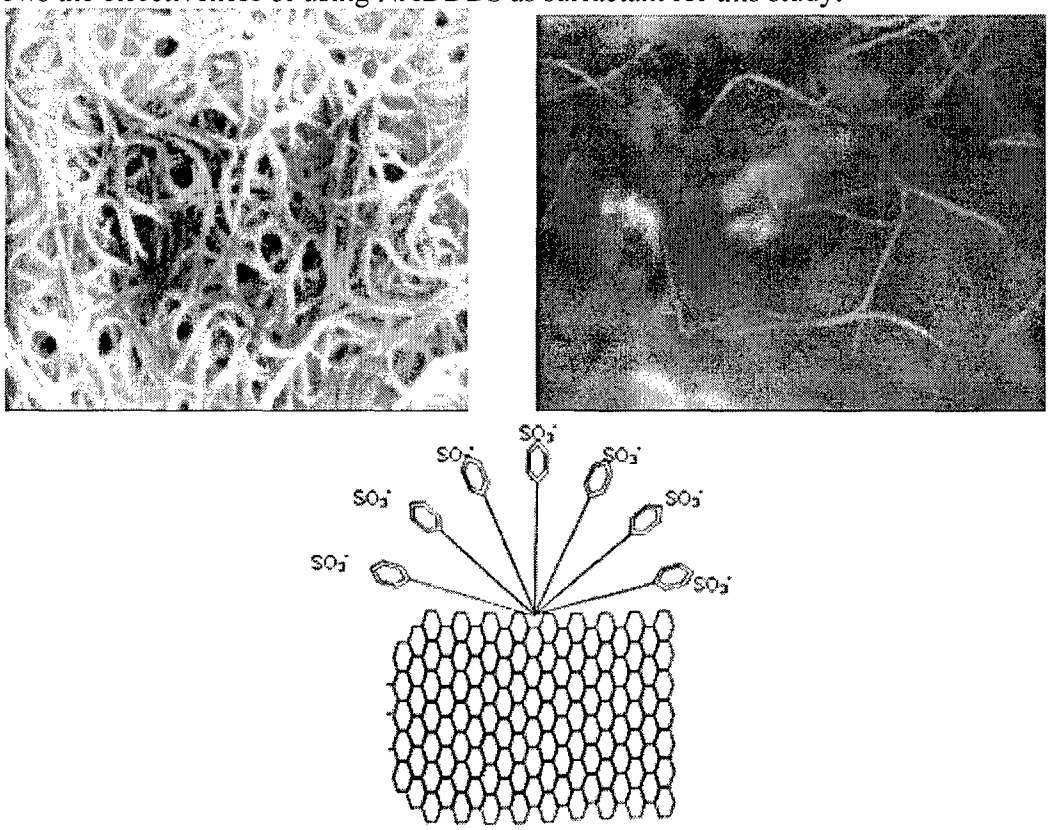

Figure 3 (a) Carbon nanotube in bundles before use of surfactant (b) nanotube bundles separated into individual tubes (c) schematic illustration of how surfactant may adsorb onto the nanotube surface to separate the nanotubes.

II.C. 2. Visualization of Individual Carbon Nanotubes in Confocal Microscope using Conventional Flourophores:

Labeling CNTs with conventional flourophores places several advantages for studying the interaction of biological molecules on carbon nanotubes. First, it allows the visualization of smaller carbon nanotubes approaching individual nanotubes using confocal microscopy with out aid from electron microscopic techniques. It doesn't damage the nanotube lattice thereby preserving the electronic transport properties of the nanotubes. When antibodies are functionalized on the nanotube, the resultant change in the electronic properties of the nanotube stems from the antibodies as the flourophores does not change the Sp^2 bonded grapheme sidewall. Further, nanotubes coated with flourophores can also be used as contrast agents to visualize internal parts of the cellular structure and even may enable high contrast imaging for breast cancer imaging and vaccine delivery applications using carbon nanotubes. For successful imaging and for higher contrast images, it is essential that the nanotubes are well separated and labeled using flourophores. In the recent past, the interaction of carbon nanotubes with different types of flourophores has been successfully investigated [3]. It was shown that nanotubes could be labeled successfully using DiIC16 and DiOC6. It was found that DiOC2, DiOC5, BODIPY or hydrazide did not produce any successful labeling of carbon nanotubes.

In our preliminary experimentation with flourophores, we have integrated our nanotube fabrication, purification and separation technology using surfactant solutions, with labeling using DiOC6, thereby preserving the sidewalls of the nanotube for tagging biologically active molecules such as antibodies. We also don't see any carbonaceous residue as all the nanotubes that we use for this purpose are purified nanotubes.

Single wall carbon nanotubes after fabrication were ultrasonically agitated for upto 8 hours in water at a density of approximately 0.001mg/ml, and labeled with dihexyloxacarbocyanine iodide ($DiOC_6$ – Molecular Probes Inc), by allowing interaction of the two components for 2-3 hours. Following labeling, the surfactant solution was added to make CNT:surfactant of 1:20 by weight as mentioned above and agitated for 6 hours. The resultant samples were imaged using Zeiss LSM 510 Multiphoton Confocal Microscope. Figure 5 (a) is the confocal image of nanotubes treated with DiOC6 with out the use of any surfactants and Figure 5 (b) is the fluorescence image of nanotubes treated with surfactant solution. This shows that well separated CNTs could be easily located in a fluorescence image and is an important step for studying the interactions of biomolecules on nanotubes using confocal microscopy. The smallest nanotube that has been viewed using confocal microscopy is ~10 nm using $DiOC_6$. The addition of surfactant increases the contrast during fluorescent imaging of the carbon nanotubes and reduces background noise due to the separation of the nanotubes. This study also shows that carbon nanotubes could be used as contrast agents in the study of cancer cells in vivo. Nanotubes coated with fluorescent labels or radioactive dyes can be injected into the body and conventional techniques such as Magnetic Resonance Imaging can be used to locate the nanotubes within the tissues. This is very important if nanotubes are to be used as drug delivery vehicles and the present study clearly shows the feasibility of such an approach. However, more studies needs to be done on the in vivo utility of carbon nanotubes as it is not clear whether injecting a nanotube into tissues in mice or human body is safe.

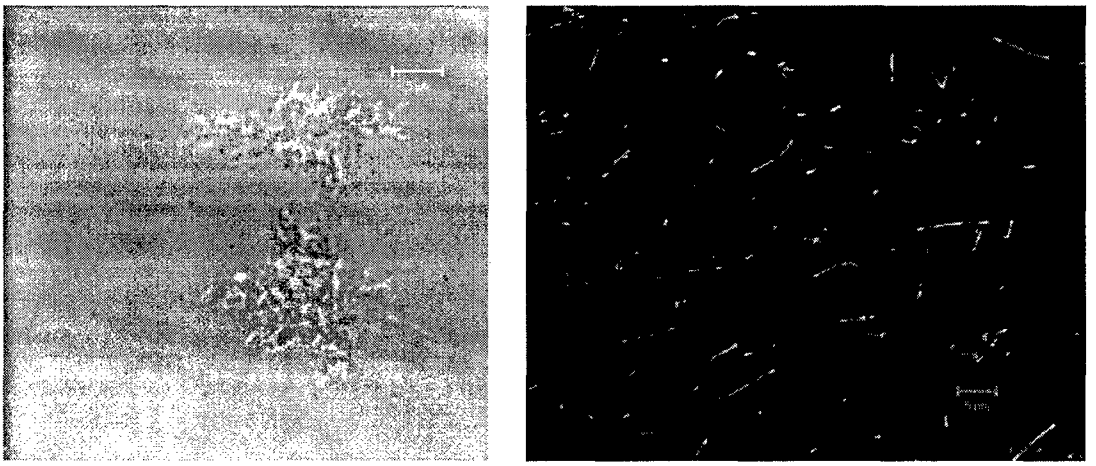

Figure 4 (a): CNT labeled with DiOC6 with out using surfactant showing background noise and no contrast (b) Nanotubes labeled using DiOC6 and separated using NaDDBS surfactant solution showing better contrast and no background noise. Note: both images have 5 micron scale bar.

II. C. 3. Antibody Functionalization of Carbon Nanotubes:

The CNT solution was prepared by agitating the CNTs for 24 hours after adding sodium dodecyl benzene sulfonate, a surfactant, to the solution at a ratio of 1:20 (CNT : surfactant) by weight. The nanotubes were then labeled with dihexyloxacarbocyanine iodide ($DiOC_6$), a dye that fluoresces at 488nm. The $DiOC_6$ was prepared at 2mg/ml in methanol and diluted in distilled water just prior to use with the CNT solution. The dye and nanotube solution were mixed at a 1:1 ratio and allowed to incubate for 1-2 hours. They were then viewed using a Zeiss LSM 510 Multiphoton Confocal Microscope to verify their dispersion.

Two antibodies were used, a secondary polyclonal goat anti-mouse IgG (Molecular Probes Inc.) and primary mouse monoclonal IgG (EMD Biosciences). The secondary antibody is only for labeling purposes to visualize in a confocal microscope. It is the primary monoclonal mouse IgG that will dock with the Her2 cell surface receptors in cell experiments. The antibodies were prepared in Phosphate Buffered Saline (PBS) solution (0.138M NaCl, 0.0027M KCl, pH 7.4), by diluting a 2mg/ml antibody solution with PBS to a ratio of 1:10 (antibody : PBS), just prior to use. The secondary antibody was pre-labeled with Alexa 546 (Molecular Probes Inc), a dye that fluoresces at 543 nm. The CNT solution and secondary antibody solution were then mixed in a micro-centifuge tube and allowed to interact for up to 2 hours. Centrifuging was done to the antibody solution when necessary to eliminate unnecessary fluorescence. The un-labeled primary was first tagged with the fluorescently labeled secondary antibody by allowing them to interact for ~1 hour, and then introduced to the CNT solution in the same way as the secondary.

We have used confocal microscopy to view fluorescently tagged CNTs in a method similar to that of viewing biological proteins such as antibodies to accurately analyze and quantify their interaction [4]. Co-localization is seen to increase with incubation time as evaluated by the change in weighted co-localization coefficient (WCC) [5], which is defined as the ratio of the intensity of co-localized area of a particular channel (color) to

the intensity of total area above threshold intensity of that channel (color). The value of WCC was observed to increase from 65% to 88% for the red channel with the increase in incubation time from 5 min to 2 hours between the nanotubes and secondary antibodies as previously reported in our earlier work [6]. This is the first time to show such hifgh degree of functionalization of antibodies on nanotube surfaces. A high degree of co-localization (88%) was seen between CNTs and secondary rabbit anti-goat IgG antibodies upon ~2 hours of incubation in Figure 5(a).

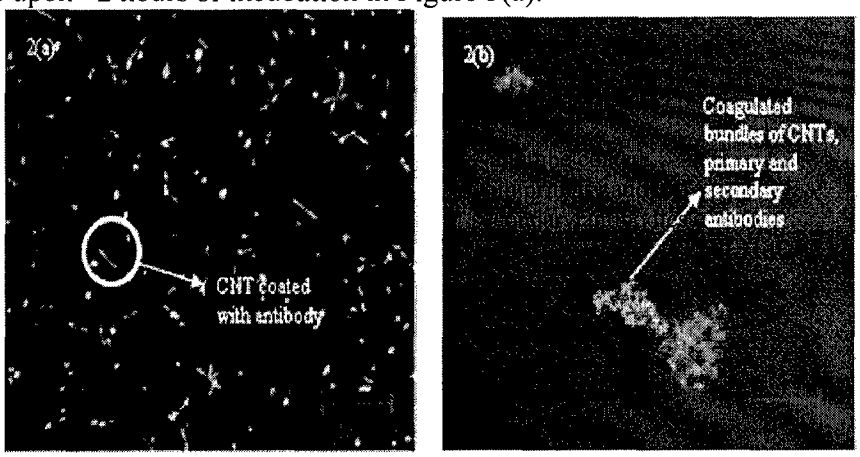

Figure 5: (a) Flourescence image of CNTs functionalized using secondary rabbit anti-goat IgG antibodies upon 2 hours of incubation. The WCC was measured to be 88% showing high degree of co-localization of secondary antibodies on nanotubes; (b) Flourescence image of nanotubes with primary and secondary antibodies

To effectively view and evaluate binding of the primary antibody (monoclonal mouse IgG) to the CNTs, the primary antibodies were conjugated with secondary antibody (polyclonal goat anti mouse IgG). Upon viewing the primary antibody in conjugation with the secondary on the nanotubes, considerable binding was observed (see Figure 5 (b) top corner), although separation of the CNTs was no longer effective (Figure 5(b)). The effect can be attributed to the fact that the binding site is formed due to clustering of the hydrophobic amino acid groups that interact with the CNT surfaces similar to the fullerene interaction on antibodies as referenced in [7, 8]. When the primary and secondary IgG interact, the resultant cohesive forces force the antibodies together and the nanotubes that are bound to them.

To verify the selective attachment of antibodies on carbon nanotubes, the nanotubes were labeled with a green dye using DiOC6 and the antibodies with a red dye. Figure 6 shows the selective attachment in confocal microscopy analysis. Confocal microscopy image of a green-dye-labeled CNTs and subsequently coated with the red-dye-conjugated antibodies. The green dye (labeling CNTs) in the inner rectangular region is bleached to verify the selective attachment of the antibodies to the CNTs (i.e. CNTs appear in red color due to the antibody binding) and the weighted co-localization coefficient was found to be 88% for antibody functionalization.

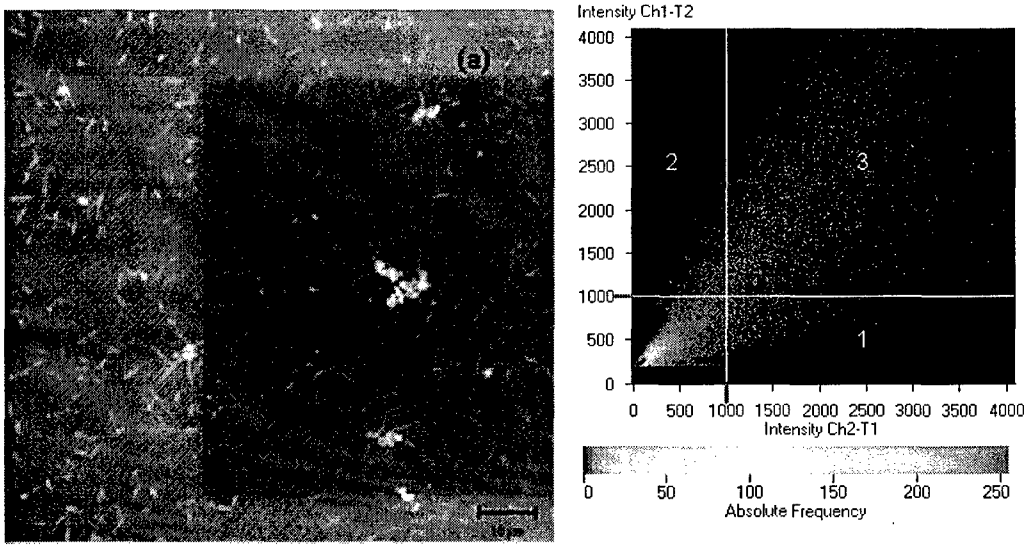

Figure 6: (a) Confocal microscopy image of a green-dye-labeled CNTs and subsequently coated with the red-dye-conjugated antibodies. The green dye (labeling CNTs) in the inner rectangular region is bleached to verify the selective attachment of the antibodies to the CNTs (i.e. CNTs appear in red color due to the antibody binding); (b) WCC found to be 88% for antibody functionalization.

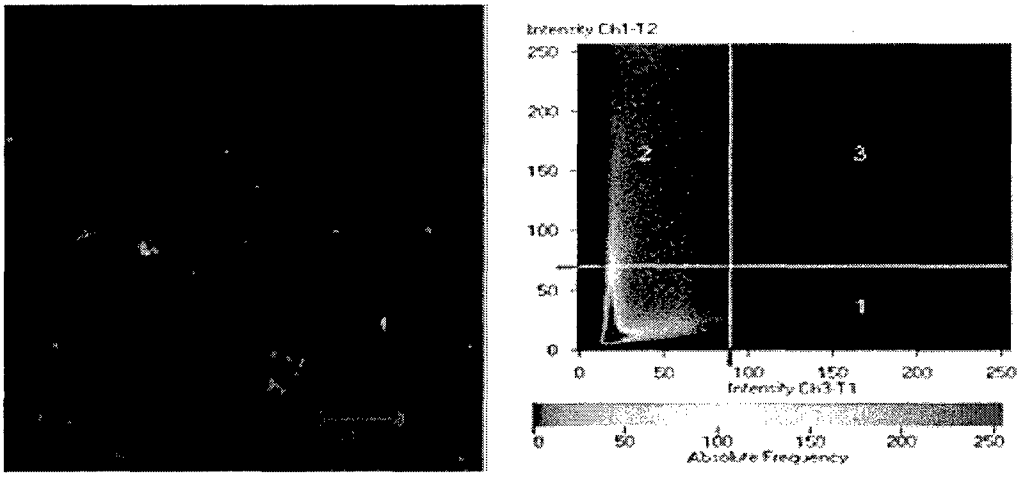

Figure 7: (a) Confocal images of (a) CNTs coated with $DiOC_6$ (green) and incubated with PEG for ~2 hours (b) Graph to mark the threshold intensities of the WCC data; (region 1 represents the red channel, region 2 the green channel and region 3 represents the co-localized area); WCC found to be 0% for the co-localized regions.

To prevent non-specific binding of antibodies to the CNTs, polyethyleneglycol (PEG), a bio-compatible polymer that has been widely used to prevent non-specific binding of proteins to the surfaces of nanostructures in sensing applications, has been used against the secondary IgG. In studies on specific binding of streptavidin on CNT surfaces, the hydrophilic PEG molecules were used to block the streptavidin molecules from binding

to the CNT surfaces [9]. We have performed similar experiments with antibodies and are seen to produce the same effect. Figure 6(a) is a confocal microscope image of the CNTs (green), coated with PEG and then incubated with the primary IgG combined with secondary IgG (red) for ~2 hours. Upon co-localization analysis, under the influence of PEG, co-localization coefficient (WCC) is seen to be zero.

One method of measuring the degree of co-localization of objects in confocal dual-color images is calculation of co-localization coefficients. It was reported that the co-localization coefficients can provide quantitative information, when the numbers of the objects in the two components of the image are not equal[18]. In order to measure the degree of co-localization between CNTs (green) and antibodies (red), multiple images were obtained from each sample. Furthermore, the images were taken under the same conditions. The images were then analyzed using the Zeiss LSM 510 software by creating a scattergram, which is interactively linked to data table and the image display, for each image. Threshold intensities in the scattergram are determined such a way to eliminate the background intensities. In fact, the threshold intensities for both channels (red and green) were kept same for all the images. The co-localization data is presented in Table 1.

Samples	CNT co-localization coefficient	Antibody co-localization coefficient
1	0.84	0.86
2	0.69	0.97
3	0.62	0.85
4	0.86	0.92
5	0.89	0.76
6	0.92	0.87

Table 1. Co-localization coefficients for CNTs and antibodies.

II.D. Atomic Force Microscope (AFM) Imaging of Primary Antibodies and Conductance Measurements:

The energy gap between the valence and conduction band is of fundamental importance to the properties of solid. Most of the material's behavior, such as intrinsic conductivity, optical transitions and electronic transistions depend on it. Any change in

the gap can alter the material physics and chemistry. The effects such as structural changes, lattice construction, atomic relaxation, surface passivation, surface reconstruction, strain induced changes due to coating, can change the local electronic density of states and the energy gap which is a quantum effect, and can result in dramatic modulation in the conductivity. It is this quantum effect that we tend to take advantage of in sensing cancer cells using nanotube probes. Initial studies on 5 nm silicon nanoparticles have shown that the band gaps can change with particle size (quantum size effect), electronic coupling between particles and cross-linking [10]. Nanotubes have many of their atoms in their surface positions. A surface is a strong perturbation to any lattice, creating many dangling bonds. These unsaturated bonds are energetically unfavorable. The dangling bonds, originally present at the surface of the nanotube can be passivated with their interacting neighbors (antibodies), thereby reducing their energy and in the process changing their localized surface electronic charge density and conductivity. It is this approach that will be utilized in this research for detecting cancer cells.

Figure 8 (a) is the AFM image of a single nanotube coated with primary antibody in PBS after incubation for 2 hours followed by rinsing in distilled water and drying. Preliminary work on the conductance of nanotubes and nanotubes functionalized with antibodies has been studied recently by using atomic force microscope tips that is attached to the tips of a semiconductor prober attached to a parameter analyzer. The AFM tips that were used has a tip radius of 10 nm and tip height of 17 nm. The tips are attached by bonding the tungsten probe tip directly to the base of the AFM tip. Following bonding, 10 nm of gold is evaporated making the tips suitable for electrical measurements. The tips are mounted onto the probe station attached to a semiconductor parameter analyzer.

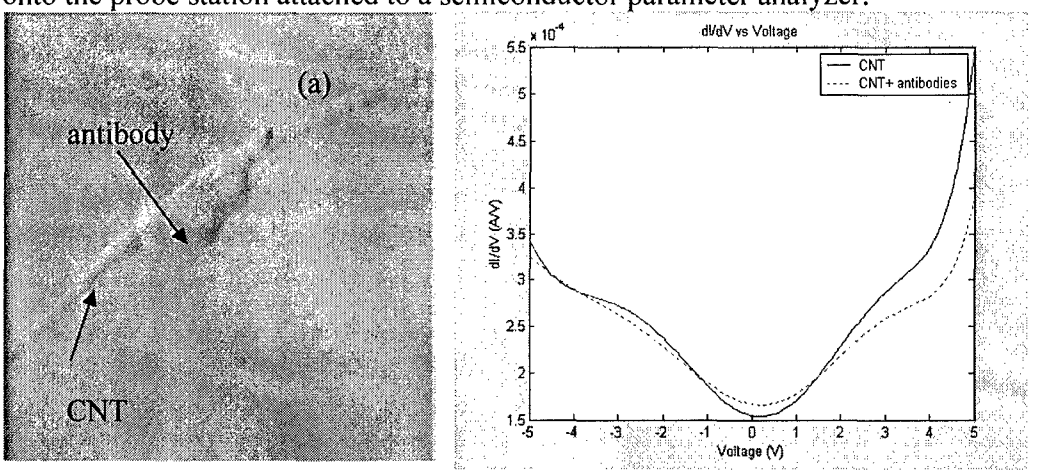

Figure 8: (a) AFM image of primary antibody functionalized on SWNT, the scan size is 1.25 x 1.25 μm. (b) Change in I-V as a function of the applied voltage between -5 to +5 V for CNT and antibody functionalized CNT in PBS after an incubation period of 2 hours followed by rinsing in DI water and drying in air.

Figure 8(b) is the data graph of the differential conductance vs voltage between -5V to +5 V measured at room temperature for nanotubes from PBS with out the antibody and the nanotube functionalized with primary antibody in phosphate buffer solution after

incubation period of 2 hours. The conductance was measured after rinsing the samples in water and drying them in air. The dip in the conductance plot shows the conductance gap. It can be seen that as the nanotubes are functionalized with the primary antibodies, it results in an increase in the conductance gap due to the broadening of the curve. The nanotubes that were used for this study were semiconducting in nature. This is the first study to show that the quantum electronic properties can be altered by antibody functionalization and is a fundamental step towards realizing sophisticated biological sensor systems in the future. Using this principle, we have achieved astonishing results in detecting live cancer cells in different cell cultures.

II. E. Detection and Killing of Cancer Cells in Culture:

We adsorbed monoclonal antibodies (mAb) specific to insulin-like growth factor 1 receptor (IGF1R) onto interconnected single wall carbon nanotube (SWCNT) networks, then placed the mAb-SWCNT conjugates between lithographically patterned electrodes (Fig. 1). The increase in conductance of the mAb-SWCNT devices was 3.0±0.1-fold for human BT474 breast cancer cells and 8.0±0.2-fold for human MCF7 breast cancer cells added to nanotube devices with adsorbed IGF1R-specific mAb, relative to nanotube devices with non-specific mAb of the same isotype. No conductance jump was induced by R- cells lacking IGF1R.

Knowing the change in electronic properties of SWCNT devices upon mAb adsorption, we hypothesized that interaction of adsorbed mAb with breast cancer cell surface targets would produce a further change in the electrical conductance of the SWCNT devices, proportional to the number of adsorbed mAb per cell, dependent upon the density of those surface antigens on breast cancer cells. The interconnected SWCNT that we grow are primarily semiconducting in nature, with positively charged holes carrying the current (p-type behavior)

Human BT474 breast cancer cells exhibit negligible expression of estrogen receptor-α, moderate expression of IGF1R, and high expression of human endothelial receptor 2 (Her2). Conversely, human MCF7 breast cancer cells exhibit significant expression of estrogen receptor-α, high expression of IGF1R, and low expression of Her2, confirmed by QRT-PCR. The control R- cells are nontumorigenic, nonmalignant, immortalized mouse embryonic fibroblast cells derived from mice with a targeted disruption of the *IGF1R* gene.

We tested our hypothesis for the interaction of breast cancer cells with mAb-SWCNT devices in five steps: 1) non-covalent functionalization of SWCNT, 2) fabrication of nanodevices with SWCNT patterned between the source and drain electrodes, 3) measurement of electrical conductance of the SWCNT as they were patterned and SWCNT coated with mAb specific to IGF1R, 4) control experiments to determine charge transfer between adsorbed mAbs and BT474 or MCF7 cells, 5) measurement of electrical conductance of the devices during cellular interactions with non-specific mAbs and specific mAb.

To study the binding of breast cancer cells, SWCNT were grown using methane-based chemical vapor deposition using iron nanoparticles as catalyst materials. The grown SWCNT consisted of interconnected bundles of SWCNT. For controlled dispersion and solubilization, the SWCNT were prepared in water with sodium

dodecylbenzene sulfonate (NaDDBS), a surfactant that ensured their separation in an aqueous environment (*27, 28*). The entire mixture was gently agitated for 24 hr in a sonicator (Fisher Scientific Ultrasonic Cleaner, 60 Hz frequency, FS60H) that resulted in nonspecific adsorption of surfactant on the sidewalls of the SWCNT and separation of the SWCNT bundles into individual SWCNT. Following SWCNT dispersion, devices were prepared using lithography, titanium/gold deposition, and lift-off (*4*).

Non-specific mouse myeloma IgG1 (EMD Biosciences) and specific anti-IGF1 receptor mouse mAb Ab-3 (33255.111, EMD Biosciences) were prepared in 0.138 M NaCl, 0.0027 M KCl, pH 7.0 (phosphate buffered saline, PBS) by diluting a 1 mg/mL mAb solution with PBS to a ratio of 1:10 (mAb:PBS). Following mAb dilution, 1 μL of the SWCNT dispersed in deionized water was mixed with 1 μL of the mAb solution and the mixture was allowed to interact for 1 hr at room temperature in a 4 μL microcentrifuge tube. Confocal microscopy and atomic force microscopy (AFM) were used to image and ascertain the non-specific adsorption of mAbs onto SWCNT surfaces. Following AFM imaging, SWCNT devices were prepared by placing 4 μL of the mAb-SWCNT conjugates onto the patterned regions between the electrodes. The devices were then annealed at 180°C for 15 min to reduce the contact resistance of the SWCNT from 300 kΩ to 80 kΩ. The resistance of the device was monitored using a semiconductor parameter analyzer (HP 4516) that is capable of measuring femto-amps (fA) of current with high accuracy with limits of 5 fA.

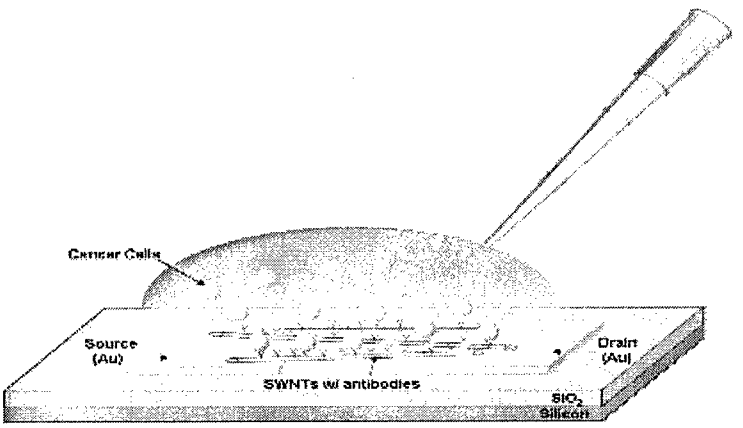

Figure.9 Schematic of the device used for detecting breast cancer cells by SWCNT-mAb binding to surface antigens on live breast cancer cells.

Figure. 9 shows the schematic of the SWCNT device that we prepared using photolithography, metal deposition, and lift-off. The source and drain electrodes were patterned as pads, and the interconnected SWCNT coated with mAb were patterned in the regions between the electrodes. Figure. 10a is the optical micrograph of the device that was prepared as described above. Figure. 10b is the AFM scan of the region that was patterned with SWCNT conjugated with mAb. First the SWCNT were patterned in the regions, followed by adsorption of mAb. The conductance was measured continuously during mAb adsorption, and then during cell adsorption to the devices. The device was biased at 5 mV to minimize charge injection effects and also to minimize current due to ionic conduction. Keeping the bias voltage low also enhances the actual signal

transduction between the mAb and cells and the actual surface electronic charge transfer process is visualized in the results.

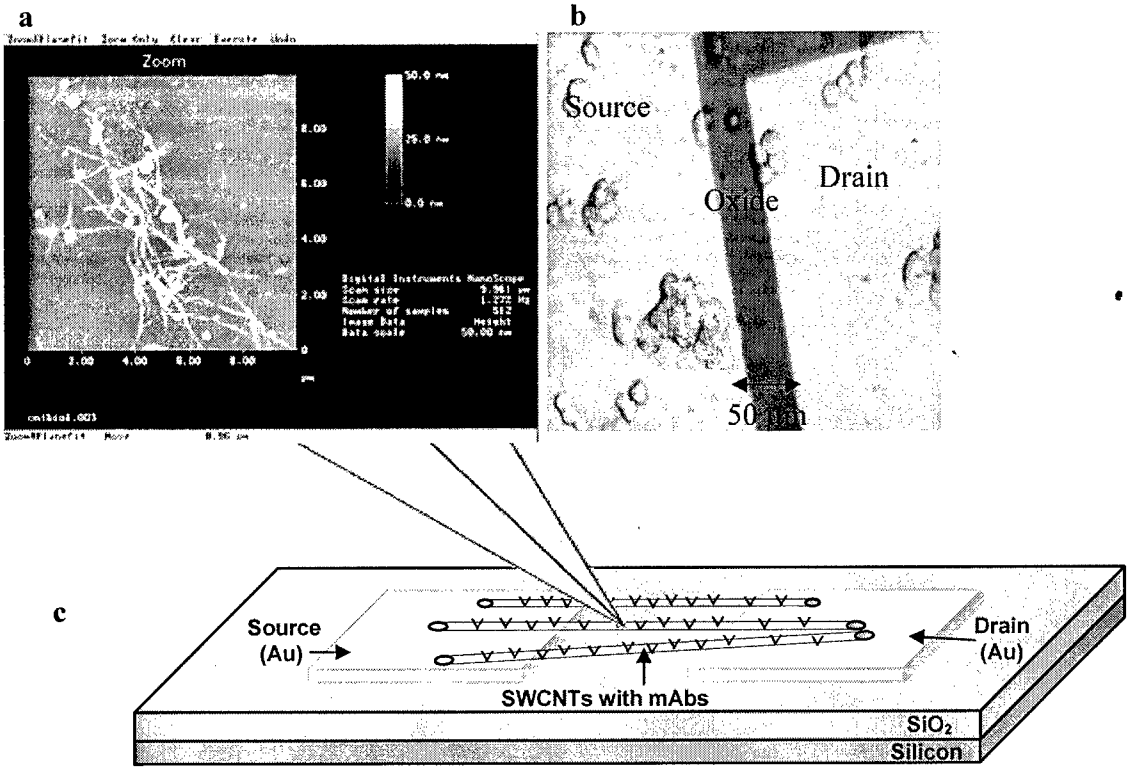

Figure. 10. Overview of the SWCNT-mAb device. **a**, AFM scan of the patterned areas in the schematic; **b**, optical micrograph of the actual device; **c**, schematic.

Electronic sensing of bound mAb and breast cancer cells was carried out by monitoring the electrical current through the SWCNT device under a 5 mV bias during mAb and breast cancer cell additions to a 4 μL drop of PBS on the surface of the device. Low bias was used to minimize charge injection into the device and to monitor the actual surface electronic events that happen between the mAbs and the breast cancer cells on the device. Under these low bias conditions control experiments revealed no ionic currents (Fig. 11). To measure breast cancer cell binding, we applied 1 μL of the 0.2 mg/mL mAb solution onto the surface of the biased SWCNT device while the current was monitored continuously in a probe station attached to a semiconductor parameter analyzer. Once the current stabilized, 4 μL of breast cancer cells (≈1,000 cells) were applied to the device and the current was monitored continuously. We studied the interactions of IGF1R-specific mAb adsorbed onto the SWCNT devices with BT474 and MCF7 breast cancer cells. Non-specific control mAb interactions between BT474 and MCF7 breast cancer cells were studied as controls.

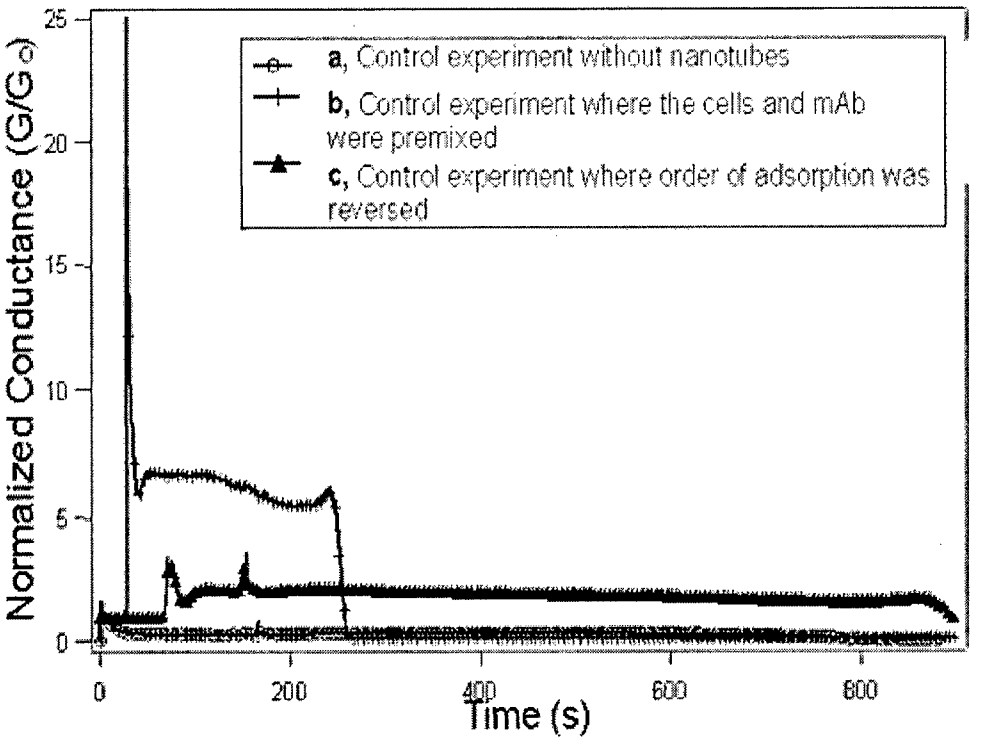

Figure.11: Negative control experiments: **a**, No SWCNT on device; IGF1R-specific mAbs were added, followed by BT474 breast cancer cells. **b**, Order of adsorption reversed for the SWCNT device: BT474 cells added first, followed by IGF1R-specific mAbs. **c**, Conductance of SWCNT device when the IGF1R-specific mAbs and BT474 cells were mixed together before addition.

Control experiments were carried out to test the specificity of change in conductance of the SWCNTs during mAb and breast cancer cell adsorption on the SWCNT surface (Fig. 3). Three types of control experiments were carried out: 1) monitoring the conductance during mAb adsorption without any SWCNT on the device; 2) monitoring conductance evolution with the order of mAb and breast cancer cell adsorption reversed; 3) monitoring the conductance evolution of the device when the mAbs and breast cancer cells were initially premixed. All these control experiments were repeated twice to determine the nature of the charge transfer process and to test the specificity of the mechanism.

Figure.11a shows the conductance as a function of time when there was no SWCNT on the device. No dramatic modulation in the conductance of the device was observed upon adsorption of IGF1R mAb and BT474 breast cancer cell adsorption on the device. This experiment demonstrated that the charge transfer process that resulted in an increase in conductance of the device for the interaction of marker-specific mAb with their specific targets on breast cancer cells was mediated by the SWCNT.

Figure. 11b shows the conductance as a function of time when the IGF1R mAbs and BT474 breast cancer cells were premixed and adsorbed on the surface of the SWCNT device. The observed spike train was due to the adsorption of the mAb-cell mixture onto the device, not to surface interaction between the IGF1R mAbs and BT474 breast cancer cells on the SWCNT surface. When the BT474 cells were premixed with the IGF1R mAbs, the IGF1R mAbs were expected to bind to their IGF1R targets on the BT474

breast cancer cells, in which case no significant change in the conductance was expected. Adsorption of antibodies and cells in general produce a small spike train in all our measurements. This is due to physical adsorption effects that result in a transient jump in conductance of the device.

Figure. 11c shows the conductance as a function of time when the order of IGF1R mAb and BT474 breast cancer cell adsorption was reversed. As seen in Figure. 11b, we observed two spikes, the first one due to the adsorption of BT474 cells onto the device, and the second one due to the adsorption of IGF1R mAbs onto the device. It is interesting to note that cells and antibodies produced similar effects when the order of adsorption was reversed, implying that the spikes were due to physical adsorption on the surface of the SWCNT, which are extremely sensitive to changes at their surfaces. From our earlier work on mAb adsorption, (*11,12*), we conclude that the result seen in Figure. 11c was due to physical adsorption. In general, when antibodies or other proteins adsorb to the surface of p-type SWCNT, they lower the conductance of the SWCNT, rather than increasing the conductance, as we observed here upon breast cancer cell binding. Hence this control experiment implies that when the order of adsorption was reversed, the charge transfer process was altered significantly. All these controls suggest that the mechanism for the significant increase in conductance upon breast cancer cell binding depends upon the charge transfer process between the adsorbed mAbs on the SWCNT and their specific antigens on cancer cells.

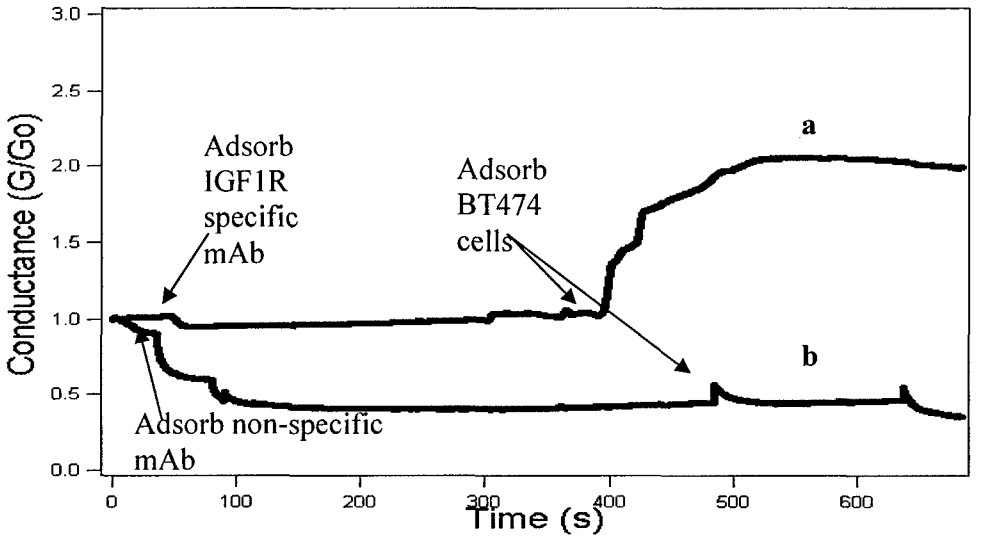

Figure.12 : Change in normalized conductance for BT474 breast cancer cells applied to SWCNT devices with adsorbed IGF1R-specific mAb, **a,** or non-specific mAb, **b,** followed by BT474 breast cancer cell application.

In another control experiment, Figure. 12a shows the conductance of the device during non-specific mAb adsorption (mouse myeloma IgG1), followed by adsorption of BT474 breast cancer cells, which generated two small spikes. In the first direct test of the hypothesis, Figure. 12a displays the effects of IGF1R-specific mAb adsorption, followed by adsorption of BT474 cells, which generated a 3.0±0.2-fold increase in the device conductance. It was apparent that BT474 cells interacting with the IGF1R-specific mAb-SWCNT device produced a large increase in conductance, while the non-specific mAb-

SWCNT device yielded two small transients. Previous studies from other laboratories and our own reported that the amine groups in proteins tend to donate electrons to the SWCNT, thereby decreasing the conductance of the SWCNT FETs during protein adsorption (*3, 4, 29-32*). A single amine group donates 0.04 electrons to the p-type SWCNT, thereby decreasing the conductance of the device. When breast cancer cells are adsorbed onto the device, association of mAb with the cell surface targets on the cancer cells is likely to produce an increase in device conductance due to the charge transfer process between the SWCNT and the breast cancer cells.

In other words, as the cell surface proteins interact with the specific mAbs, electrons transfer from the surface of the p-type SWCNT to the bound cell, thereby increasing the conductance of the device. It should be mentioned that the devices consisted of nanotube networks that were adsorbed with mAb to provide high surface area for mAb adsorption as well as for cell interaction. Hence although the breast cancer cells themselves are much bigger than individual nanotubes, the devices that we present here are network of nanotubes that are collectively bigger than the cells. The mAb exhibited specific interactions with their target proteins. Figure. 12b illustrates that the non-specific mAb did not produce any significant modulation in the electrical conductance of the SWCNT. The BT474 breast cancer cell adsorption experiments were carried out twice, producing the same effects each time.

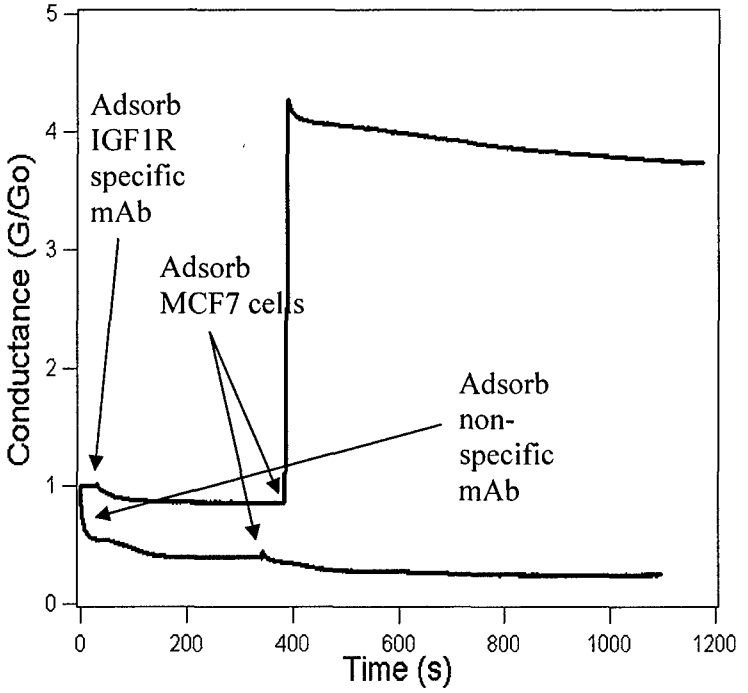

Figure.13 Change in normalized conductance for MCF7 breast cancer cells applied to SWCNT devices with adsorbed IGF1R-specific mAb, **a,** or non-specific mAb, **b,** followed by MCF7 breast cancer cell application.

The hypothesis of charge transfer upon breast cancer cell surface protein binding to a mAb adsorbed to the surface of SWCNTs was tested again with MCF7 breast cancer cells, which express a higher density of IGF1R than do BT474 cells (*13,14,15*). Figure. 13b shows minimal perturbation of device conductance after non-specific mAb

adsorption (mouse myeloma IgG1) and MCF7 cell adsorption to the SWCNT device. Figure. 13a, however, shows a large jump in the electrical conductance of the device, after IGF1R-specific mAb adsorption, upon MCF7 cell adsorption to the SWCNT device. MCF7 cell binding increased device conductance by 8.0±0.2-fold, compared to non-specific mAb experiments in Figure. 13b. Compared to BT474 breast cancer cells (Figure. 12), the MCF7 breast cancer cells produced a greater increase in device conductance upon binding to IGF1R-specific mAb-SWCNTs. We also observed that the non-specific mAb-SWCNT conductance data for the BT474 and MCF7 breast cancer cells were quite similar. Our experimental results suggest that charge transfer between SWCNT and breast cancer cells takes place through the mAbs that link the SWCNT to the cells. Binding to an antigen-specific mAb produced several-fold higher increases in the electrical conductance of the SWCNT devices than did binding to the non-specific mAbs.

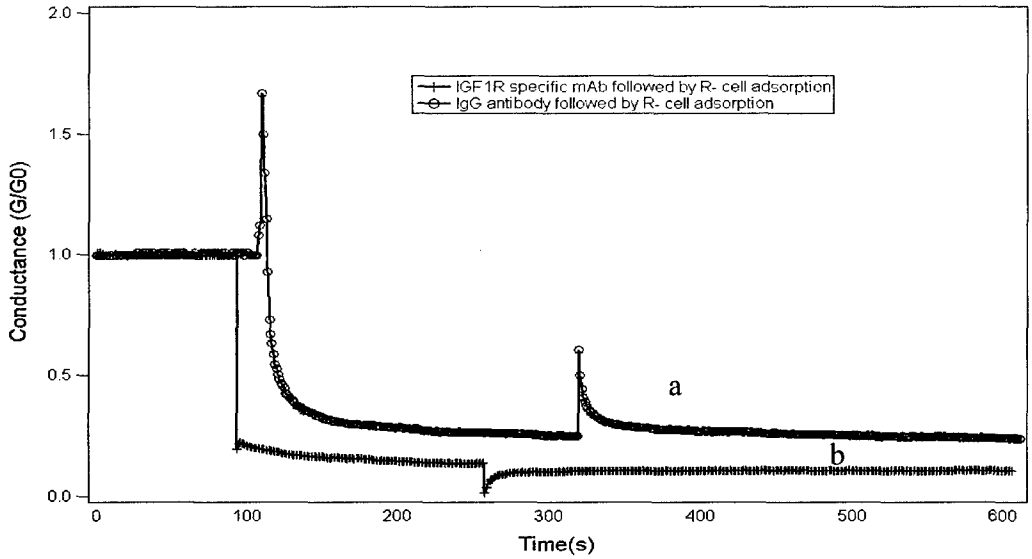

Fig. 14 Change in normalized conductance for R- cells applied to SWCNT devices with adsorbed non-specific mAb, **a,** or IGF1R-specific mAb, **b**, followed by R- cell application.

In contrast, application of R- cells, which do not express IGF1R, to IGF1R-specific mAb-SWCNTs yielded no sustained increase in conductivity (Figure. 14a), just like R- cell application to non-specific mAb-SWCNTs (Figure. 14b). This control experiment revealed that the conductivity jump seen with IGF1R-specific mAb-SWCNTs requires cell surface expression of IGF1R.

This study investigated the charge transfer process between adsorbed mAbs and their corresponding surface protein targets on breast cancer cells using SWCNT devices. We found that adsorption of antigen-specific and non-specific mAb to SWCNT resulted in a small decrease in the conductance of the SWCNT device. Subsequent adsorption of BT474 breast cancer cells (expressing significant IGF1R) or MCF7 breast cancer cells (overexpressing IGF1R) to IGF1R-specific mAb on the surfaces of the SWCNT dramatically increased the conductance of the devices. Non-specific mAbs did not yield a large increase in conductance. The increase in conductance was roughly proportional to the density of IGF1R expressed on the surfaces of the breast cancer cells. For example,

when IGF1R was targeted on BT474 breast cancer cells, cell binding to SWCNT devices produced a 3.0±0.1-fold increase in conductance. However, targeting the same receptor on MCF7 breast cancer cells produced an 8.0±0.2-fold change in the conductance of the SWCNT device. However, R- cells lacking IGF1R produced no conductance change.

These results imply that our observed large increase in device conductance when live breast cancer cells that overexpress IGF1R on their surfaces interact with the mAb on the surface of the SWCNT, is a general phenomenon due to charge transfer between the SWCNT and cells through the mAb, as opposed to the 1-2% decrease in conductivity of the SWCNT device upon mAb adsorption [12]. Importantly, we found that breast cancer cell interaction with antigen-specific mAb-SWCNTs produced a much greater increase in the device conductance compared to non-specific mAbs. Equally important, no such conductivity jump was observed with cells that do not express IGF1R.

Although adsorption of mAb onto the surface of the SWCNT was noncovalent, nevertheless SWCNT with adsorbed mAb were extremely sensitive to changes in the surface electrostatic charge density upon surface adsorption of live breast cancer cells. These results are consistent with the hypothesis that modulating the surface electrostatic charges in SWCNT could be utilized to detect breast cancer cells based on overexpression of cell surface antigens.

These results suggest that the binding of breast cancer cells via a cell surface receptor to mAb on the surface of the SWCNT devices caused those remarkable jumps in conductance. Our observations highlight a generic pathway for using the high surface area to volume ratio and the unique conductivity of SWCNT to detect overexpressed surface proteins on breast cancer cells. Furthermore, the mAb-SWCNT approach could in principle detect the molecular signatures of other types of circulating cancer cells. These findings suggest applications of mAb-SWCNT to detect a wide variety of surface markers on diseased cells, which could lead to sensitive nanotube-based biosensors for detecting specific cell surface antigens on circulating cells, in fine needle aspirates, or in masses probed by laparoscopy.

Carbon Nanotube Nano-bomb Agents for Killing Breast Cancer Cells:

In this report we show that by hydrating nanotubes both in sheets as well as by co-localizing them to cells, potent nano-bombs can be created to blow cancer cells completely. This process is highly localized with minimum collateral damage to neighboring cells. Nano-bombs are created due to the optical-thermal transitions in nanotubes. Hydrating nanotubes and exposure to light causes the thermal energy to heat the water molecules, which in turn creates pressure inside the nanotube bundles that causes them to explode. When co-localized with cells, they completely destroy the cells causing 100% cell destruction. This method is simple, robust and highly effective in killing cancer cells. Further, the technique uses low laser power compared to competing techniques with bigger explosions that may ensure complete destruction of cancer cells. Recent reports have shown that nanotubes could be highly toxic for in vivo applications[15]. Our method of using nano-bombs may indeed overcome the toxicity problems as the tubes are completely destroyed due to the explosions.

Single wall carbon nanotubes are first grown in-house using methane-based thermo-chemical vapor deposition technique at 900°C and atmospheric pressures using

iron and nickel as catalyst metals. The growth is set in the reaction rate-limited regime with high temperatures facilitating high kinetic energy of the gas molecules and with low supply of carbon, allowing the formation of single wall carbon nanotubes. The grown nanotubes are purified by first heating in dry air at 400°C for removing the soot and an acid reflux (3 M HCL for 10 hrs) to remove the catalyst particles. Following fabrication, SWCNT were dispersed in deionized water and a sheet was created by vacuum filtration. The SWCNT sheets were made by vacuum filtration of 20 mL of a 0.6 mg/mL SWCNT suspension through a poly(tetrafluoroethylene) filter (Millipore LS, 47 mm in diameter, 5-μm pores). The SWCNT sheet was washed with 200 mL of deionized water and then 100 mL of methanol to remove residual NaOH and surfactant, respectively. The sheets were allowed to dry under continued vacuum purge for 1 hour before being peeled from the filter. The typical SWCNT sheet was fabricated into circular discs about 100 mm in diameter and about 50 μm thick.

Two 1 mm wells, 1 mm apart, were created on the SWCNT sheet as sites to deposit 1.0 μL aliquots of ~1×10^5 BT474 breast cancer cells freshly resuspended in PBS after release from culture dishes. Clusters of BT474 cells on the bottoms of the wells were stained with Trypan blue dye to investigate membrane permeability and cell damage before and after light exposure. Second, the BT474 cells in one well were illuminated with 800 nm laser light at 200 mW/cm^2 for 60 sec. Finally, 0.1 μg of nanotubes were dispersed in PBS solution and agitated for 24 hours till all the nanotubes were dispersed. The nanotubes in PBS do not precipitate even after 24 hours and are quite stable. The resulting suspension consisting of nanotubes were directly adsorbed onto the center of a larger cell cluster that was treated with the Trypan blue dye and light was irradiated directly to see the effectiveness of the localized cell killing.

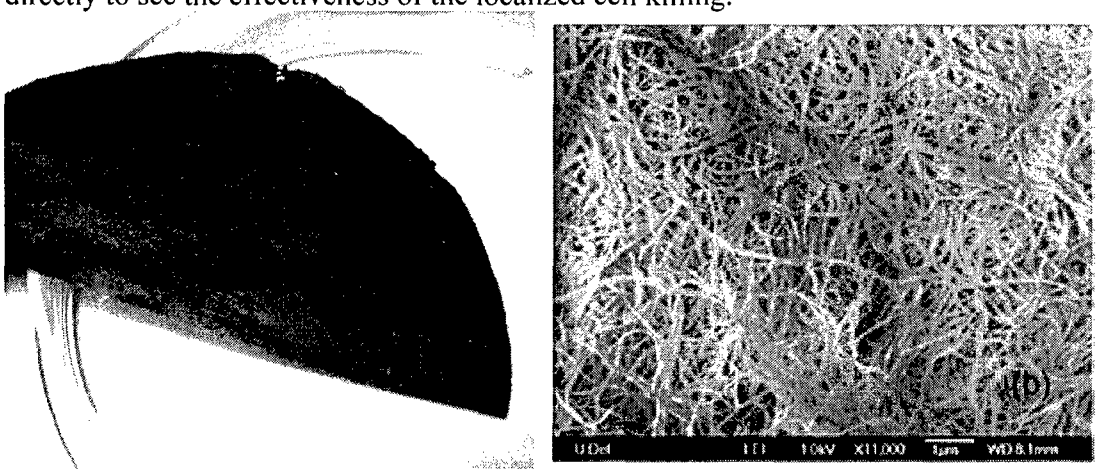

Figure 15 (a) SWNT sheets fabricated using vacuum filtration, (b) SEM image of nanotube sheet showing highly entangled nanotubes.

Figure 15 (a) shows the macroscopic sheet of single wall carbon nanotubes that was fabricated using vacuum filtration technique. Figure 15(b) shows the scanning electron micrograph of the sheet consisting of highly entangled nanotubes. We created sheets to make arrays of immobilized cells to clearly demonstrate the explosion effect that were treated with nanotubes. What we found was nanotube sheets that are highly entangled in DI water and in PBS can explode on exposure to near infra red light. Figure

16 (a) to (d) shows the explosions of nanotube sheets in DI water on exposure to 200 mW/cm^2 of laser light. These dramatic explosions are caused due to the opto-thermal transitions in nanotubes which heat the water molecules to more than 100°C that are present in the nano-pores between bundles, creating explosions. From Figure 3 (b), it can be conjectured that the temperatures must have been in excess of 700°C to create such explosions.

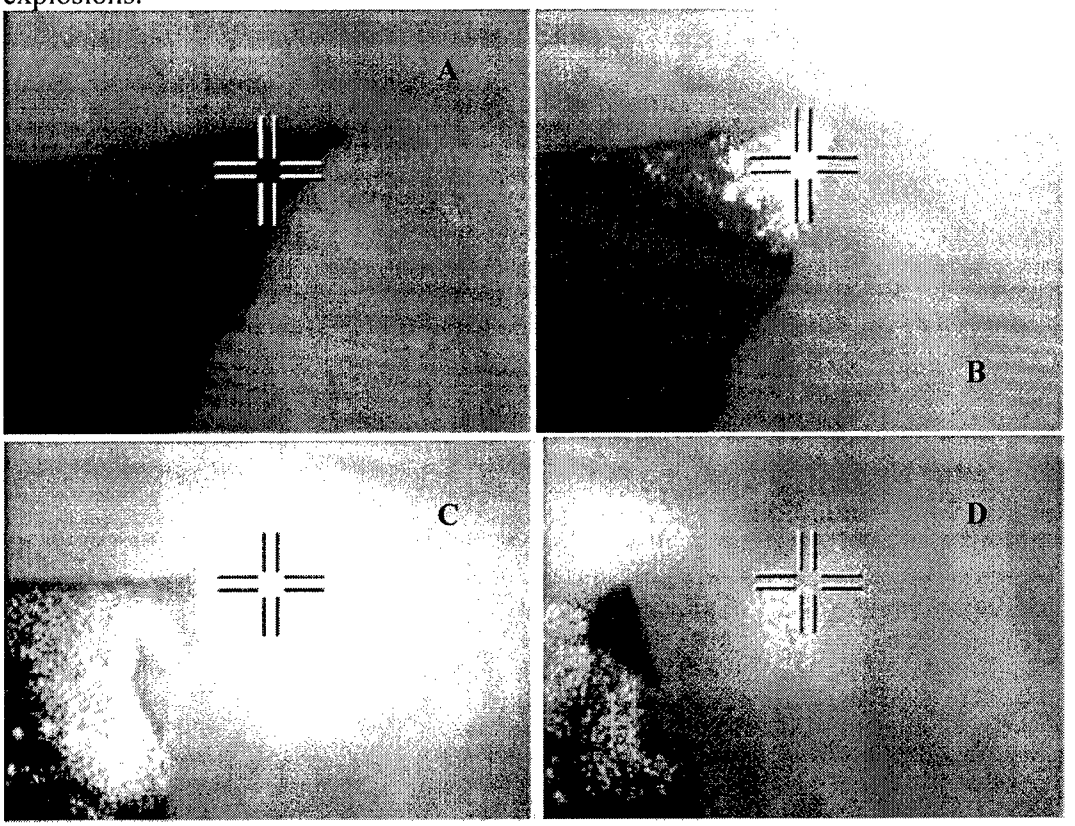

Figure 16. Series of dramatic explosions in single wall carbon nanotubes. (A) Nanotubes before light exposure, (B), (C) and (D) Nanotube explosions at t= 3, 7 and 10 s. The entire series of explosions were completed in 12 seconds. Scale bars for all the images is 1 mm

Explosions in air of loosely packed nanotubes have been observed before [16]. However, such explosions were ascribed to the thermal energy confinement in loosely packed nanotubes and the burning due to adsorption of oxygen creating ignition. It was noted that when nanotubes were compacted, the thermal energy was dissipated rapidly to the surroundings that made the explosions occur only at high laser energy. What we have found that nanotubes could explode even in the compacted form as sheets and bundles at laser intensities of 50-200 mW/cm^2. We postulate that this phenomenon arises both from high heat confinement inside the tubes, and from high heat confinement between the tubes when nanotubes are compacted together. The high optical absorbance in single wall carbon nanotubes originates between the first and second van Hove singularities in nanotubes [16, 17]. Heat is also generated in nanotubes due to the electron-phonon coupling causing molecular vibrations. While such thermal vibrations can be dissipated easily in single nanotubes without explosions at low laser intensities, when nanotubes are

in sheets or bundles, the thermal energy is confined between the tubes creating explosions of this nature at low laser intensity in distilled water. Although nanotubes have excellent thermal conductivity, when nanotubes are in bundles, the dissipation of thermal energy to the surrounding water molecules is not fast enough compared to the heating process itself. While the thermal conductivity of nanotubes along the tube axis is high [18-21], the thermal conductivity in sheets is almost an order of magnitude smaller [22]. This creates an imbalance in thermal energy dissipation to the surroundings and heat confinement between the tubes. This can create localized hot spots where the water molecules that are just adsorbed onto the surface of the nanotubes are vaporized. These vaporized water molecules have no place to escape as they are tightly confined between the bundles. This in turn starts building up intense pressures between the bundles causing the nanotubes to explode creating nano-bombs. Explosions occur only when the pressure is high enough and not all the nanotubes explode simultaneously in the presence of light. This is witnessed in Figure 16 (b), at a moment when parts of the area are exploding while some of the nanotube bundles remain unexploded. This imbalance in the thermal energy generation and dissipation in nanotube bundles causes such explosions. Heating single nanotubes requires much more laser energy because the heat is dissipated rapidly to the surroundings. Asserting that local energy imbalance induces explosions is a simple model, but such imbalances and gradients in nano-scale materials can be extremely high.

We also found that the explosions were more dramatic in phosphate buffered saline, which we utilized to kill cells dramatically. This may be due to the presence sodium in saline solutions and to the strongly ionic nature of the solution, providing electrons to the nanotube and creating a localized electrostatic effect that may have caused the explosions to be more powerful than in distilled water. The nanotubes that we have used consist of both metallic and semiconducting nanotubes mixed together. When we shine light on a metal-semiconductor junction, charge separation and accumulation can occur leaving an excess amount of charges creating localized electrostatic effects that can also trigger explosions. Further, nanotubes can act as nano-electrodes in electrolytic solutions, and metallic ions in electrolytes reduce themselves on the surface of the nanotubes. This nature of the nanotube may also be attracting ionic sodium from the PBS to reduce to metallic sodium, which then explodes when excited with light in the presence of water.

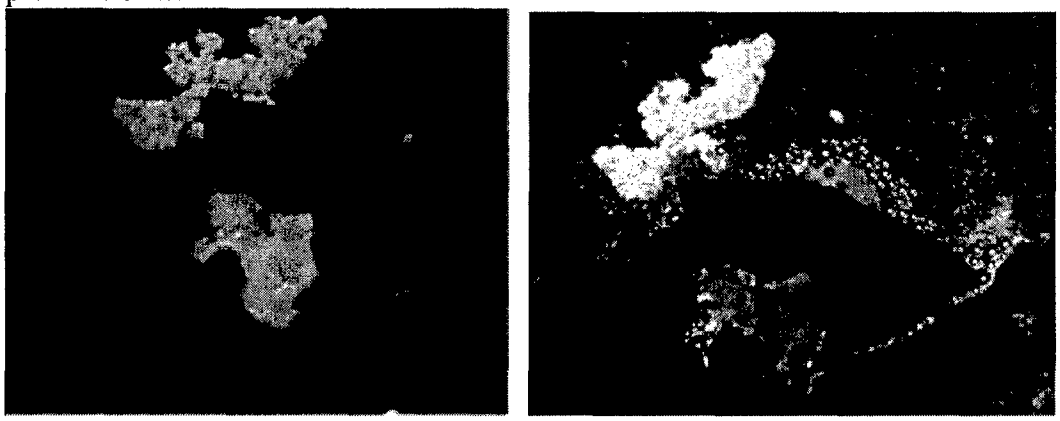

Figure.17 : (a) BT474 breast cancer cells placed inside two etched holes on nanotube sheet before light exposure, (b) after exposure to 200 mW/cm^2 of light intensity. The cells

in the well of the nanotube sheet that received light were ablated. Scale bars for both images: 1 mm

Figure 17 (a) shows the nanotube sheet with cells placed on top of the wells before light exposure. The cells in the bottom well were treated with nanotubes dispersed in PBS, while the cells in the top well were just treated with PBS solution to serve as controls. Figure 17 (b) shows the same image in Figure 17 (a) after exposure to 200 mW/cm^2 of 800 nm laser light. As one can see the appearance of Figure 17 (b) is dramatic compared to Figure 17 (a). The cells in the bottom well were blown to pieces and the cells appeared charred. The cells were also seen to be dislodged from the cluster showing that the explosions were indeed dramatic. The pattern of dead cells looks like the explosions started from the center of the cell clusters and moved all the mass to the surrounding areas, including the bubbles. Bubbles can be seen around the dead cells, which we ascribe to violent boiling effect of the PBS solution permeating the nanotubes. No bubbles were seen around the cells that were not treated with nanotubes but were exposed to light. These results imply that the localized temperature when nanotubes explode in PBS solution should be in excess of the boiling point of PBS. To control the explosions and create selective effects, cluster of cells were placed in a dish and nanotube in PBS solution was dropped on to the center of a large cell cluster. Upon shining 50 mW/cm^2 of 800 nm light, the cells started to turn blue, showing the cell membrane was permeated by the Trypan blue dye. This is shown in Figure 18 (a) and Figure 18 (b).

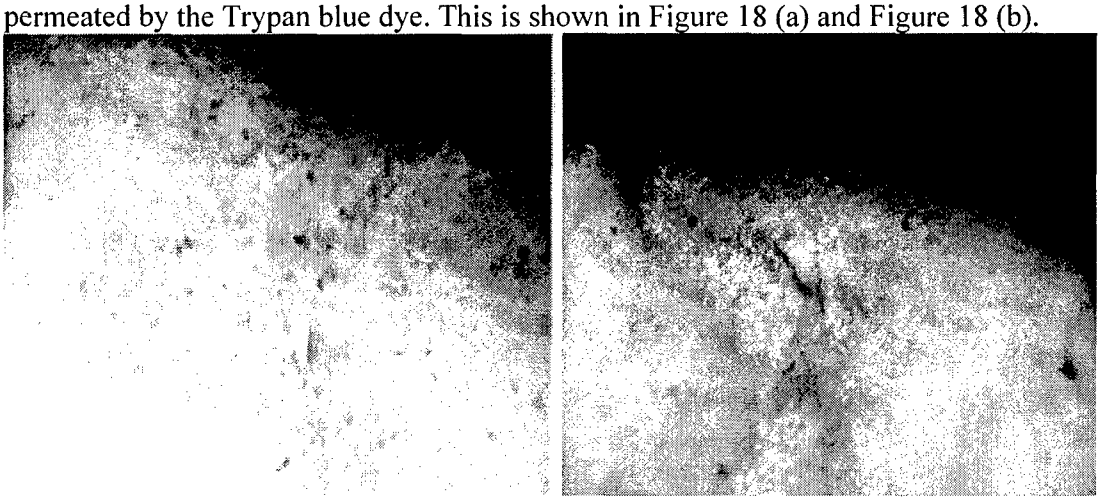

Figure.18: (a) BT474 cells that were treated with nanotubes in PBS suspension before light exposure, (b) after light exposure to 50 mW/cm^2. Note that the center part that turned blue is the site that was exposed to light, while the surrounding cells appear normal. This illustrates the precision of cancer cell killing in the central region by this approach. Scale bars for both the images: 1 cm

III. Key Research Accomplishments:

The following are the key research accomplishments that have emanated through this research:

- This is the first time to show the effective separation of carbon nanotubes and their labeling to be viewed in confocal microscopy. The smallest nanotubes observed were about 10 nm.
- The use of surfactant and labeling using $DiOC_6$ has shown to increase the contrast in confocal imaging which shows the utility of carbon nanotubes for high contrast imaging with techniques such as MRI
- This is the first study to show antibody functionalization of carbon nanotubes for direct applications in breast cancer research. Previous research had pointed that antibodies cannot be functionalized on nanotubes due to their size and geometry. We have proved that it can be done through effective separation of the nanotubes using surfactants and labeling.
- Specific functionalization has been achieved by using di-amino PEG molecules to the nanotube surfaces that can attach to the primary antibody.
- This is the first study to show the differences in quantum conductance of nanotubes and nanotubes coated with antibodies. Coating nanotubes with antibodies shifts their energy gap and the associated conductance which can be measured using nano-probes, which is also the basis of the biosensor that is being developed for cancer detection applications.
- Our cell detection technique shows the feasibility of the concept that nanotube devices can be used for molecular targeting of cancer cells
- Finally, nano-bombs can find applications as potent therapeutic agents in the fight against breast cancer.

IV. Reportable Outcomes:

The following are the reportable outcomes of this award:

- Two manuscripts has already been accepted in Nanobiotechnology. Uncorrected proofs are attached.
- A manuscript on selective molecular targeting has been submitted in Nature Biotechnology for review.
- A presentation was given at the IEEE Sensors conference in Vienna in Biosensors. This is a very prestigious conference with an acceptance rate of 55% and top 10% are allowed presentations. The PI is one of the top 10 presenters at the conference.
- A presentation was given in Nanotech 2005 in Anaheim, CA.
- A paper has been accepted in IEEE sensors journal and is in press.
- The PI has been invited to be on the editorial board of the Journal Nanobiotechnology that caters directly to the medical applications of nanotechnology. This wouldn't have been possible with out the dissemination of the current results.

- A student Ranjani Sirdeshmukh has obtained her Masters degree due to this research and her thesis is "Antibody Functionalization of Carbon Nanotubes".
- A patent has been applied on the antibody functionalization of carbon nanotube and the biosensors based on this award.
- Collaborations with medical schools such as Thomas Jefferson University has been strengthened due to this award.
- Collaborations with Oakridge National Laboratory has been established due to this award.

V. Conclusions:

In this research, a new technique of using carbon nanotubes for detection, diagnosis and killing of cancer cells have been investigated. The most important implications of this research is to be able to demonstrate the functionalization of antibodies on carbon nanotubes. The high degree of functionalization is achieved due to the well separation and labeling of carbon nanotubes using surfactant and flourophore solutions. This first study demonstrates the utility of nanotubes as an epitope for delivering antibodies to cells and tissues for cancer detection. Further, tumor suppressing agents such as Tarceva and 2C4, which are monoclonal antibodies can be functionalized on carbon nanotubes and selectively delivered for suppressing tumor and promoting anti-cancer activity. The continuation of this grant will allow us to study the effect of cell interactions on antibodies coated on nanotubes, measure their electronic properties and also investigate cell killing using nanotubes by heating the nanotubes using visible-Infra-red light. The potential applications of this study are enormous as this is the first time to conclusively show that the electronic properties of nanotubes can be altered by biomolecular functionalization. It will help in the development of a cancer diagnostic system that can detect cancer cells by investigating the changes in the surface electronic properties of carbon nanotubes. Further, the optical fluorescence of nanotubes can be utilized to image cells and tissues at the sub-100 nm limits using conventional microscopic techniques. This study also shows the utility of nanotubes as contrast agents for high resolution sub-micron to sub-100 nm MRI imaging which is not possible using present day technology. The potential applications of nanotubes for cancer research are therefore enormous. Our cell detection strategy shows the effectiveness of developing early diagnostic kits for detection of cancer cells. Finally, our nanobombs can find applications as potent therapeutic agents for eradicating breast cancer. All the outcomes has been achieved successfully.

VI. References:

[1] M. F. Islam, E. Rojas, D. M. Bergey, A. T. Johnson, and A. G. Yodh, "High Weight Fraction Surfactant Solubilization of Single-Wall Carbon Nanotubes in Water," *NanoLetters*, pp. 269-273, 2003.

[2] O. Matarredona, H. Rhoads, Z. Li, J. H. Harwell, L. Balzano, and D. E. Resasco, "Dispersion of Single-walled carbon nanotubes in aqueous solutions of anionic surfactant NaDDBS," *Journal of Physical Chemistry B*, vol. 107, pp. 13357-13367, 2003.

[3] R. Prakash, S. Washburn, R. Superfine, R. E. Cheney, and M. R. Falvo, "Visualization of individual carbon nanotubes with flourescence microscopy using conventional flourophores," *Applied Physics Letters*, vol. 83, pp. 1219-1221, 2003.

[4] P. C. Cheng, T. H. Lin, W. L. Wu, and J. L. Wu, *Multidimensional Microscopy*, Springer Verlag, New York, 1994.

[5] E. M. M. Manders, F. J. Verbeek, and J. A. Aten, "Measurement of Colocalization of Objects in Dual Color Confocal Images," *Journal of Microscopy*, pp. 375-382, 1993.

[6] K. T. R. Sirdeshmukh, B. Panchapakesan, "Antibdoy Functionalization of Carbon Nanotubes," *Materials Research Society Spring Conference*, 2004.

[7] B. C. Braden, "X-ray Crystal Structure of an anti-Buckministerfullerene Antibody Fab Fragment: Biomolecular Recognition of C60," *Proceedings of the National Academy of Sciences*, pp. 12193-12197, 2000.

[8] B. C. B F Erlanger, M Zhu, L Brus, "Binding of an Anti-Fullerene IgG Monoclonal Antibody to Single Wall Carbon Nanotubes," *NanoLetters*, pp. 465-467, 2001.

[9] N. W. S. K. M Shim, R J Chen, Y Li, H Dai,, "Functionalization of Carbon Nanotubes for Biocompatibility and Biomolecular Recognition," *NanoLetters*, pp. 285-288, 2002.

[10] K. Sattler, "The energy gap of clusters nanopraticles and quantum dots", Hand book of thin film materials," *edited by H.S. Nalwa, Academic Press*, 2002.

[11] K. Teker, G. Cesarone, E. Wickstrom, B. Panchapakesan, "Electronic sensing of antibodies and surface receptors in cancer cells using nanotube devices" paper presented at the Nanotech 2005, Anaheim, CA 2005.

[12] K. Teker, R. Sirdeshmukh, K. Sivakumar, S. Lu, B. Panchapakesan, E. Wickstrom, "Applications of Carbon Nanotubes for Cancer Research", Nanobiotechnology Vol 1(2)1-12, 2005

[13] X. Tian *et al.*, *Journal of Nuclear Medicine* **45**, 2070-2082 (2004).

[14] X. Le Roy *et al.*, *Oncogene* **6**, 431-7 (1991).

[15] K. J. Martin *et al.*, *Cancer Res* **60**, 2232-8 (Apr 15, 2000).

[16] M. J. O'Connell, S. M. Bachilo, C. B. Huffman, V. C. Moore, M. S. Strano, E. H. Haroz, K. L. Railon, P. J. Boul, W. H. Noon, and C. Kitrell, *Science*, vol. 297, pp. 593-596, 2002.

[17] S. M. Bachilo, M. S. Strano, C. Kittrell, R. H. Hauge, R. E. Smalley, and R. B. Weisr, *Science*, vol. 298, pp. 2361-2366, 2002.

[18] A. M. Rao, P. C. Eklund, S. Bandow, A. Thess, and R. E. Smalley, "Evidence for charge transfer in doped carbon nanotube bundles from Raman scattering," *Nature*, vol. 388, pp. 257-259, 1997.
[19] S. Berber, Y. K. Kwon, and D. Tomanek, *Physical Review Letters*, vol. 84, pp. 4613, 2000.
[20] P. Kim, L. Shi, A. Majumdar, and P. L. McEuen, *Physical Review Letters*, vol. 87, pp. 215502, 2001.
[21] M. A. Osman and D. Srivatsava, *Nanotechnology*, vol. 12, pp. 21, 2001.
[22] J. Hone, M. Whitney, C. Piskoti, and A. Zettl, *Physical Review B*, vol. 59, pp. R2514, 1999.

APPENDIX

Job: NANO 1/1 Journal
Chapter: Panchapakesan
Template: 8.5x11/comp/22.05.05

Operator: IBH
Date: 25.04.2005
Revision: 1st Proof

Nanobiotechnology

ISSN 1551-1286/05/01:1–12/$30.00
DOI: 10.1385/Nano:1:1:1

Research Article

Applications of Carbon Nanotubes for Cancer Research

Kasif Teker,[1] Ranjani Sirdeshmukh,[1] Kousik Sivakumar,[1] Shoaxin Lu,[1] Balaji Panchapakesan,[,1] Eric Wickstrom,[2] Hsin-Neng Wang,[3] and Tuan Vo-Dinh[3]*

[1]Delaware Nanotechnology Laboratory, Department of Electrical and Computer Engineering, University of Delaware, Newark, DE 19716, USA; [2]Department of Biochemistry and Molecular Pharmacology, Thomas Jefferson University, Philadelphia 19107, USA; *and* [3]Center for Advanced Biomedical Photonics, Oak Ridge National Laboratory, Oak Ridge, TN 37831-6101, USA

Abstract

Carbon nanotubes have many unique properties such as high surface area, hollow cavities, and excellent mechanical and electrical properties. Interfacing carbon nanotubes with biological systems could lead to significant applications in various disease diagnoses. Significant progress in interfacing carbon nanotubes with biological materials has been made in key areas such as aqueous solubility, chemical and biological functionalization for biocompatibility and specificity, and electronic sensing of proteins. In addition, the bioconjugated nanotubes combined with the sensitive nanotube-based electronic devices would enable sensitive biosensors toward medical diagnostics. Furthermore, recent findings of improved cell membrane permeability for carbon nanotubes would also expand medical applications to therapeutics using carbon nanotubes as carriers in gene delivery systems. This article reviews the current trends in biological functionalization of carbon nanotubes and their potential applications for breast cancer diagnostics. The article also reports the applications of confocal microscopy for use in understanding the interactions of biological materials such as antibodies on carbon nanotubes that are specific to HER2 surface receptors in breast cancer cells. Furthermore, a nanotube-field-effect transistor is demonstrated for electronic sensing of antibodies that are specific to HER2 surface receptors in cancer cells.

Key Words: Single-wall carbon nanotubes; nanotube-field-effect transistors; biomolecular sensing; antibodies; HER2; confocal microscopy.

(Nanobiotechnology DOI: 10.1385/Nano:1:1:1)

*** Correspondence and reprint requests to:**
Balaji Panchapakesan, Delaware Nanotechnology Laboratory, Department of Electrical and Computer Engineering, University of Delaware, Newark, DE 19716, USA.
E-mail: baloo@ece.udel.edu

Humana Press

Introduction

Carbon nanotubes (CNTs) are remarkable synthetic materials with many fascinating properties, such as high mechanical strength, high surface area, excellent electronic and chemical properties, and thermal stability *(1–7)*. CNTs are nanometer-diameter cylinders consisting of single or multiple graphene sheets wrapped up to form a single-wall (SWNT) or multiwall (MWNT) carbon nanotube, respectively. Since the discovery of carbon nanotubes, researchers have been exploring their applications as building blocks for nanodevices such as probes *(8)*, electron-field-emission sources *(9)*, chemical sensors *(10)*, and transistors *(11)*. Furthermore, novel biological devices have been fabricated by integrating nanotubes with organic molecules *(12–14)*. These devices will enable new research fields and applications such as *in situ* modification of living cells or their physiological activities. For example, covalently functionalized carbon nanotube probes have been found to be chemically sensitive to be

used in the scanning probe microscopy mapping of biofunctional receptors *(12)*. The research for the development of CNT-based nanoscale biosensors has been intensified by the successful immobilization of biological species, such as proteins and enzymes, either in the interior cavity or on the surface of nanotubes without any drastic conformational or bioactivity change *(15,16)*. Very recent advances in the fabrication of CNT based devices, such as field-effect transistors (CNTFETs), have increased the expectations for the utilization of CNTs as superior biosensor materials *(17–19)*. These CNTFETs have shown appreciable changes in the electrical conductance suggesting the possibility of using them for electronic biosensing applications. Meanwhile, recent advances in aqueous solubility of CNTs have accelerated the biocompatibility evaluations toward biomedical applications including the potential use of CNTs as carriers in drug or gene delivery systems. Furthermore, conjugation of CNTs with biomolecules such as proteins, carbohydrates, and nucleic acids will play a very critical role in the research effort toward bioapplications of CNTs.

In this review article we present the recent advances and achievements in the CNT-based technologies and methodologies aimed toward biomedical applications. The following subjects will be presented sequentially: (i) CNTs, (ii) aqueous solubility of CNTs, (iii) functionalization of CNTs with biomolecules, (iv) electronic detection of protein adsorption using CNT devices, (v) utilization of CNTs in biomolecular delivery systems, (vi) antibody functionalization of CNTs for breast cancer applications, and (vii) electronic detection of antibodies using CNTFETs.

Carbon Nanotubes

Owing to their unique electronic and extraordinary mechanical properties, CNTs have grown to be interesting materials in recent years ever since they were discovered by Ijiima in 1991 *(20)*. CNTs can be considered as a rolled up single layer of graphite, with diameters of 0.4–2 nm for SWNTs and 2–100 nm for coaxial MWNTs, and lengths from several hundred nanometers to millimeters. MWNTs are essentially concentric single-walled tubes, where each individual tube can have different chirality. The concentric tubes are held together through secondary, van der Waals bonding. Although the exact interactions are not well understood, both chirality and morphology influence nanotube mechanical and electronic properties. From unique electronic properties and thermal conductivity roughly twice that of diamond, to mechanical properties such as stiffness, strength and resilience exceeds any current material. The unique electronic features include the ballistic (scattering-free) and spin-conserving transport of electrons along the tubes, the ability to have metallic as well as semiconducting behavior, and the access to the energy gap, which depends on the diameter of the tubes. Metallic or semiconducting nanotubes can be achieved by rolling them up differently. Figure 1 shows that the armchair configuration always leads to metallic tubes, while two-thirds of those with zigzag configuration

Fig. 1

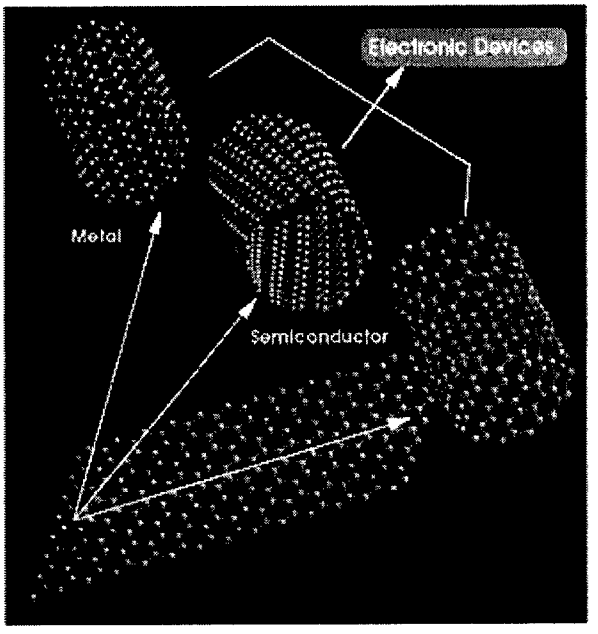

Fig. 1. Different morphological configurations and corresponding electrical conduction types for carbon nanotubes *(21)*. Left: armchair; right: zigzig; middle; intermediate chirality.

are semiconducting. They can also be rolled up with different chiralities. Two-thirds of all possible configurations show semiconducting characteristics.

CNTs are grown by combining at elevated temperatures a source of carbon with various catalytic nanostructured metals such as iron or cobalt. Common sources of carbon employed include bulk graphite, hydrocarbons, and carbon monoxide. The most common methods for bulk fabrication are arc synthesis *(22)*, laser vaporization of graphite *(23)* and thermal chemical vapor deposition (CVD) *(24)*. Unfortunately, the bulk synthesized tubes are highly tangled and bundled. For device applications, they need to be separated. This will be discussed in the next section. The CVD method allows nanotubes to grow directly on a wafer. Nanoparticles of iron are used as catalyst for the growth of CNTs. The catalyst material is placed on the surface of a wafer, which is inserted in a furnace at 700–1000°C in a flow of a carbon source gas. The tubes grow from the catalyst on the wafer surface. Engineering the properties of the catalyst and controlling the growth conditions determine the nature of the tube and their properties. In order to make devices, the tubes need to be integrated with electrodes on a wafer. Although the growth of randomly oriented and bundled nanotubes has been perfected in recent years, one of the major challenges is the repeatable placement of the tubes relative to the patterned features on the substrate. Although the "top-down" and "bottom-up" approaches of nanomanufacturing developed for integration of nanotubes to electronic and sensor devices are quite satisfactory for research purposes, there is still quite a lot of work ahead on the manufacturability of electronic and sensor devices using CNTs.

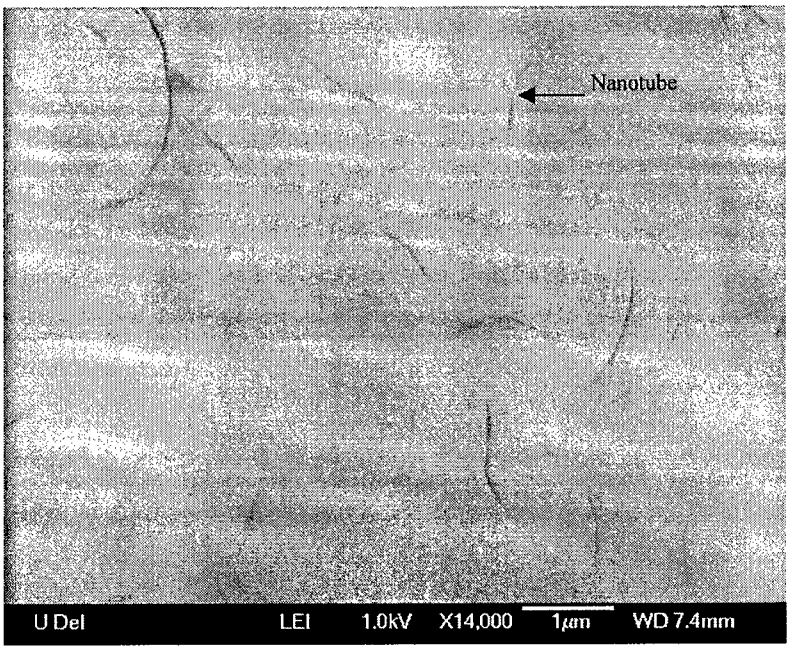

Fig. 2. SEM image of carbon nanotubes treated with the surfactant NaDDBS. The CNTs are very well separated and dispersed.

Aqueous Solubility of Carbon Nanotubes

The insolubility of carbon nanotubes in aqueous media has been a major obstacle for biological and biomedical applications. Recent studies have demonstrated water-soluble SWNTs by functionalization with amines *(25,26)* and DNA adducts *(27,28)*. Nevertheless, it has been reported that surface modifications after functionalization can affect the inherent material properties of the nanotube *(29,30)*. Thus, many researchers have suggested the approach of noncovalent stabilization of CNTs in solution by using surfactants, which can successfully disperse and separate CNTs without the formation of chemical bonds, i.e., the inherent properties of the CNTs are preserved. Moreover, the surfactant-mediated dispersion and the separation procedures are relatively low cost and simple, involving only ultrasonication and centrifuging or filtration.

In a recent study, Islam and co-workers *(31)* studied the effectiveness of the various surfactants for SWNT aqueous dispersion and separation. The optimum nanotube–surfactant ratios were 1:5 to 1:10 by weight. The optimum ratio for sodium dodecylbenzene sulfonate (NaDDBS) was 1:10. The nanotube–NaDDBS dispersions were found to be the most stable up to nanotube concentrations of 20 mg/mL. Furthermore, the suspensions remained dispersed for at least 3 mo, i.e., sedimentation or aggregation of nanotube bundles was not observed. The authors reported that the strong interactions between NaDDBS and SWNTs are the combined effect of the long lipid chain of NaDDBS and π–π interactions between aromatic moieties on the surfactant molecule and the surface of nanotubes. In another study the interactions between the NaDDBS and nanotubes were investigated for different parameters such as pH, surfactant concentration, nanotube concentration, and sonication time *(32)*. They reported that during the adsorption of the surfactant NaDDBS on SWNT Coulombic forces do not play a central role, but are overcome by the hydrophobic interactions between the surfactant tail and the nanotube walls. The hydrophobic forces between the surfactant tail and the nanotube control the structure of the surfactant-stabilized nanotubes. Each nanotube is covered by a monolayer of surfactant molecules in which the tails remain in contact with the nanotube walls, whereas the heads form a compact outer surface. Figure 2 is a scanning electron microscopy (SEM) image of CNTs in deionized (DI) water dropped on a wafer surface showing a very effective separation of CNT bundles into individual CNTs using the surfactant NaDDBS. Fig. 2

Functionalization of Carbon Nanotubes with Biomolecules

Owing to its strength, stability, and electrical conductivity *(33)*, carbon has been the most widely used support material for the immobilization of biomolecules. For example, antibodies specific to fullerenes have been produced by researchers in recent years *(34,35)*. CNTs with higher surface area, hollow cavities, excellent mechanical and electrical properties would make nanotubes a more suitable material for bioapplications. Therefore, extensive research is necessary to study the interactions between carbon nanotubes and the fundamental components of living organisms, such as proteins, nucleic acids, carbohydrates, antibodies, cells, and tissues. Our empha-

sis will mainly be on antibodies. Davis et al. *(15)* reported the immobilization of proteins and enzymes in carbon nanotubes. They demonstrated that small proteins and enzymes can readily be placed within the interior cavity of opened nanotubes. In some instances, proteins were seen to be distorted, resulting in a concave meniscus inside the tube. Moreover, encapsulated proteins exhibited relative immunity to electron-induced disintegration implying strong immobilization. A significant amount of the immobilized enzyme remained catalytically active, indicating that no drastic conformational change had taken place. To develop a new CNT-based biosensor for specific biomolecular recognition, the biomolecules need to be densely packed on the outer surface of the CNTs, and the functionality of the biomolecule has to be maintained. A good measure for the conservation of the functional properties of the biomolecule is its ability to form ordered arrays. Balavoine et al. *(36)* reported direct crystallization of proteins such as streptavidin and HupR on the surface of the CNT. The proteins were able to crystallize in a helical conformation around the MWNTs. The strong interaction between the proteins and carbon nanotubes is due to hydrophobic domains within the protein structure. They demonstrated that a single protein layer coats the nanotubes.

Chen et al. *(16)* demonstrated protein binding to SWNTs through a noncovalent sidewall functionalization scheme. Noncovalent functionalization allows preserving the carbon sp^2 character and structure, which is significant for retaining the electrical properties of the nanotubes. A variety of proteins, such as streptavidin, ferritin, and biotinyl-3,6-dioxaoctanediamine, have been immobilized on SWNTs that were functionalized by 1-pyrene butanoic acid succinimidyl ester. The pyrenel group irreversibly adsorbs onto the hydrophobic surfaces of SWNTs through a π–π interaction, and the succinimidyl ester group reacts with amine groups on lysine residues of proteins to form amide bonds. To confirm the protein immobilization mechanism, they carried out control experiments in which CVD-grown SWNTs were incubated in aqueous ferritin solution without the pyrenel group. They reported no observable adsorption of proteins on the SWNT surfaces. Nevertheless, Azamian et al. *(37)* reported strong adsorption of ferritin onto SWNTs in water. They also demonstrated that immobilization is strong in the presence and absence of a coupling reagent, implying predominant noncovalent nature of the immobilization.

Huang et al. *(38)* have demonstrated the functionalization of CNTs with bovine serum albumin (BSA) proteins via diimide-activated amidation. The CNT–BSA conjugates were highly water soluble, and formed dark-colored aqueous solutions. They have used the total protein micro-determination assay (modified Lowry procedure) to evaluate the bioactivities of the CNT-attached proteins. The results showed that the majority of the proteins in the CNT–BSA conjugates remained bioactive.

In a recent study, Shim et al. *(39)* investigated the adsorption behavior of the proteins on the sides of SWNTs using the streptavidin/biotin system. They found that streptavidin nonspecifically binds to as-grown SWNTs. For the realization of CNT-based biosensors and biomedical applications, biocompatibility and specificity are two important requirements. Specificity requires biofunctionalization of nanomaterials for recognizing of only one type of target biomolecule in solution and rejecting others. Thus, they used a polymer to coat the nanotube surfaces to prevent nonspecific-protein adsorption. Poly(ethylene glycol), PEG, is one the most effective and widely used protein-resistant materials *(40)*. However, PEG-coated CNTs have shown appreciable protein adsorption. Therefore, they preadsorbed Triton molecules (a surfactant) on as-grown SWNTs to facilitate the subsequent PEG adsorption to prevent nonspecific-protein adsorption. Co-adsorption of Triton and PEG was found to be very effective for preventing nonspecific adsorption of streptavidin on nanotubes. Specific binding of streptavidin onto SWNTs was achieved by co-functionalization of nanotubes with biotin and protein-resistant polymers. In a similar study, Lin et al. *(41)* investigated the interactions between covalently functionalized SWNTs and ferritin in aqueous solution. The ferritin–SWNT conjugation was enhanced and stabilized in the presence of a coupling agent for amidation to promote the formation of covalent linkages. The nonspecific-protein adsorption was eliminated by the functionalization of the nanotubes with hydrophilic polymers or better with oligomeric PEG moieties. To date, PEG has been the most widely studied and accepted protein-resistant material. The alterable protein affinity of CNTs in aqueous solutions is valuable to their potential biological and biomedical applications. Although there is overwhelming evidence for both covalent and noncovalent functionalization of proteins on CNTs, it is yet to be determined which of these functionalization schemes would be more appropriate for biosensor applications. In the past two years, our group at the University of Delaware has been investigating various functionalization procedures on SWNT surfaces *(42–45)*. The results of such functionalization procedures has led to the development of CNTFETs with antibodies functionalized on CNT surfaces. In this article, the results on electronic detection of the antibody binding to the surface of carbon nanotubes using a noncovalent functionalization scheme are presented using CNT-based devices. Noncovalent functionalization has several advantages including simplicity of the steps involved, preservation of the bioactivity of the molecule, noninterference of the sensor properties from the host molecules used for tagging in covalent functionalization schemes, and tailorable surface properties of the CNT. The results presented here also hint at the possibility of the application of CNTs to detect biomolecules in fluids.

Au: Please check changes.

Electronic Sensing of Protein Adsorption using Carbon Nanotube Devices

Converting CNTs into electronic devices for biosensor applications have received significant attention in recent years. The reason for such an approach is to be able to combine nanotechnological interfaces to CMOS, MEMS, and biotechnology that can lead to creation of compact and batch-fabricated biosensors with hundreds to thousands of sensors on a single chip.

This would be a powerful approach for simultaneously detecting and screening various types of cancer. An example of such a device is a nanoscale field-effect transistor with CNTs acting as the conducting channel for detection of various biomolecules. A CNT-based field-effect transistor (CNTFET) was first fabricated in 1998 *(46)*, and extensively studied *(11)*. These CNT-based devices are small and fast, and the active detection area can be sized for individual biomolecules. Furthermore, their response to different species can be varied in a controlled way using chemical and biological functionalization.

In general, two types of measurements are performed: (i) the current through the drain contact is monitored while a variable gate voltage is applied to a metallic gate buried underneath the oxide (SiO_2) substrate and (ii) the device is immersed in a buffer solution and the gate voltage is applied through a metal (e.g., Pt) electrode immersed in the solution. Star et al. *(18)* co-adsorbed poly(ethylene imine) (PEI) and PEG on an SWNT FET device, followed by the biotinylation of PEI for specific streptavidin recognition. The CNTFET device characteristic before chemical modification is *p*-type (i.e. conduction in negative gate voltages), presumably due to exposure to oxygen *(47,48)*. Coating the device with the mixture of PEI and PEG polymers resulted in an *n*-type device characteristic. This effect, which has been observed before *(49)*, was attributed to the electron-donating property of the NH_2 groups of the polymer. Subsequently, biotinylated devices showed *p*-type conductance, suggesting that attachment of biotin was via covalent binding to the NH_2 group of PEI, thus reducing the overall electron donating property of PEI. The modified device exhibited different device characteristics compared to those with direct nonspecific-protein adsorption. A closely related study has been conducted to quantify the charge transfer between streptavidin and the CNT surfaces *(50)* using CNTFETs, both in dry and in buffer environments. They reported that proteins donate charge to CNTs.

In another study, Chen et al. investigated *(17)* CNT–protein binding to develop highly specific electronic biosensors. They used polyethylene oxide (PEO) units to prevent nonspecific binding of various proteins. They found that Tween- and P103 (PEO-containing molecules) coated SWNTs exhibited strong resistance to proteins such as streptavidin, avidin, BSA (β-glucosidase, and staphylococcal protein A (SpA). Furthermore, a Tween-coated CNTFET device did not show any conductance change upon exposure to various proteins. Based on these results, it was suggested that PEO units formed a nearly uniform layer on the CNT surface. The van der Waals interaction between the hydrophobic segment of the molecules and the CNT sidewall is robust against desorption in aqueous solutions owing to favorable hydrophobic–hydrophobic association. The PEO segments extend into the water and make the nanotube surface protein resistant *(51)*. Subsequently, they achieved specific biotin–streptavidin binding by modifying carbon nanotubes with biotinylated Tween-20. In separate experiments, they demonstrated specific detection of mAbs to the human autoantigen U1A (a protein involved in the splicing of mRNA). To do that, the nanotube device was coated with the U1A antigen–Tween-20 conjugate. The device was capable of detecting the binding of 10E3, a mAb that specifically recognizes U1A, at concentrations of 1 n*M*, while rejecting polyclonal IgG at a much greater concentration of 1 μ*M*. More recently, Chen et al. *(19)* have developed microarray of nanotube "micromat" sensors to investigate electrical conductance change by protein adsorption. They have applied various chemical functionalization schemes to block selected components of the devices from protein adsorption. They reported that much of the conductance changes due to protein binding on CNTFET devices results from the metal–CNT contact region. These studies suggest that CNT biosensors can be utilized for real-life applications such as in medical diagnostics, proteomics arrays, and gene chips.

Utilization of Carbon Nanotubes in Biomolecular Delivery Systems

Solubilization and biological functionalization of carbon nanotubes have greatly increased the usage of carbon nanotubes in biomedical applications such as biosensors and nanoprobes. More recently, Pantarotto et al. *(52)* have demonstrated that peptide-functionalized carbon nanotubes are able to penetrate cell membranes and to accumulate inside living cells without causing apparent cytotoxicity. To investigate the cell membrane permeability of carbon nanotubes, SWNTs were functionalized based on the 1,3-dipolar cycloaddition reaction *(26)*, which can increase the water solubility of CNTs and provide free amino groups along their side walls. The functionalized SWNTs were then conjugated with fluorescently labeled peptides. After a 60-min incubation of cells with functionalized CNTs, these conjugates were found to be distributed in the cytoplasm or even inside the nucleus. Based on this result, they further conjugated carbon nanotubes with plasmid DNA through electrostatic interaction between the amino groups of the functionalized CNTs and the phosphate groups of plasmid DNA *(53)*. After a 30-min incubation of cells with plasmid DNA–CNT conjugates, the gene encoded by the plasmid DNA began to be expressed, and then reached 10 times higher levels of gene expression than the incubation of cells with DNA alone after 3 h incubation. Owing to the low cytotoxicity caused by carbon nanotubes, they have demonstrated that carbon nanotubes can be used as a high-efficiency gene delivery system in various therapeutic applications.

In another study, Shi Kam et al., *(54)* demonstrated that large biomolecules such as streptavidin (MW approx 60 kDa) can be delivered into living cells by conjugating with biotin-functionalized carbon nanotubes within a short incubation period. They have proposed that the uptake mechanism of carbon nanotubes is through the endocytosis pathway driven by the nonspecific association between the unoxidized areas of the CNTs and the hydrophobic regions of the cell surface.

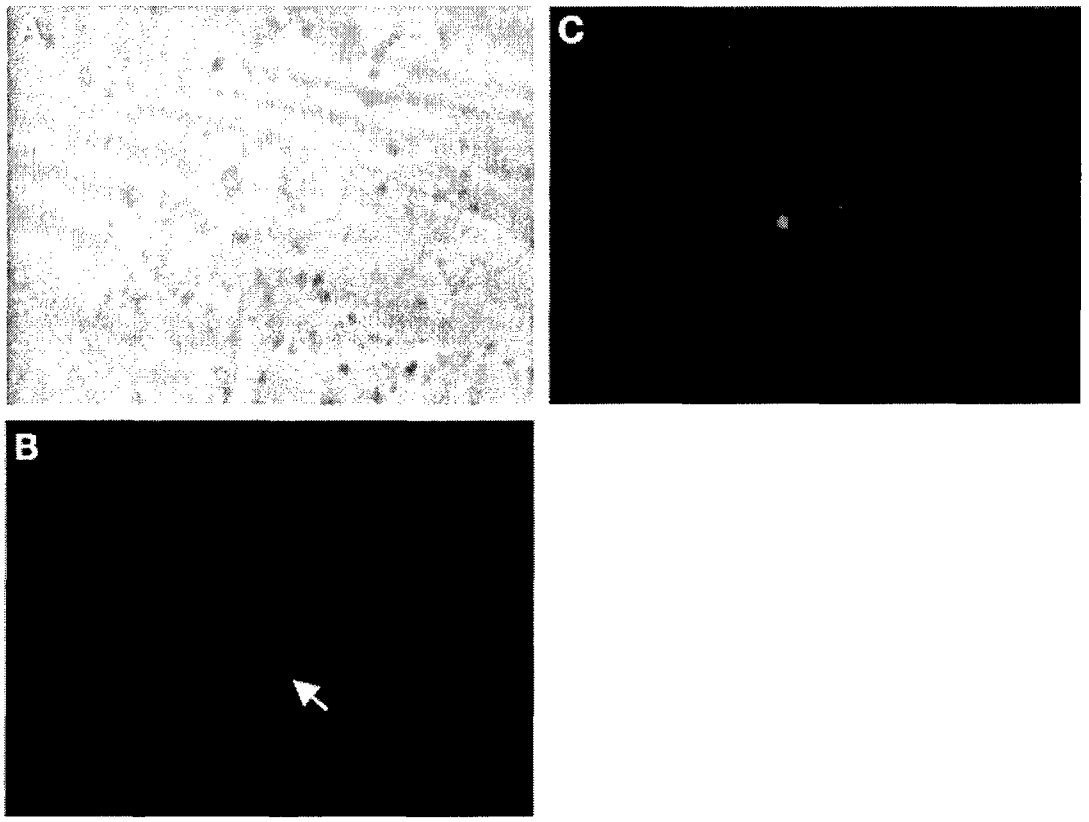

Fig. 3. Fluorescence microscopy images of CHO cells following 30-min incubation with fluorescently labeled streptavidin–biotin–SWNT conjugates: **(A)** bright-field image of cells; **(B)** fluorescence image of same area of cells; **(C)** combined bright-field and fluorescence image, showing that the streptavidin–biotin–SWNT conjugate (indicated by arrow) is able to penetrate the cell membrane after 30-min incubation.

We have investigated the use of SWNTs for delivery in Chinese hamster ovary (CHO) cells. We prepared the fluorescently labeled streptavidin–biotin–CNT conjugates using the method described in Shi Kam's report with slight modifications. Briefly, to obtain stable water solubilization of SWNTs, 20 mg CVD produced SWNTs with a length 0.5–100 μm (Nanostructured & Amorphous Materials, Inc.) were refluxed and oxidized in 50 mL, 2.6 *M* aqueous HNO_3 solution for 48 h. This oxidation step has been known to shorten CNT bundles and produce carboxylated SWNTs *(55)*. The acid-treated mixture was then filtered through a 100-nm pore size polycarbonate filter (Whatman, Inc.) on a filter holder (Millipore). After washing with 1 L deionized water, a small amount of 1 *N* NaOH solution was poured over the filter, which was then washed with 50 mL deionized water to neutralize the sample and to remove the small nanoparticulate impurities *(56)*. This step was repeated until the pH of the solution in the funnel was approx 7. The SWNT mixture on the filter was then resuspended in pure water by sonication for 60 min. To remove insolubilized SWNTs, the solution was centrifuged at 8000 rpm for 10 min. The solubilized SWNTs were obtained from the dark supernatant and stored at a concentration of 1 mg/mL.

Au: Please provide the g-force.

The carboxylated SWNTs were then biotinylated by reacting overnight with 1 mg/mL 1-ethyl-3-(3-dimethylamino-propyl) carbodiimide (EDC) and 1 m*M* biotin-LC-PEO-amine (Pierce) in 50 m*M* MES buffer (pH 5.5). To remove unreacted reagents, the mixture was dialyzed against deionized water in a 12–14K MWCO membrane (Spectrum Laboratories, Inc.) for 3 d. The streptavidin–biotin–CNT conjugates were obtained by mixing the biotinylated SWNTs with 1 μ*M* Rhodamine B labeled streptavidin (Molecular Probes) at room temperature for 1 h. To demonstrate the cell membrane permeability for CNTs, the CNT conjugates were incubated with CHO cells at 37°C in 5% CO_2. Figure 3 shows that the fluorescently labeled streptavidin–biotin–CNT conjugates are able to penetrate the cell membrane after 30-min incubation with CHO cells. Although the cytotoxicity and cellular uptake mechanism of CNTs are still topics to be investigated in more detail, these observations of the cell membrane permeability for carbon nanotubes have offered a great opportunity for medical applications involving delivery of drugs, proteins, or genes into living cells.

Fig. 3

Fig. 4. Confocal microscopy image of carbon nanotubes labeled with $DiOC_6$. The CNTs are very well separated and dispersed.

Antibody Functionalization of Carbon Nanotubes for Breast Cancer Applications

Rapid advances in nanotechnology will enable CNT devices to be used effectively to detect clinically and biologically important interactions between antibodies and antigens. Owing to their small size and very high conductivity, CNTs coated with antibodies could be used as probes of cell or membrane function. For example, Erlanger et al. *(57)* demonstrated that a monoclonal antibody specific for fullerenes recognized and bound specifically to SWNTs. They found that the binding cavity was formed by the clustering of hydrophobic amino acids, and the hydrophobic binding site of the antibody is sufficiently flexible to recognize SWNTs as well.

In order to exploit the unique nanomaterials, CNTs, in biological and biomedical applications, we have functionalized SWNTs with antibodies. This functionalization approach is used toward developing a biosensor for breast cancer detection, by conjugating the SWNTs with antibodies that are specific to cell surface receptors (HER2) of breast cancer cells. To develop CNT- based cancer diagnostic systems, the following steps need to be achieved: (i) separation of CNTs in aqueous solutions, (ii) functionalization of CNTs with antibodies that are specific to cancer cell surface receptors, (iii) assembling the antibody-coated CNTs with the cancer cells to detect overexpressed cell surface receptors (HER2). We have functionalized CNTs with three different antibodies: (i) monoclonal mouse IgG, (ii) polyclonal rabbit anti-goat IgG, (iii) polyclonal goat-anti-mouse IgG. The monoclonal mouse antibody is sensitive to cell-surface receptors (HER2) on a breast cancer afflicted cell. It should be pointed that BT474 human breast cancer cells, overexpress *HER2 (Her2$^+$)* and *c-MYC* oncogenes, but not the estrogen receptor (ER^-) or IGF1 receptor ($IGF1R^-$) with MCF7M human breast cancer cells, which express the estrogen receptor (ER^+) and overexpress *cyclin D1* and *c-MYC* oncogenes and the IGF1 receptor ($IGF1R^+$) *(58–60)*. Therefore, CNTs are used as probes for detecting and killing cancer cells by assembling specific anti-oncogene antibodies on CNT surfaces for detecting overexpressed cell surface receptors (HER2). The interaction between CNTs and antibodies is studied mainly using confocal microscopy.

Au: Check to be sure that all genes are set in italics.

Confocal microscopy is a widely used tool for fluorescent imaging of biological objects. Confocal microscopy can constitute the bridge connecting high-resolution analysis and observation of spatially extended areas. Fluorescence provides the possibility to analyze location and expression of many target molecules at the same time. Furthermore, confocal microscopy has the unique feature to optically section a sample into thin slices almost in real time, thereby providing a full three-dimensional view of the sample. Therefore, we have used confocal microscopy to view fluorescently tagged CNTs in a method similar to that of viewing biological materials such as antibodies to accurately analyze and quantify their interaction.

Most applications employing the unique electronic, thermal, optical, and mechanical properties of individual CNTs will require large-scale manipulation of stable suspensions at a high weight fraction. CNT solubilization provides access to

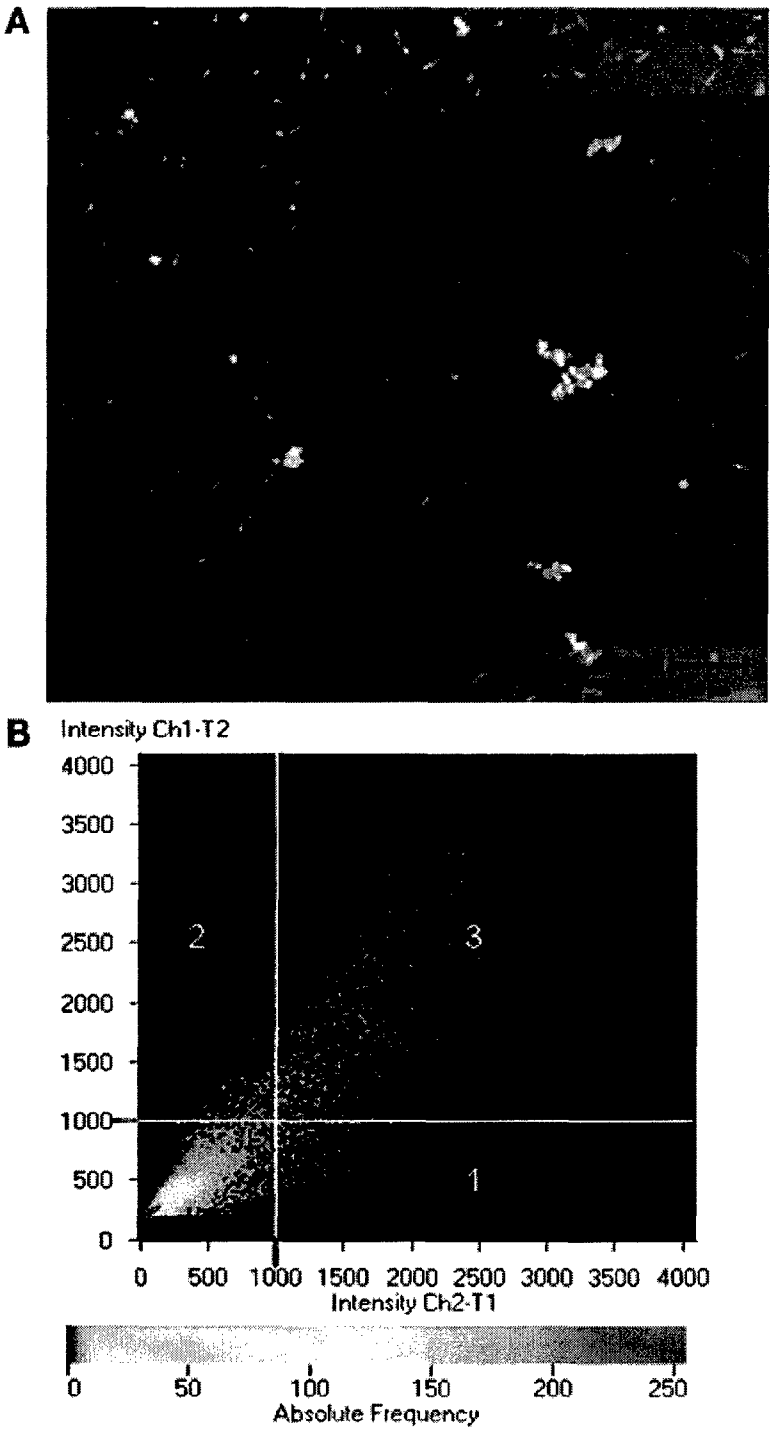

Fig. 5. (A) Confocal microscopy image of a green-dye-labeled CNTs and subsequently coated with the red-dye-conjugated antibodies. The green dye (labeling CNTs) in the inner rectangular region is bleadched to verify the selective attachment of the antibodies to the CNTs (i.e., CNTs appear in red color due to the antibody binding). **(B)** Scattergram to measure the co-localization between antibodies and CNTs via calculation of WCC. Region 1 represents pixels in green channel; region 2 represents pixels in red channel; and region 3 represents co-localizing pixels.

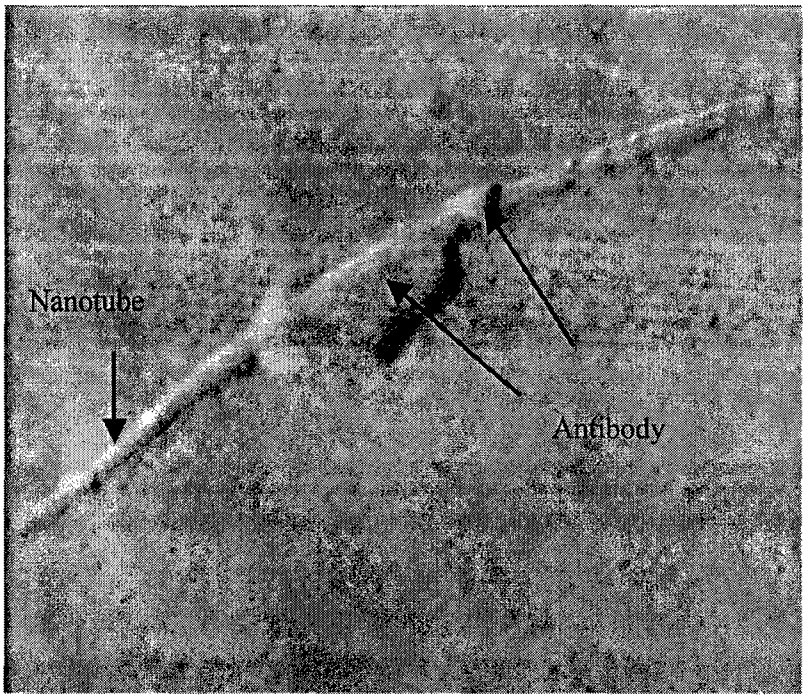

Fig. 6. AFM image of the same sample (Fig. 5a) showing the attachment of the antibodies to a single CNT. The entire scan size is 1.25 x 1.25 μm.

solution-phase separation methodologies, facilitates chemical derivatization and controlled dispersion, which are critical for antibody functionalization.

For controlled dispersion and solubilization, the CNTs were prepared in water with f-NaDDBS, a surfactant that ensured their separation in aqueous environment *(31)*. The entire mixture was gently agitated for 24 h in a sonicator, which resulted in nonspecific adsorption of surfactant on the sidewalls of the carbon nanotube and separation of the nanotube bundles into individual nanotubes. The superior dispersing capability of NaDDBS can be explained in terms of graphite–surfactant interactions, alkyl chain length, head group size, and charge as pertains to the molecules that lie along the surface, parallel to the central tube axis. The separation is due to the π-like stacking of the benzene rings onto the surface of the graphite that causes the surfactant to bind to the surface of the nanotube, which is in good agreement with previously reported literature on CNT solubilization *(31,32)*. Following separation, the CNTs are labeled using a flourophore before antibody functionalization for studying the extent of antibody interaction with nanotubes using confocal microscopy. Thus, the well-separated CNTs were labeled with dihexyloxacarbocyanine iodide ($DiOC_6$), a dye that fluoresces at 488 nm.

Labeling CNTs with conventional flourophores has several advantages for studying the interaction of biological molecules on carbon nanotubes. First, it allows the visualization of smaller CNTs approaching individual CNTs using confocal microscopy without aid from electron microscopic techniques. It does not damage the CNT lattice, thereby preserving the electronic transport properties of the CNTs *(61)*. When antibodies are functionalized on the CNT, the resultant change in the electronic properties of the CNT stems from the antibodies as the flourophores and surfactant do not change the sp^2-bonded graphene sidewall. Furthermore, CNTs coated with flourophores can also be used as contrast agents for high contrast imaging of cells and tissues for biomedical imaging applications. For successful imaging and for higher contrast images, it is essential that the CNTs are well separated and labeled using flourophores. Figure 4 shows the well-separated and labeled CNTs. Fig. 4

Following labeling, the antibody solutions were prepared in phosphate-buffered saline (PBS) (0.138 *M* NaCl, 0.0027 *M* KCl, pH 7.4) by diluting a 2 mg/mL antibody solution with PBS to a ratio of 1:10 (antibody:PBS). Then, the antibody solutions were prelabeled with Alexa 546 (Molecular Probes, Inc.), a dye that fluoresces at 543 nm. The labeled CNT solution and the prelabeled antibody solution were mixed in a microcentrifuge tube and allowed to interact for up to 2 h prior to confocal microscopy analysis. Centrifuging was done to the antibody solution to eliminate unnecessary fluorescence. A slightly different procedure was carried out to view the monoclonal mouse IgG antibodies by confocal microscopy, because the presence of BSA with the antibody interferes the labeling of the antibodies. Therefore, the unlabeled mouse antibody was first tagged with the fluorescently labeled polyclonal goat anti-mouse antibody, which selectively binds to the monoclonal mouse antibody. Then, the

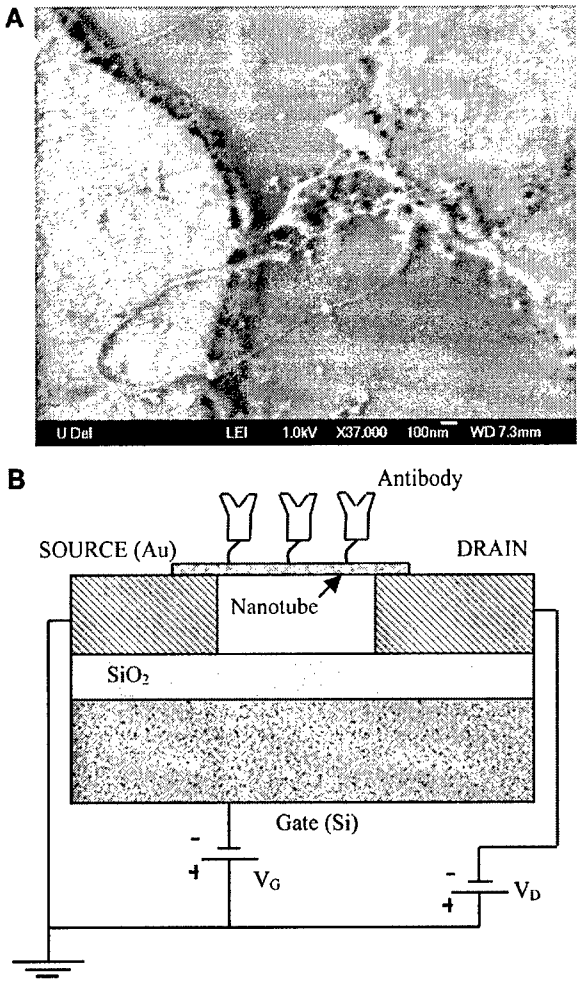

Fig. 7. (A) SEM image of the CNTFET with antibodies on top; **(B)** a schematic of a CNTFET with antibody (Si acts as the back gate).

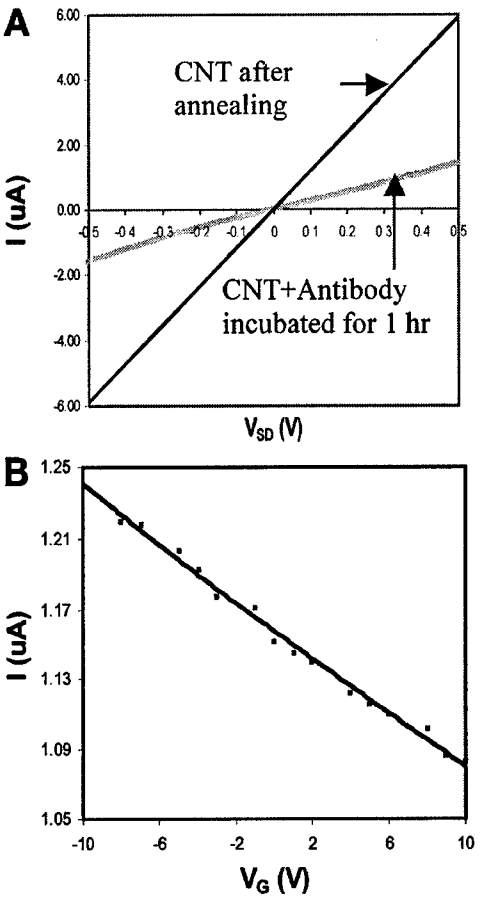

Fig. 8. Change in device characteristic I–V_{SD} at V_G = 0: (A) exposure to antibody for 1 h. The source-drain current was significantly reduced by antibody incubation. **(B)** Change in device characteristic I–V_G at V_{SD} = 100 mV showing gate effect.

monoclonal mouse and polyclonal goat anti-mouse antibody conjugate were introduced to the dye-labeled CNT solution. Besides confocal microscopy, scanning electron microscopy (SEM) and atomic force microscopy (AFM) were used for analysis. Figure 5A is an overlap confocal image of CNTs (green) and antibodies (red). The green dye in the inner rectangular region is bleached out to verify the attachment of the antibodies to the CNTs. In order to measure the degree of binding, weighted co-localization coefficients (WCC) for both the CNTs and antibodies were calculated. WCC can be defined as the ratio of the intensity of co-localized area of a particular channel (color) to the intensity of total area above threshold intensity of that channel (color). It has been demonstrated that the co-localization coefficients can provide quantitative information in dual-color images *(62)*. Figure 5B is a scattergram that provides quantitative information about the image. The WCCs were found to be over 85% for both the CNTs and antibodies. In order to determine the repeatability, six consecutive experiments have been conducted under the same conditions. The calculations yielded a high degree of co-localization with an average WCC of 0.80 for CNTs and 0.87 for antibodies *(63)*. The key to such a high WCC is the separation of CNTs using a surfactant solution. When CNTs are separated using a surfactant, they yield a high surface area that enables attachment of antibodies on the CNT surface, thereby yielding a high WCC. Figure 6 is an AFM image of the same sample from Fig. 5 showing the attachment of the antibodies to a single nanotube. The scan size for the AFM image was 1.25 μm x 1.25 μm.

Fig. 5

Fig. 6

Electronic Sensing of Antibodies using Carbon Nanotube Devices

CNTFET devices have been fabricated on a doped silicon wafer that is coated with silicon dioxide. First, metal electrodes were patterned using microfabrication techniques such as photolithography, metal evaporation, and lift-off. The electrodes consist of 10 nm titanium and 100 nm gold with a spacing of 1–4 μm between source and drain. Following that, the nanotubes

were integrated between the electrodes by an electrophoretic self-assembly technique. This process has been carried out using AC electrophoresis with a frequency of 10 MHz and voltage of
Fig. 7 6 V peak to peak. Figure 7A is an SEM image of the CNTFET device. Following the electrophoretic self-assembly, the devices were dried, and electrical measurements were performed using a probe station attached to a semiconductor parameter analyzer. The silicon substrate was used as back gate. Figure 7B is a schematic of a CNTFET. After the measurements, the devices were annealed at 180°C for 15 min to reduce contact resistance between nanotube and the electrodes. In fact, the resistance of the device dropped from 289 kΩ to 84 kΩ. Following annealing, 2 μL of monoclonal antibody solution prepared in PBS and DI water (3.35 μ*M*) was dropped on the surface of the CNT. The CNT and antibodies were allowed to incubate for 1 h. The sam-
Fig. 8 ple was then thoroughly rinsed with deionized water. Figure 8A compares the output characteristics I–V_{SD} of the same device at zero gate voltage: CNT device after annealing and antibody incubation. Furthermore, the devices exhibited significant gate effect as determined by I–V_G measurements (Fig. 8B). The source-drain current of the devices decreased with increasing gate voltage indicating that the dominant conduction process is due to hole transport. It should be emphasized that a significant loss of source-drain current was observed upon exposure to antibody (see Fig. 8A, the current decreased from 5.94 μA to 1.43 μA). This decrease in current results from the electron-donating property of the NH_2 groups of the antibodies to CNTs similar to the previous reports in literature *(50,64–66)*. The measurements have show that 0.04 electron per adsorbed amine is donated to nanotubes *(64,65)*. Thus, this electron-donating effect will result in a reduction in the number of majority carriers (holes) in semiconducting CNT, thereby reducing the source-drain current. These preliminary studies suggest that CNTFET devices can be utilized for electronic sensing of antibodies that could be used as probes against breast cancer.

Conclusions

Solid progress in interfacing novel nanomaterials, CNTs, with biological materials could enable significant advances in biomedical applications such as disease diagnosis and treatment. Advances in aqueous solubility of CNTs now allow effective research of the CNTs in physiological environments. Furthermore, noncovalent stabilization of CNTs in water is particularly important due to the preservation of inherent properties of the CNTs. The studies on chemical and biological functionalization of CNTs have demonstrated their biocompatibility and specificity. In addition, the findings of improved cell membrane permeability for CNTs have expanded the potential applications of CNTs in biomolecular delivery systems. The bioconjugated CNTs combined with the sensitive CNT-based electronic devices would enable sensitive and specific biosensors toward medical diagnostics.

We have successfully demonstrated antibody functionalization of CNTs. Initially, the CNT bundles were separated to individual nanotubes in aqueous solutions. Following that, the individual CNTs were functionalized with antibodies. In fact, a high degree of binding and co-localization has been observed by confocal microscopy. This suggests that CNTs can be used as probes for detecting cancer cells by assembling specific anti-oncogene antibodies on CNT surfaces for detecting overexpressed cell surface receptors (HER2). Electronic sensing of antibodies specific to cell surface receptors suggests the possibility of detecting overexpressed receptors in cancer cells using nanotechnological interfaces such as CNTs.

The approach of combining bioconjugated CNTs with CMOS and MEMS technology can lead to creation of compact and batch-fabricated arrays of biosensors on a single chip. Microfluidics integration with biosensors can lead to the development of compact active devices that can lead to continuous monitoring of proteins, antibodies, and cells against various tumor markers.

Acknowledgments

The authors wish to acknowledge the help provided by Dr. Kirk Czymek on Confocal Microscopy. Funding for this research was generously provided by Department of Defense: Congressionally Directed Medical Research Program–BCRP Concept Award Number: BC024244.

References

Au: Please supply complete page range where appropriate.

1. Ruoff, R. S. and Lorents, D. C. (1995), *Carbon* **33,** 925–930.
2. Dresselhaus, M. S., Dresselhaus, G., and Eklund, P. C. (1996), *Science of Fullerenes and Carbon Nanotubes*, Academic Press, New York.
3. Ebbesen, T. W. (1997), *Carbon Nanotubes: Preparation and Properties*, CRC Press, Boca Raton, FL.
4. Bockrath, M., Cobden, D. H., McEuen, P. L., et al. (1997), *Science* **275,** 1922–1925.
5. Yakobson, B. I. and Smalley, R. E. (1997), *Am. Scientist* **85,** 324.
6. Ajayan, P. M. (1999), *Chem. Rev.* **99,** 1787.
7. Edelmann, F. T. (1999), *Angew. Chem. Int. Ed.* **38,** 1381.
8. Dai, H., Hafner, J. H., Rinzler, A. G., Colbert, D. T., and Smalley, R. E. (1996), *Nature* **384,** 147.
9. De Heer, W. A., Chatelain, A., and Ugarte, D. (1995), *Science* **270,** 1179.
10. Kong, J., Franklin, N. R., Zhou, et al. (2000), *Science* **287,** 622.
11. Bachtold, A., Hadley, P., Nakanishi, T., and Dekker, C. (2001), *Science* **294,** 1317.
12. Wong, S. S., Joselevich, E., Woolley, A., Cheung, C. L., and Lieber, C. M. (1998), *Nature* **394,** 52.
13. Koshino, A., Yudasaka, M., Zhang, M., and Iijima, S. (2001), *Nano Lett.* **1,** 361.
14. Georgakilas, V., Kordatos, K., Prato, M., Guldi, D. M., Holzinger, M., and Hirsch, A. (2002), *J. Am. Chem.* **124,** 760.
15. Davis, J. J., Green, L. H. M., Hill, H. A. O, et al. (1998), *Inorg. Chem. Acta.* **272,** 261–266.
16. Chen, R. J., Zhang, Y., Wang, D., and Dai, H. (2001), *J. Am. Chem. Soc.* **123,** 3838.
17. Chen, R. J., Bangsaruntip, S., Drouvalakis, K. A., et al. (2003), *Proc. Natl. Acad. Sci. USA* **100,** 4984.
18. Star, A., Gabriel, J. C. P., Bradley, K., and Gruner, G. (2003), *Nano Lett.* **3,** 459.

Job: NANO 1/2 Journal
Chapter: Panchapakesan
Template: 8.5x11/temp/22.05.05

Operator: IBH
Date: 17.09.2005
Revision: 1st Proof

NanoBiotechnology

ISSN 1551-1286/05/01:1–8/$30.00
DOI: 10.1385/Nano:1:2:1

Rapid Communications

Single-Wall Carbon Nanotube Nanobomb Agents for Killing Breast Cancer Cells

Balaji Panchapakesan,[1] Shaoxin Lu,[1] Kousik Sivakumar,[1] Kasif Teker,[1,†] Gregory Cesarone,[2] and Eric Wickstrom[2,3]

[1]Delaware MEMS and Nanotechnology Laboratory, Department of Electrical and Computer Engineering, University of Delaware, Newark DE 19716; [2]Department of Biochemistry and Molecular Biology and [3]Kimmel Cancer Center, Thomas Jefferson University, Philadelphia PA 19107

Abstract

We report the first application of single-wall carbon nanotubes (SWCNT) as potent therapeutic nanobomb agents for killing breast cancer cells. We show here that by adsorbing water molecules in SWCNT sheets or loosely adsorbed on top of cells, potent nanobombs were created that heated the water molecules inside them to more than 100°C upon exposure to laser light of 800 nm at light intensities of approx 50–200 mW/cm^2. Conversion of optical into thermal energy, and the subsequent confinement of thermal energy in nanotubes, caused the water molecules to evaporate and develop extreme pressures in nanotubes causing them to explode in solutions. Co-localized nanobombs killed human BT474 breast cancer cells in physiological phosphate-buffered saline (PBS) solution. Cells that were treated with nanobombs exploded into fragments, while the surrounding cells not treated with nanobombs were viable. Nanotube-based nanobomb agents can potentially outperform most nanotechnological approaches in killing cancer cells with out toxicity.

(Nanobiotechnology DOI: 10.1385/Nano:1:2:1)

Key Words: Nanobomb; single-wall carbon nanotube; heat dissipation; therapeutics; cancer nanotechnology; photothermal cell killing.

Correspondence and reprint requests to:
Balaji Panchapakesan,
Delaware MEMS
and Nanotechnology Laboratory,
Department of Electrical
and Computer Engineering,
University of Delaware,
Newark DE 19716
E-mail: baloo@ece.udel.edu

†Current address:
Department of Physics
& Engineering, Frostburg State
University, Frostburg, MD 21532

Humana Press

Introduction

Although there has been outstanding advances in fundamental cancer biology, these have not translated into comparable advances in the clinic. Inadequacies in the ability to administer therapeutic agents with high selectivity and with minimum collateral damage have largely accounted for the discrepancies in cancer therapeutics. Furthermore, it is most striking to recognize that only 1 and 10 parts per 100,000 of intravenously injected monoclonal antibodies reach their targets in vivo *(1)*. Therefore, new therapeutic technologies that can potentially reach their targets with maximum selectivity and minimum collateral damage needs to be explored. Nanotechnology, owing to its small size and unique physical properties, has generated interest in the area of cancer nanotechnology.

Today, cancer-related nanotechnology research is progressing on two main fronts: laboratory-based diagnostics and in vivo diagnostics and therapeutics. Nanoscale devices, such as nanowire grids, that are designed in the laboratory use sophisticated lithographic techniques to fabricate the grids *(2–4)*. Following fabrication, the silicon nanowires are coated with monoclonal antibodies directed against various tumor markers. With minimal sample preparation, substrate binding to even a small number of antibodies produces a 100-fold increase in detection sensitivity over current solution-phase diagnostic techniques. Meanwhile,

nano-cantilevers have been coated with molecules capable of binding specific substrates–DNA complementary to a specific gene sequence and can detect a single molecule of DNA or protein due to the change in the surface stresses that bend the nano-cantilever, which is detected using optical techniques *(5)*. Recently, DNA-labeled magnetic nanobeads have been used to detect DNA and proteins that may serve as diagnostic or prognostic indicators of cancer *(6)*. Much interest in using nanoparticles for cancer detection arose with the use of semiconductor nanocrystals or quantum dots of cadmium selenide as a tool for laboratory diagnostics of cancer. These quantum dots change their optical properties with their size. When linked to an antibody or a molecule capable of binding to a substance of interest, quantum dots act like beacons that light up when binding occurs *(7)*. These have the potential for creating assays capable of detecting multiple substances simultaneously, such as Her2, actin, microfibril protein, and nuclear antigens *(8,9)*. On an unconventional front, researchers have used empty RNA virus capsules from cowpea mosaic virus and flockhouse virus as potential contrast agents for magnetic resonance imaging (MRI) by attaching homing molecules such as monoclonal antibodies or cancer cell–specific receptor antagonists, and reporter molecules. Therapeutic agents loaded inside the capsule can also serve as drug-delivery vehicles *(10,11)*. Recently, silica-coated lipid micelles contain luteinizing hormone–releasing hormone (LH-RH) as a targeting agent have been used to deliver iron oxide nanoparticles to LH-RH receptor positive cancer cells. Once the iron oxide nanoparticles are delivered, oscillating magnetic fields are applied to heat the nanoparticles to kill the cancer cells *(12)*. Studies on nanoshell, and more recently nanotube, technology to kill cancer cells by using infrared radiation and imaging has proved to be a successful approach for cancer cell killing in vivo and has increased the interest in nanotechnology to kill cancer cells *(13–15)*. In both these technologies lasers with very high power (35 W/cm^2 for nanoshell and 1–4 W/cm^2 for nanotubes) were used to heat the nanoshell and nanotubes to 55–70°C. However, we have taken the level of temperature increase in nanotubes to an extraordinary level to create nanobombs that explode at low laser intensities. By exploding nanotubes that are co-localized with cancer cells, one can selectively destroy the nanotubes as well as the cancer cells. This approach may be the only way of using nanotubes for therapeutics without causing any toxicity problems. Nanobombs are created due to the thermal-energy confinement in nanotube bundles and subsequent vaporization of liquids between nanotubes in bundles creating pressures that cause the eventual explosion. This phenomenon works in a host of different liquids such as alcohol, deionized (DI) water, and phosphate-buffered saline solutions.

Au: word change ok?

In this report we show that by hydrating nanotubes in sheets as well as by co-localizing them to cells, potent nanobombs can be created to explode cancer cells completely. This process is highly localized with minimum collateral damage to neighboring cells. Nanobombs are created due to the optical–thermal transitions in nanotubes. Hydrating nanotubes and exposure to light causes the thermal energy to heat the water molecules, which in turn creates pressure inside the nanotube bundles that causes them to explode. When co-localized with cells, they completely destroy the cells causing 100% cell destruction. This method is simple, robust, and highly effective in killing cancer cells. Furthermore, this technique, which uses low laser power compared to competing techniques, can produce larger explosions that may ensure complete destruction of cancer cells. Recent reports have shown that nanotubes could be highly toxic for in vivo applications *(16)*. Our method using nanobombs may indeed overcome the toxicity problems as the nanotubes are completely destroyed due to the explosions.

Methods and Experiments

Single-wall carbon nanotubes (SWCNT) are first grown in-house using methane-based thermochemical vapor deposition technique at 900°C and atmospheric pressures using iron and nickel as catalyst metals. The growth is set in the reaction rate–limited regime with high temperatures facilitating high kinetic energy of the gas molecules and with low supply of carbon, allowing the formation of single-wall carbon nanotubes. The grown nanotubes are purified by first heating in dry air at 400°C to remove the soot and an acid reflux (3 *M* HCl for 10 h) to remove the catalyst particles. Following fabrication, SWCNT were dispersed in deionized water and a sheet was created by vacuum filtration. The SWCNT sheets were made by vacuum filtration of 20 mL of a 0.6-mg/mL SWCNT suspension through a poly(tetrafluoroethylene) filter (Millipore LS, 47 mm in diameter, 5-μm pores). The SWCNT sheet was washed with 200 mL of deionized water and then 100 mL of methanol to remove residual NaOH and surfactant, respectively. The sheets were allowed to dry under continued vacuum purge for 1 h before being peeled from the filter. The typical SWCNT sheet was fabricated into circular discs about 100 mm in diameter and about 50 μm thick.

Two 1-mm wells, 1 mm apart, were created on the SWCNT sheet as sites to deposit 1.0 μL aliquots of approx 1×10^5 BT474 breast cancer cells freshly resuspended in PBS after release from culture dishes. Clusters of BT474 cells on the bottoms of the wells were stained with Trypan blue dye to investigate membrane permeability and cell damage before and after light exposure. Second, the BT474 cells in one well were illuminated with 800 nm laser light at 200 mW/cm^2 for 60 s. Finally, 0.1 μg of nanotubes were dispersed in PBS solution and agitated for 24 h until all the nanotubes were dispersed. The nanotubes in PBS do not precipitate even after 24 h and are quite stable. The resulting suspension consisting of nanotubes were directly adsorbed onto the center of a larger cell cluster that was treated with the Trypan blue dye and light was irradiated directly to see the effectiveness of the localized cell killing.

Job: NANO 1/2 Journal
Chapter: Panchapakesan
Template: 8.5x11/acmp/22.05.05

Operator: BSH
Date: 17.09.2005
Revision: 1st Proof

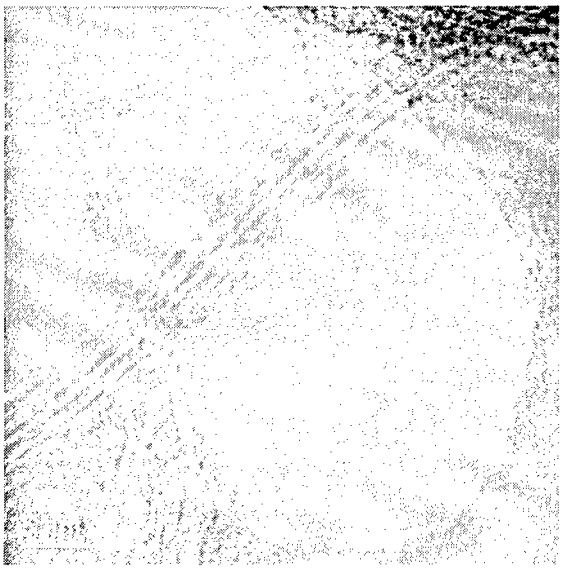

Fig. 1. TEM image of single-wall carbon nanotube. The nanotubes are about 1.5 nm in diameter.

Results and Discussion

Fig. 1. Figure 1 shows the transmission electron micrograph of single-wall carbon nanotubes grown using the procedure described above. The nanotubes grown are about 1.5–4 nm in diameter. Figure 2A shows the macroscopic sheet of SWCNT that was fabricated using vacuum filtration technique. Figure 2B shows the scanning electron micrograph of the sheet consisting of highly entangled nanotubes. We created sheets to make arrays of immobilized cells that were treated with nanotubes to clearly demonstrate the explosion effect. We found the nanotube sheets that were highly entangled in DI water and in PBS can explode on exposure to near infrared light. Figures 3A–D show the explosions of nanotube sheets in DI water on exposure to 200 mW/cm^2 of laser light. These dramatic explosions are caused by the optothermal transitions in nanotubes, which heat to more than 100°C the water molecules that are present in the nanopores between bundles, creating explosions. From Fig. 3B, it can be conjectured that the temperatures must have been in excess of 700°C in order to create such explosions, in agreement with a previous report *(17)*.

Fig. 2.

Fig. 3.

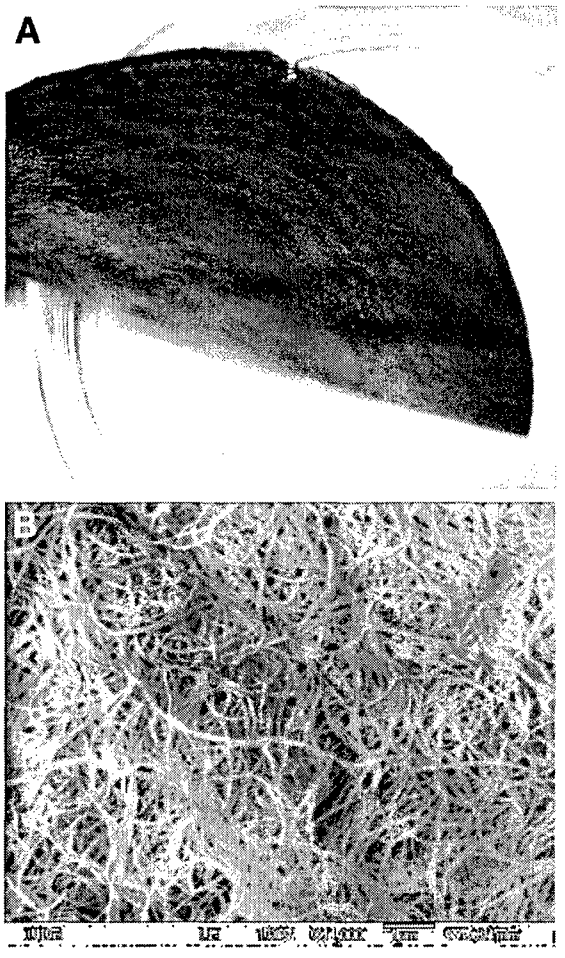

Fig. 2. (A) SWNT sheets fabricated using vacuum filtration; **(B)** SEM image of nanotube sheet showing highly entangled nanotubes.

Au: Please check image scale for clarity.

Explosions in air of loosely packed nanotubes have been observed previously *(17)*. However, such explosions were ascribed to the thermal energy confinement in loosely packed nanotubes and the burning due to adsorption of oxygen causing ignition. It was noted that when nanotubes were compacted, the thermal energy was dissipated rapidly to the surroundings, which made the explosions occur only at high laser energy. We have found that nanotubes could explode even in the compacted form as sheets and bundles at laser intensities of 50–200 mW/cm^2. We postulate that this phenomenon arises both from high heat confinement inside the tubes, and from high heat confinement between the tubes when the nanotubes are compacted together. The high optical absorbance in SWCNTs originates between the first and second van Hove singularities in nanotubes *(18,19)*. Heat is also generated in nanotubes due to the electron–phonon coupling causing molecular vibrations. While such thermal vibrations can be dissipated easily in single nanotubes without explosions at low laser intensities, when nanotubes are in sheets or bundles, the thermal energy is confined between the tubes creating explosions of this nature at low laser intensity in distilled water. Although nanotubes have excellent thermal conductivity, when nanotubes are in bundles, the dissipation of thermal energy to the surrounding water molecules is not fast enough compared to the heating process itself. Although the thermal conductivity of nanotubes along the tube axis is high *(20–23)*, the thermal conductivity in sheets is almost an order of magnitude smaller *(24)*. This creates an imbalance in thermal energy dissipation to the surroundings and heat confinement between the tubes. This can create localized hot spots where the water molecules that are just adsorbed onto

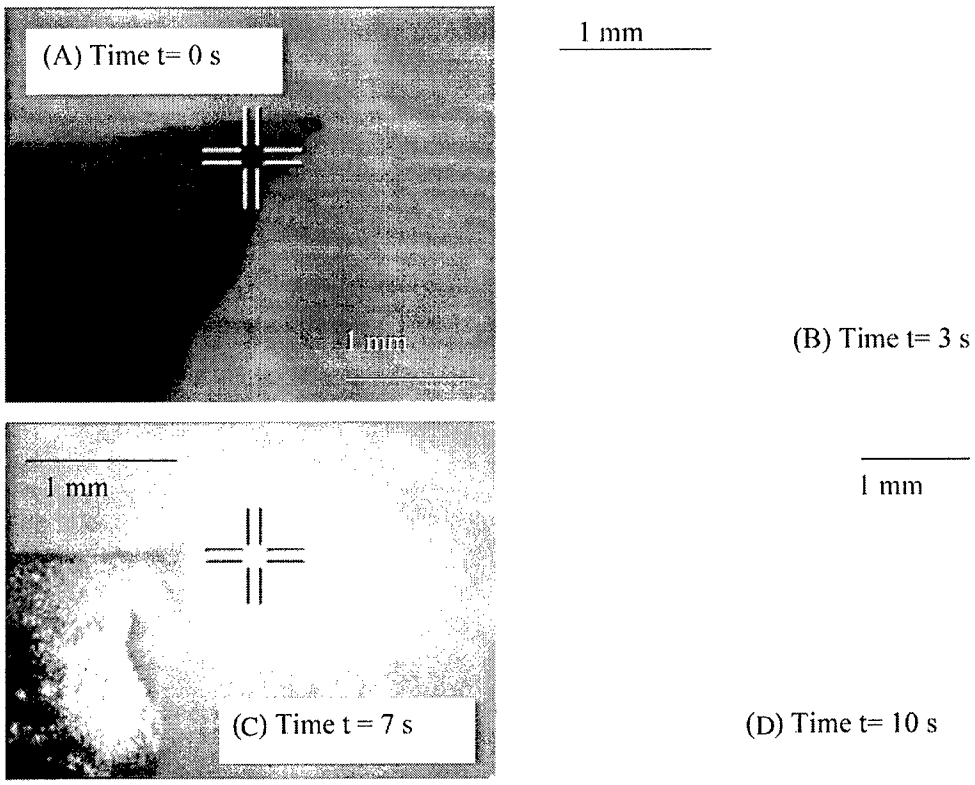

Au: Please provide images for B and D.

Fig. 3. Series of dramatic explosions in single-wall carbon nanotubes. **(A)** Nanotubes before light exposure, **(B)**, **(C)** and **(D)** nanotube explosions at t = 3, 7, and 10 s. The entire series of explosions were completed in 12 s.

the surface of the nanotubes are vaporized. These vaporized water molecules have no place to escape, as they are tightly confined between the bundles. This in turn starts building up intense pressures between the bundles causing the nanotubes to explode, thus creating nanobombs. Explosions occur only when the pressure is high enough, and not all the nanotubes explode simultaneously in the presence of light. This is depicted in Fig. 2B, which shows a moment when parts of an area are exploding while some of the nanotube bundles remain unexploded. This imbalance in the thermal-energy generation and dissipation in nanotube bundles causes such explosions. Heating single nanotubes requires much more laser energy because the heat is dissipated rapidly to the surroundings. Asserting that local energy imbalance induces explosions is a simple model, but such imbalances and gradients in nanoscale materials can be extremely high.

We also found that the explosions were more dramatic in phosphate-buffered saline, which we utilized to kill cells dramatically. This may be due to the presence sodium in saline solutions and to the strongly ionic nature of the solution, providing electrons to the nanotube and creating a localized electrostatic effect that may have caused the explosions to be more powerful than in distilled water. The nanotubes that we have used consist of both metallic and semiconducting nanotubes mixed together. When we irradiate light on a metal–semiconductor junction, charge separation and accumulation can occur leaving an excess amount of charges creating localized electrostatic effects that can also trigger explosions. Furthermore, nanotubes can act as nanoelectrodes in electrolytic solutions, and metallic ions in electrolytes reduce themselves on the surface of the nanotubes. This type of nanotube may also be attracting ionic sodium from the PBS to reduce to metallic sodium, which then explodes when excited with light in the presence of water.

Figure 4A shows the nanotube sheet with cells placed on top of the wells before light exposure. The cells in the bottom well were treated with nanotubes dispersed in PBS, while the cells in the top well were just treated with PBS solution to serve as controls. Figure 4B shows the same image in Fig. 4A after exposure to 200 mW/cm^2 of 800 nm laser light. As one can see, the appearance of Fig. 4B is dramatic compared to Fig. 4A. The cells in the bottom well were blown to pieces and the cells appeared charred. The cells were also seen to be dislodged from the cluster showing that the explosions were indeed dramatic. The pattern of dead cells looks like the explosions started from the center of the cell clusters and moved all the mass to the surrounding areas, including the bubbles. Bubbles can be seen around the dead cells, which we ascribe to the violent boiling effect of the PBS solution permeating the nanotubes. No bubbles were seen around the cells that were not treated with nanotubes but were exposed to light. These results imply that the localized temperature

Fig. 4.

Job: NANO 1/2 Journal
Chapter: Panchapakesan
Template: 8.5x11/temp/22.05.05

Operator: IBH
Date: 17.09.2005
Revision: 1st Proof

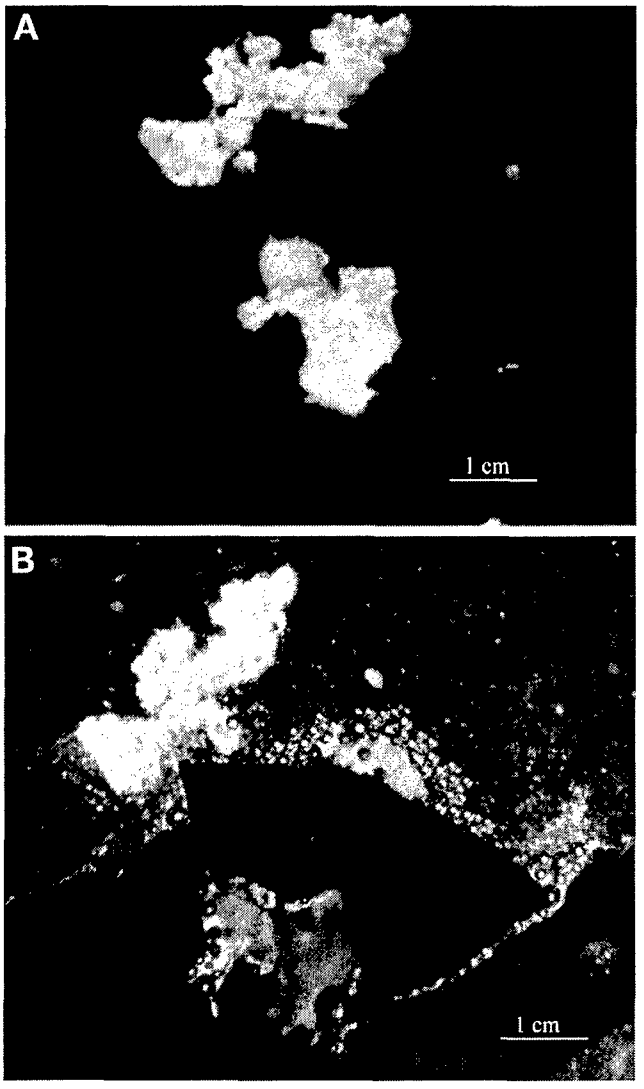

Fig. 4. (A) BT474 breast cancer cells placed inside two etched holes on nanotube sheet before light exposure; **(B)** after exposure to 200 mW/cm^2 of light intensity. The cells in the well of the nanotube sheet that received light were ablated.

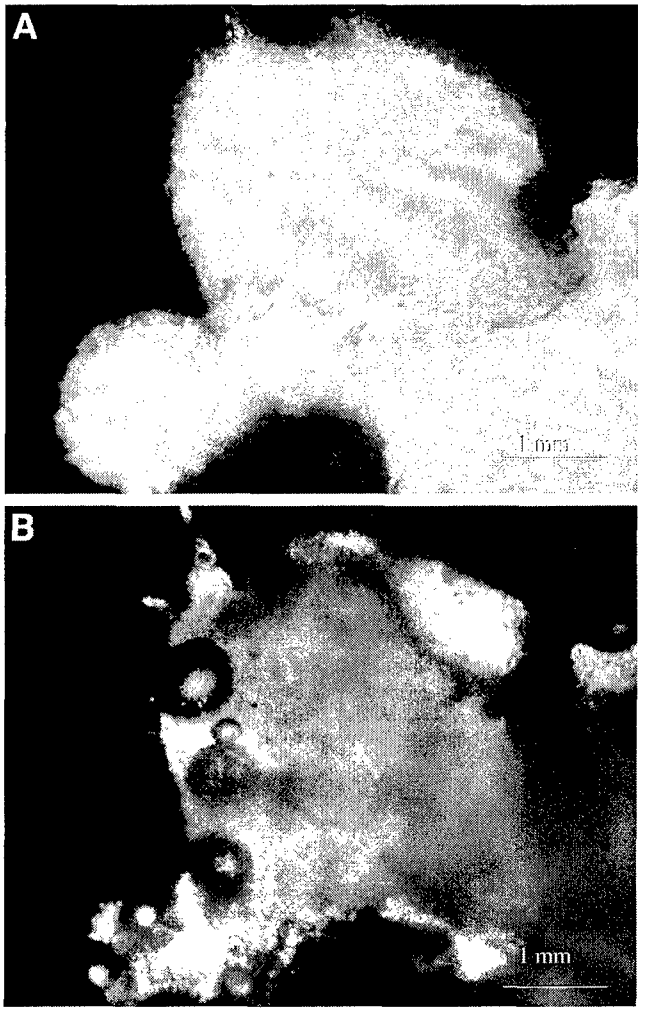

Fig. 5. (A) High magnification image of BT474 cell cluster treated with nanotube and Trypan blue dye before light exposure; **(B)** on exposure to 200 mW/cm^2 of light intensity. Note that there are bubbles on the cell cluster indicating the boiling of PBS due to nanotube heat emission.

when nanotubes explode in PBS solution should be in excess of the boiling point of PBS. Figure 5A is the high magnification optical image of cell clusters that were initially treated with nanotubes. Upon light exposure, the cells were completely destroyed as shown in Fig. 5B and one can see the bubbles showing the localized boiling effect of PBS around the cells. In Figs. 5A,B, it can be seen that the background looks the same and any dramatic explosive and boiling effects only occurred within the cell clusters. This shows that the explosive effects were highly localized for killing cancer cells.

Fig. 5.

To control the explosions and create selective cell killing effects, cluster of cells were placed in a dish and nanotube in PBS solution was dropped onto the center of a large cell cluster. Upon shining 50 mW/cm^2 of 800 nm light, the cells started to turn blue, showing the cell membrane was permeated by the Trypan blue dye. Figure 6A shows the viable cells before light exposure and Fig. 6B shows the same area after light exposure. Note that the center regions, which were treated with nanotubes, turned blue upon shining light. This result clearly shows the selective nature of this technology for killing cancer cells. While the selective cell killing was shown by directly integrating nanotubes in parts of cell clusters, nanotubes could be potentially coated with different types of biomolecules for targeted delivery of nanotubes to cancer cell clusters. Furthermore, magnetic guiding and minimally invasive laproscopic techniques could extend the applications of nanobomb agents to selectively kill cancer cells in vivo.

Fig. 6.

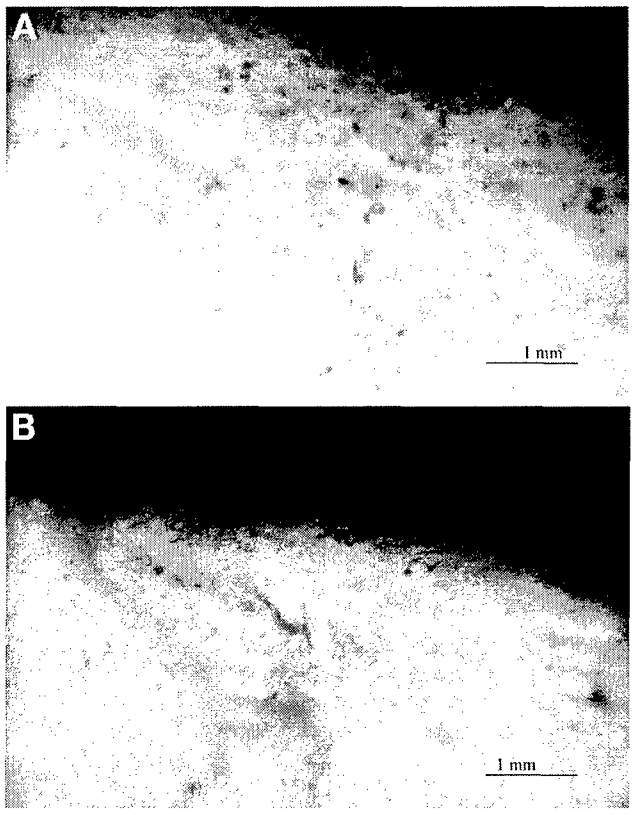

Fig. 6. (A) BT474 cells that were treated with nanotubes in PBS suspension before light exposure; **(B)** after light exposure to 50 mW/cm^2. Note that the center part that turned blue is the site that was exposed to light, while the surrounding cells appear normal. This illustrates the precision of cancer cell killing in the central region by this approach.

Conclusions

We have demonstrated the applicability of SWCNTs as potent nanobomb agents to kill cancer cells. Nanotubes were fabricated using a methane-based chemical-vapor-deposition process. Following nanotube fabrication, sheets of SWCNTs were fabricated. Two wells were etched and clusters of BT474 breast cancer cells were placed in these wells to immobilize the cells. One of the cell clusters were treated with a suspension of nanotube in PBS solution, while the other cluster received only the PBS solution. When near infrared light about 800 nm and 200 mW/cm^2 was incident on the samples, dramatic explosions from the nanotubes caused the cells to explode, killing all the cells in less than 60 s. The presence of bubbles around the dead cells indicated the boiling effect that happened due to nanotube explosions. The nanobombs were created as a result of heat confinement in bundles of nanotubes and the presence of adsorbed water molecules that heat rapidly causing extreme pressures in between the bundles of nanotubes causing explosions. These explosions are controllable by changing the intensity of light and for light at lower intensity, the explosions were less dramatic. These initial results indicate that potent nanobombs can be created using nanotubes at low light intensities that may be more acceptable for clinical applications than previously reported nanotube- and nanoshell-based cell killing vehicles that use high light intensities. Furthermore, our nanobomb cell killing technique can potentially overcome toxicity problems that are associated with nanotubes, as we completely destroy the nanotubes. Although these preliminary results show the feasibility of this concept, much work is necessary to understand this phenomenon. The first application of this technology may be to be used in a laproscope that could kill cancer cells with minimum invasiveness. Nanobombs could be developed as a generic tool for targeting and killing different types of cancer cells. Nanobombs treated with radiological nanoparticles and anticancer monoclonal antibodies could not only destroy the cancer cells, but also severe the biological cell signaling pathways, thereby improving therapeutic efficacies in a localized environment. Furthermore, nanotube-based nanosurgical or microsurgical tools can be integrated with traditional surgical tools to kill microscopic cancer foci that are often left behind in surgery. Finally, nanotube-based tools reported here can be used to kill developing cancer cells in parts of the body that are considered inaccessible to traditional surgery.

Acknowledgments

The authors wish to acknowledge the funding for this research provided by the Department of Defense, Office of the Congressionally Directed Medical Research Program, DAMD:170310701, to B. Panchapakesan, and the Department of Energy, Office of Biological Research, ER63055, to E. Wickstrom.

References

1. Ferrari, M. (2005), *Nat. Rev. Cancer* **5,** 161–171.
2. Schmittel, M., Kalsani, V., Fenske, D., and Wiegrefe, A. (2004), *Chem. Communi.* **5,** 490–491.
3. Yan, H., Finkelstein, G., Reif, J. H., and LaBean, T. H. (2003), *Science* **301,** 1882–1884.
4. Spillmen, H., Dmitriev, A., Lin, N., Messina, P., Barth, J. V., and Kern, K. (2003), *J. Amer. Chem. Soci.* **125,** 10,725–10,728.
5. L. R. and Allain, T. V.-D. (2002), *Anal. Chim. Acta* **469,** 149–154.
6. Lizard, G., Duvillard, L., Wedemeyer, N., et al. (2003), *Pathol. Biol.* **51,** 418–427.
7. Dubertret, S. B., Norris, D. J., Noireaux, V., Brivanlou, A. H., and Libchaber, A. (2002), *Science* **298,** 1759–1762.
8. Mansson, S. A., Balaz, M., Bunk, R., et al. (2004), *Biochem. Biophys. Res. Communi.* **314,** 529–534.
9. Wu, X., Liu, J., Haley, K. N., et al. (2003), *Nat. Biotechnol.* **21,** 41–46.
10. Heverhagen, J. T., Fahr, A., Muller, R., and Alfke, H. (2004), *Magne. Reson. Imaging* **22,** 483–487.
11. Toyoda, K., Tooyema, I., Kato, M., et al. (2004), *Neuroreport* **15,** 589–593.
12. Roy, I., Pudavar, H. E., Bergey, E. J., et al. (2003), *J. Ameri. Chem. Soci.* **125,** 7860–7865.

Au: Please spellout authors names.

13. Hirsch, L., Stafford, R. J., Bankson, J. A., et al. (2003), *Proc. Natl. Acad. Sci. USA* **100,** 12,549–12,554.
14. Loo, C., Lin, A., Hirsch, L., et al. (2004), *Technolo. Cancer Res. Treat.* **3,** 33–40.
15. Kam, N. W. S., O'Connell, M., Wisdom, J. A., and Dai, H. (2005), *Proc. Natl. Acad. Sci. USA* **102,** 11,600–11,605.
16. Lam, C. W., James, J. T., McCluskey, R., and Hunter, R. L. (2004), *Toxicol. Sci.* **77,** 126–134.
17. Ajayan, P., Terrones, M., de la Gaurdia, A., et al. (2002), *Science* **296,** 705.
18. O'Connell, M. J., Bachilo, S. M., Huffman, C. B. (2002), *Science* **297,** 593–596.
19. Bachilo, S. M., Strano, M. S., Kittrell, C., Hauge, R. H., Smalley, R. E., and Weisr, R. B. (2002), *Science* **298,** 2361–2366.
20. Rao, A. M., Eklund, P. C., Bandow, S., Thess, A., and Smalley, R. E. (1997), *Nature* **388,** 257–259.
21. Berber, S., Kwon, Y. K., and Tomanek, D. (2000), *Phys. Rev. Lett.* **84,** 4613.
22. Kim, P., Shi, L., Majumdar, A., and McEuen, P. L. *Phys. Rev. Lett.* **87,** 215502.
23. Osman M. A. and Srivatsava, D. (2001), *Nanotechnology*, **12,** 21.
24. Hone, J., Whitney, M., Piskoti, C., and Zettl, A. (1999), *Phys. Rev. B*, **59,** R2514.

Circulating cancer cells often express characteristic cell surface markers, which provide an opportunity for early diagnosis of disease. Effective early detection of precancerous and neoplastic lesions remains an elusive goal today. Clinical cancer imaging technologies do not possess sufficient spatial resolution for early detection based on the molecular signatures of proteins that are overexpressed in cancer cells. Serum markers for the early detection of most cancers are still not available (*1*). Most of the markers that are in clinical use, such as prostate specific antigen (PSA) and carcinoembryonic antigen (CEA), are not very specific, with widely different baseline expressions in the population, and are of limited effectiveness for early detection (*1*). While sensing of oncogene expression from outside the body (*2*) could precisely direct clinicians to appropriate molecular intervention at the onset of disease, such radioimaging is only appropriate for high-risk subjects. Therefore, development of new technologies for reliable early detection of cancer from biological fluids through minimally invasive or non-invasive procedures are a high priority.

Monoclonal antibodies (mAb) specific to cell surface antigens overexpressed on cancer cells can be adsorbed to single wall carbon nanotube (SWCNT) devices, resulting in a slight drop in conductance (*3-5*). Both non-covalent and covalent functionalization of SWCNT with biological molecules such as proteins, antibodies, and peptides produces changes in the surface electronic properties of SWCNT devices (*3-5*). Knowing the change in electronic properties of SWCNT devices upon mAb adsorption, we hypothesized that interaction of adsorbed mAb with breast cancer cell surface targets would produce a further change in the electrical conductance of the SWCNT devices, proportional to the number of adsorbed mAb per cell, dependent upon the density of those surface antigens on breast cancer cells. The interconnected SWCNT that we grow are primarily semiconducting in nature, with positively charged holes carrying the current (p-type behavior) (*5*).

Human BT474 breast cancer cells exhibit negligible expression of estrogen receptor-α, moderate expression of IGF1R, and high expression of human endothelial receptor 2 (Her2) (*6*).

Conversely, human MCF7 breast cancer cells exhibit significant expression of estrogen receptor-α, high expression of IGF1R, and low expression of Her2 (*7*), confirmed by QRT-PCR (*2*). The control R- cells are nontumorigenic, nonmalignant, immortalized mouse embryonic fibroblast cells derived from mice with a targeted disruption of the *IGF1R* gene (*8*).

We tested our hypothesis for the interaction of breast cancer cells with mAb-SWCNT devices in five steps: 1) non-covalent functionalization of SWCNT, 2) fabrication of nanodevices with SWCNT patterned between the source and drain electrodes, 3) measurement of electrical conductance of the SWCNT as they were patterned and SWCNT coated with mAb specific to IGF1R, 4) control experiments to determine charge transfer between adsorbed mAbs and BT474 or MCF7 cells, 5) measurement of electrical conductance of the devices during cellular interactions with non-specific mAbs and specific mAb.

Carbon nanotubes (CNTs) are remarkable synthetic materials with many fascinating properties, such as high mechanical strength, high surface area, unique electronic and chemical properties, and thermal stability (*9-14*). CNTs are nanometer-diameter cylinders consisting of single or multiple graphene sheets wrapped up to form a single-wall (SWCNT) or multi-wall (MWCNT) carbon nanotube, respectively. Since the discovery of carbon nanotubes, investigators have been exploring their applications as building blocks for nanodevices such as probes (*15*), electron-field emission sources (*16*), chemical sensors (*17*), and transistors (*18*). Furthermore, novel biological devices have been fabricated by integrating nanotubes with organic molecules (*19-21*). These devices will enable new research fields and applications such as *in situ* modification of living cells or their physiological activities. For example, covalently functionalized carbon nanotube probes have been found to perform well as solid phase ligands for scanning probe microscopy mapping of biofunctional receptors (*18*).

Development of carbon nanotube-based nanoscale biosensors has been intensified by the successful immobilization of biological macromolecules, such as proteins and enzymes, either in the interior cavity or on the surface of nanotubes without any drastic conformational or bioactivity change (*22, 23*). Recent advances in the fabrication of nanotube-based devices, such as field effect transistors (CNTFETs), have increased the expectations for the utilization of carbon nanotubes as superior biosensor materials (*24, 25*). These CNTFETs have shown appreciable changes in electrical conductance, suggesting the possibility of using them for electronic biosensing applications. Meanwhile, recent advances in aqueous solubility of carbon nanotubes have accelerated biocompatibility evaluations toward biomedical applications, including the potential usage of carbon nanotubes as carriers in drug or gene delivery systems. Furthermore, conjugation of carbon nanotubes with biomolecules such as proteins, carbohydrates, and nucleic acids are likely to facilitate bio-applications of carbon nanotubes.

Non-covalent functionalization allows preservation of the carbon sp^2 character and structure, which is essential for retaining the electrical properties of the nanotubes (*4, 24, 26*). Furthermore, non-covalent functionalization benefits from the simplicity of the steps involved, preservation of bioactivity of the molecules, non-interference with the sensor properties by host molecules used for tagging in covalent functionalization schemes, and tailorable surface properties of the SWCNT. Previously we investigated non-covalent functionalization of SWCNT with mAb using confocal and atomic force microscopy (*5*). SWCNT were first separated using a surfactant, sodium dodecyl benzene sulfonate (NADDBS) and labeled using $DiOC_6$, a dye that fluoresces at 488 nm. We found that combining NADDBS surfactant with $DiOC_6$ produced excellent separation as well as labeling SWCNT that could potentially be used for high contrast imaging applications. The excellent separation and labeling revealed SWCNT as small as 15 nm in diameter, much smaller than most biological entities that are visualized using confocal techniques. Furthermore, the labeling allowed

us to image the SWCNT inside CHO cells using streptavidin-biotin-SWCNT conjugates that showed the effectiveness of the SWCNT conjugate for penetrating cell membranes and also visualization of SWCNT using fluorescence microscopy. Following labeling, the SWCNT were exposed to monoclonal as well as polyclonal antibodies that were fluorescently labeled and interacted with the SWCNT using micro-centrifugation. Both confocal and atomic force microscopy (AFM) revealed that more than 85% of the surfaces of the SWCNT were functionalized with mAbs. It was also found that separation of the SWCNT using sonication introduced defects that acted as sites for cross-linking mAbs directly to the surface of the SWCNT using covalent functionalization (*5*). Hence a high degree of functionalization was observed due to the combination of non-covalent binding through surface forces, and covalent binding due to defective sites in the SWCNT. Defects in SWCNT allow covalent cross-linking directly without the need for any tagging or host molecules that often interfere with the bioactivity in covalent functionalization schemes.

To study the binding of breast cancer cells, SWCNT were grown using methane-based chemical vapor deposition using iron nanoparticles as catalyst materials. The grown SWCNT consisted of interconnected bundles of SWCNT. For controlled dispersion and solubilization, the SWCNT were prepared in water with sodium dodecylbenzene sulfonate (NaDDBS), a surfactant that ensured their separation in an aqueous environment (*27, 28*). The entire mixture was gently agitated for 24 hr in a sonicator (Fisher Scientific Ultrasonic Cleaner, 60 Hz frequency, FS60H) that resulted in nonspecific adsorption of surfactant on the sidewalls of the SWCNT and separation of the SWCNT bundles into individual SWCNT. Following SWCNT dispersion, devices were prepared using lithography, titanium/gold deposition, and lift-off (*4*).

Non-specific mouse myeloma IgG1 (EMD Biosciences) and specific anti-IGF1 receptor mouse mAb Ab-3 (33255.111, EMD Biosciences) were prepared in 0.138 M NaCl, 0.0027 M KCl, pH 7.0 (phosphate buffered saline, PBS) by diluting a 1 mg/mL mAb solution with PBS to a ratio of

1:10 (mAb:PBS). Following mAb dilution, 1 μL of the SWCNT dispersed in deionized water was mixed with 1 μL of the mAb solution and the mixture was allowed to interact for 1 hr at room temperature in a 4 μL microcentrifuge tube. Confocal microscopy and atomic force microscopy (AFM) were used to image and ascertain the non-specific adsorption of mAbs onto SWCNT surfaces. Following AFM imaging, SWCNT devices were prepared by placing 4 μL of the mAb-SWCNT conjugates onto the patterned regions between the electrodes. The devices were then annealed at 180°C for 15 min to reduce the contact resistance of the SWCNT from 300 kΩ to 80 kΩ. The resistance of the device was monitored using a semiconductor parameter analyzer (HP 4516) that is capable of measuring femto-amps (fA) of current with high accuracy with limits of 5 fA.

Fig. 1 shows the schematic of the SWCNT device that we prepared using photolithography, metal deposition, and lift-off. The source and drain electrodes were patterned as pads, and the interconnected SWCNT coated with mAb were patterned in the regions between the electrodes. Fig. 2a is the optical micrograph of the device that was prepared as described above. Fig. 2b is the AFM scan of the region that was patterned with SWCNT conjugated with mAb. First the SWCNT were patterned in the regions, followed by adsorption of mAb. The conductance was measured continuously during mAb adsorption, and then during cell adsorption to the devices. The device was biased at 5 mV to minimize charge injection effects and also to minimize current due to ionic conduction. Keeping the bias voltage low also enhances the actual signal transduction between the mAb and cells and the actual surface electronic charge transfer process is visualized in the results.

Electronic sensing of bound mAb and breast cancer cells was carried out by monitoring the electrical current through the SWCNT device under a 5 mV bias during mAb and breast cancer cell additions to a 4 μL drop of PBS on the surface of the device. Low bias was used to minimize charge injection into the device and to monitor the actual surface electronic events that happen between the

mAbs and the breast cancer cells on the device. Under these low bias conditions control experiments revealed no ionic currents (Fig. 3). To measure breast cancer cell binding, we applied 1 μL of the 0.2 mg/mL mAb solution onto the surface of the biased SWCNT device while the current was monitored continuously in a probe station attached to a semiconductor parameter analyzer. Once the current stabilized, 4 μL of breast cancer cells (≈1,000 cells) were applied to the device and the current was monitored continuously. We studied the interactions of IGF1R-specific mAb adsorbed onto the SWCNT devices with BT474 and MCF7 breast cancer cells. Non-specific control mAb interactions between BT474 and MCF7 breast cancer cells were studied as controls.

Control experiments were carried out to test the specificity of change in conductance of the SWCNTs during mAb and breast cancer cell adsorption on the SWCNT surface (Fig. 3). Three types of control experiments were carried out: 1) monitoring the conductance during mAb adsorption without any SWCNT on the device; 2) monitoring conductance evolution with the order of mAb and breast cancer cell adsorption reversed; 3) monitoring the conductance evolution of the device when the mAbs and breast cancer cells were initially premixed. All these control experiments were repeated twice to determine the nature of the charge transfer process and to test the specificity of the mechanism.

Fig 3a shows the conductance as a function of time when there was no SWCNT on the device. No dramatic modulation in the conductance of the device was observed upon adsorption of IGF1R mAb and BT474 breast cancer cell adsorption on the device. This experiment demonstrated that the charge transfer process that resulted in an increase in conductance of the device for the interaction of marker-specific mAb with their specific targets on breast cancer cells was mediated by the SWCNT.

Fig. 3b shows the conductance as a function of time when the IGF1R mAbs and BT474 breast cancer cells were premixed and adsorbed on the surface of the SWCNT device. The observed

spike train was due to the adsorption of the mAb-cell mixture onto the device, not to surface interaction between the IGF1R mAbs and BT474 breast cancer cells on the SWCNT surface. When the BT474 cells were premixed with the IGF1R mAbs, the IGF1R mAbs were expected to bind to their IGF1R targets on the BT474 breast cancer cells, in which case no significant change in the conductance was expected. Adsorption of antibodies and cells in general produce a small spike train in all our measurements. This is due to physical adsorption effects that result in a transient jump in conductance of the device.

Fig. 3c shows the conductance as a function of time when the order of IGF1R mAb and BT474 breast cancer cell adsorption was reversed. As seen in Fig. 3b, we observed two spikes, the first one due to the adsorption of BT474 cells onto the device, and the second one due to the adsorption of IGF1R mAbs onto the device. It is interesting to note that cells and antibodies produced similar effects when the order of adsorption was reversed, implying that the spikes were due to physical adsorption on the surface of the SWCNT, which are extremely sensitive to changes at their surfaces. From our earlier work on mAb adsorption, (*4, 29*), we conclude that the result seen in Fig. 3c was due to physical adsorption. In general, when antibodies or other proteins adsorb to the surface of p-type SWCNT, they lower the conductance of the SWCNT, rather than increasing the conductance, as we observed here upon breast cancer cell binding. Hence this control experiment implies that when the order of adsorption was reversed, the charge transfer process was altered significantly. All these controls suggest that the mechanism for the significant increase in conductance upon breast cancer cell binding depends upon the charge transfer process between the adsorbed mAbs on the SWCNT and their specific antigens on cancer cells.

In another control experiment, Fig. 4b shows the conductance of the device during non-specific mAb adsorption (mouse myeloma IgG1), followed by adsorption of BT474 breast cancer cells, which generated two small spikes. In the first direct test of the hypothesis, Fig. 4a displays the

effects of IGF1R-specific mAb adsorption, followed by adsorption of BT474 cells, which generated a 3.0±0.2-fold increase in the device conductance. It was apparent that BT474 cells interacting with the IGF1R-specific mAb-SWCNT device produced a large increase in conductance, while the non-specific mAb-SWCNT device yielded two small transients. Previous studies from other laboratories and our own reported that the amine groups in proteins tend to donate electrons to the SWCNT, thereby decreasing the conductance of the SWCNT FETs during protein adsorption (*3, 4, 29-32*). A single amine group donates 0.04 electrons to the p-type SWCNT, thereby decreasing the conductance of the device. When breast cancer cells are adsorbed onto the device, association of mAb with the cell surface targets on the cancer cells is likely to produce an increase in device conductance due to the charge transfer process between the SWCNT and the breast cancer cells.

In other words, as the cell surface proteins interact with the specific mAbs, electrons transfer from the surface of the p-type SWCNT to the bound cell, thereby increasing the conductance of the device. It should be mentioned that the devices consisted of nanotube networks that were adsorbed with mAb to provide high surface area for mAb adsorption as well as for cell interaction. Hence although the breast cancer cells themselves are much bigger than individual nanotubes, the devices that we present here are network of nanotubes that are collectively bigger than the cells. The mAb exhibited specific interactions with their target proteins. Fig. 4b illustrates that the non-specific mAb did not produce any significant modulation in the electrical conductance of the SWCNT. The BT474 breast cancer cell adsorption experiments were carried out twice, producing the same effects each time.

The hypothesis of charge transfer upon breast cancer cell surface protein binding to a mAb adsorbed to the surface of SWCNTs was tested again with MCF7 breast cancer cells, which express a higher density of IGF1R than do BT474 cells (*2, 6, 7*). Fig. 5b shows minimal perturbation of device conductance after non-specific mAb adsorption (mouse myeloma IgG1) and MCF7 cell

adsorption to the SWCNT device. Fig. 5a, however, shows a large jump in the electrical conductance of the device, after IGF1R-specific mAb adsorption, upon MCF7 cell adsorption to the SWCNT device. MCF7 cell binding increased device conductance by 8.0±0.2-fold, compared to non-specific mAb experiments in Fig. 5b. Compared to BT474 breast cancer cells (Fig. 4), the MCF7 breast cancer cells produced a greater increase in device conductance upon binding to IGF1R-specific mAb-SWCNTs. We also observed that the non-specific mAb-SWCNT conductance data for the BT474 and MCF7 breast cancer cells were quite similar. Our experimental results suggest that charge transfer between SWCNT and breast cancer cells takes place through the mAbs that link the SWCNT to the cells. Binding to an antigen-specific mAb produced several-fold higher increases in the electrical conductance of the SWCNT devices than did binding to the non-specific mAbs.

In contrast, application of R- cells, which do not express IGF1R, to IGF1R-specific mAb-SWCNTs yielded no sustained increase in conductivity (Fig. 6a), just like R- cell application to non-specific mAb-SWCNTs (Fig. 6b). This control experiment revealed that the conductivity jump seen with IGF1R-specific mAb-SWCNTs requires cell surface expression of IGF1R.

This study investigated the charge transfer process between adsorbed mAbs and their corresponding surface protein targets on breast cancer cells using SWCNT devices. We found that adsorption of antigen-specific and non-specific mAb to SWCNT resulted in a small decrease in the conductance of the SWCNT device. Subsequent adsorption of BT474 breast cancer cells (expressing significant IGF1R) or MCF7 breast cancer cells (overexpressing IGF1R) to IGF1R-specific mAb on the surfaces of the SWCNT dramatically increased the conductance of the devices. Non-specific mAbs did not yield a large increase in conductance. The increase in conductance was roughly proportional to the density of IGF1R expressed on the surfaces of the breast cancer cells. For example, when IGF1R was targeted on BT474 breast cancer cells, cell binding to SWCNT

devices produced a 3.0±0.1-fold increase in conductance. However, targeting the same receptor on MCF7 breast cancer cells produced an 8.0±0.2-fold change in the conductance of the SWCNT device. However, R- cells lacking IGF1R produced no conductance change.

These results imply that our observed large increase in device conductance when live breast cancer cells that overexpress IGF1R on their surfaces interact with the mAb on the surface of the SWCNT, is a general phenomenon due to charge transfer between the SWCNT and cells through the mAb, as opposed to the 1-2% decrease in conductivity of the SWCNT device upon mAb adsorption (*5*). Importantly, we found that breast cancer cell interaction with antigen-specific mAb-SWCNTs produced a much greater increase in the device conductance compared to non-specific mAbs. Equally important, no such conductivity jump was observed with cells that do not express IGF1R.

Although adsorption of mAb onto the surface of the SWCNT was noncovalent, nevertheless SWCNT with adsorbed mAb were extremely sensitive to changes in the surface electrostatic charge density upon surface adsorption of live breast cancer cells. These results are consistent with the hypothesis that modulating the surface electrostatic charges in SWCNT could be utilized to detect breast cancer cells based on overexpression of cell surface antigens.

These results suggest that the binding of breast cancer cells via a cell surface receptor to mAb on the surface of the SWCNT devices caused those remarkable jumps in conductance. Our observations highlight a generic pathway for using the high surface area to volume ratio and the unique conductivity of SWCNT to detect overexpressed surface proteins on breast cancer cells. Furthermore, the mAb-SWCNT approach could in principle detect the molecular signatures of other types of circulating cancer cells. These findings suggest applications of mAb-SWCNT to detect a wide variety of surface markers on diseased cells, which could lead to sensitive nanotube-based

biosensors for detecting specific cell surface antigens on circulating cells, in fine needle aspirates, or in masses probed by laparoscopy.

Acknowledgements

The authors wish to acknowledge the funding for this research provided by the Department of Defense, DAMD 170310701, to B. P., and the Department of Energy, Office of Biological Research, ER63055, to E. W.

References

1. M. Ferrari, *Nat Rev Cancer* **5**, 161-71 (Mar, 2005).
2. X. Tian *et al.*, *Journal of Nuclear Medicine* **45**, 2070-2082 (2004).
3. K. Bradley, M. Briman, A. Star, G. Gruner, *Nano Letters* **4**, 253-256 (2004).
4. K. Teker, B. Panchapakesan, E. Wickstrom, *IEEE Sensors (Accepted, in press)* (2005).
5. K. Teker *et al.*, *Nanobiotechnology* **1**, in press (November 2005).
6. X. Le Roy *et al.*, *Oncogene* **6**, 431-7 (1991).
7. K. J. Martin *et al.*, *Cancer Res* **60**, 2232-8 (Apr 15, 2000).
8. C. Sell *et al.*, *Mol Cell Biol* **14**, 3604-12 (Jun, 1994).
9. R. S. Ruoff, D. C. Lorents, *Carbon* **33**, 925-930 (1995///, 1995).
10. M. S. Dresselhaus, G. Dresselhaus, P. C. Eklund, *Science of Fullerenes and Carbon Nanotubes* (Academic Press, New York, 1996).
11. T. W. Ebbessen, *Carbon Nanotubes: Preparation and Properties* (CRC Press, Boca Raton, FL, 1997).
12. M. Bockrath, D. H. Cobden, P. L McEuen et. al., *Science* **275**, 1922-1925 (1997).
13. B. I. Yakobson, R. E. Smalley, *American Scientist* **85**, 324 (1997).
14. P. M. Ajayan, *Chemical Review* **99**, 1787 (1999).
15. H. Dai, J. H. Hafner, A. G. Rinzler, D. T. Colbert, R. E. Smalley, *Nature* **384**, 147 (1996).

16. W. A. DeHeer, A. Chatelian, D. Ugarte, *Science* **270**, 1179 (1995).

17. J. Kong *et al.*, *Science* **287**, 622-625 (Jan 28, 2000).

18. A. Bachtold, P. Hadley, T. Nakanishi, C. Dekker, *Science* **294**, 1317 (2001).

19. S. S. Wong, E. Joselevich, A. Wolley, C. L. Cheung, C. M. Lieber, *Nature* **394**, 52 (1998).

20. A. Kashino, M. Yudasaka, M. Zhang, S. Ijima, *Nano Letters* **1**, 361 (2001).

21. V. Georgakilas *et al.*, *Journal of American Chemical Society* **124**, 760 (2002).

22. J. J. Davis, L. H. M. Green, H. A. O. Hill et al., *Inorganic Chemical Acta* **272**, 261-266 (1998).

23. R. J. Chen, Y. Zhang, D. Wang, H. Dai, *Journal of American Chemical Society* **123**, 3838 (2001).

24. A. Star, J. C. P. Gabriel, K. Bradley, G. Gruner, *Nano Letters* **3**, 459-463 (2003).

25. R. J. Chen, H. C. Choi, S. Bangsaruntip et al., *Journal of American Chemical Society* **126**, 1563 (2004).

26. B. F. Erlanger, B. X. Chen, M. Zhu, L. Brus, *Nano Letters* **1**, 465-467 (2001).

27. M. F. Islam, E. Rojas, D. M. Bergey, A. T. Johnson, A. G. Yodh, *Nano Letters* **3**, 269-273 (2003).

28. O. Matarredona *et al.*, *Journal of Physical Chemistry B* **107**, 13357-67 (2003).

29. K. Teker, G. Cesarone, E. Wickstrom, B. Panchapakesan, paper presented at the Nanotech 2005, Anaheim, CA 2005.

30. H. Chang, J. D. Lee, S. M. Lee, Y. H. Lee, *Applied Physics Letters* **79**, 3863 (2001).

31. J. Kong, H. Dai, *Journal of Physical Chemistry B* **105**, 2890 (2001).

32. K. Bradley, J. C. Gabriel, M. Briman, A. Star, G. Gruner, *Physical Review Letters* **91**, 218301 (2003).

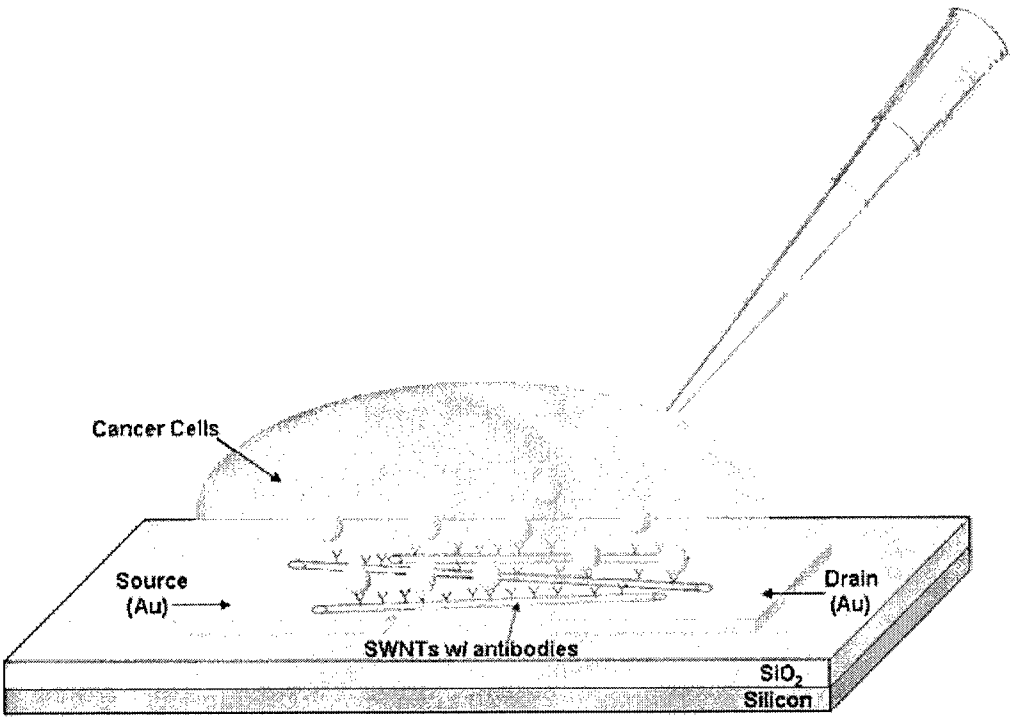

Figure 1. Schematic of the device used for detecting breast cancer cells by SWCNT-mAb binding to surface antigens on live breast cancer cells.

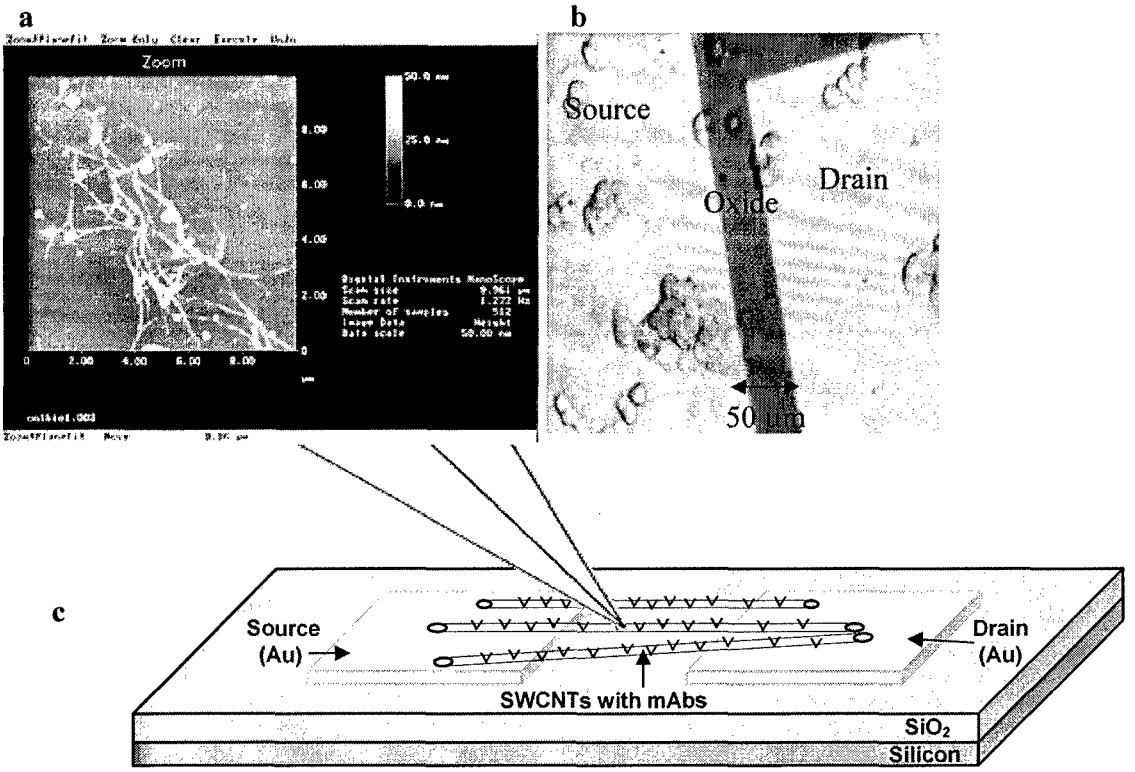

Figure 2. Overview of the SWCNT-mAb device. **a**, AFM scan of the patterned areas in the schematic; **b**, optical micrograph of the actual device; **c**, schematic.

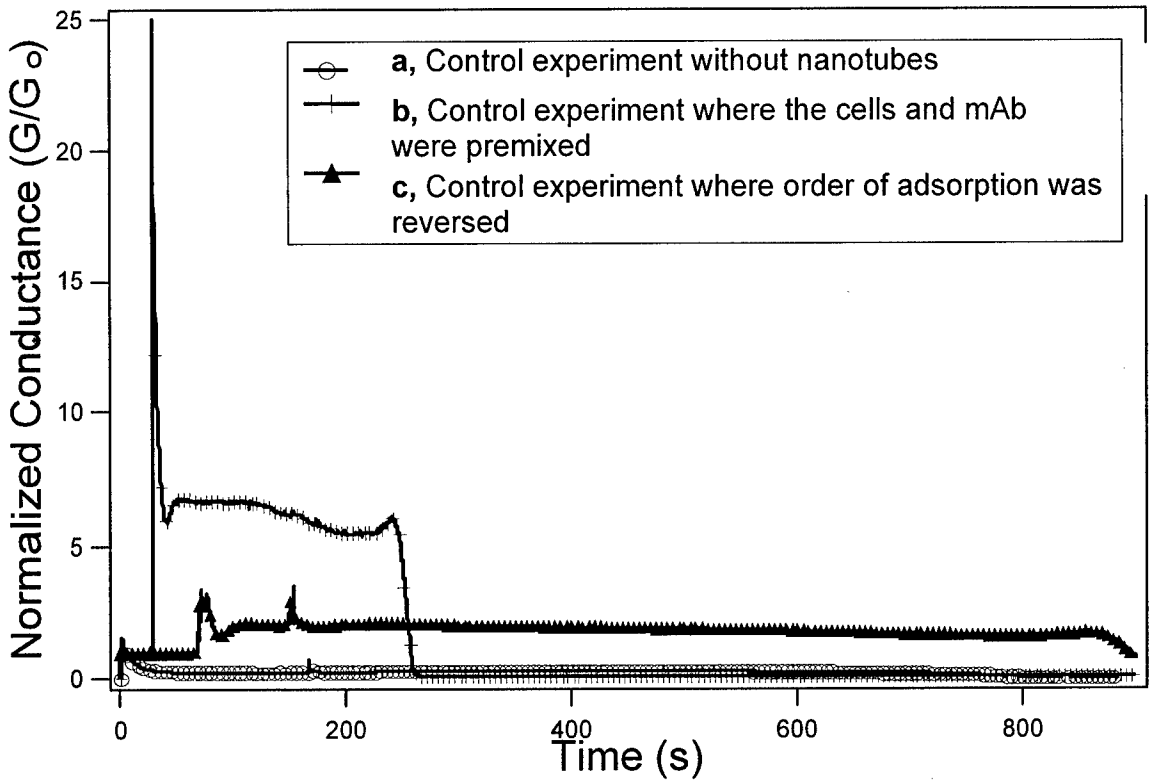

Figure 3: Negative control experiments: **a**, No SWCNT on device; IGF1R-specific mAbs were added, followed by BT474 breast cancer cells. **b**, Order of adsorption reversed for the SWCNT device: BT474 cells added first, followed by IGF1R-specific mAbs. **c**, Conductance of SWCNT device when the IGF1R-specific mAbs and BT474 cells were mixed together before addition.

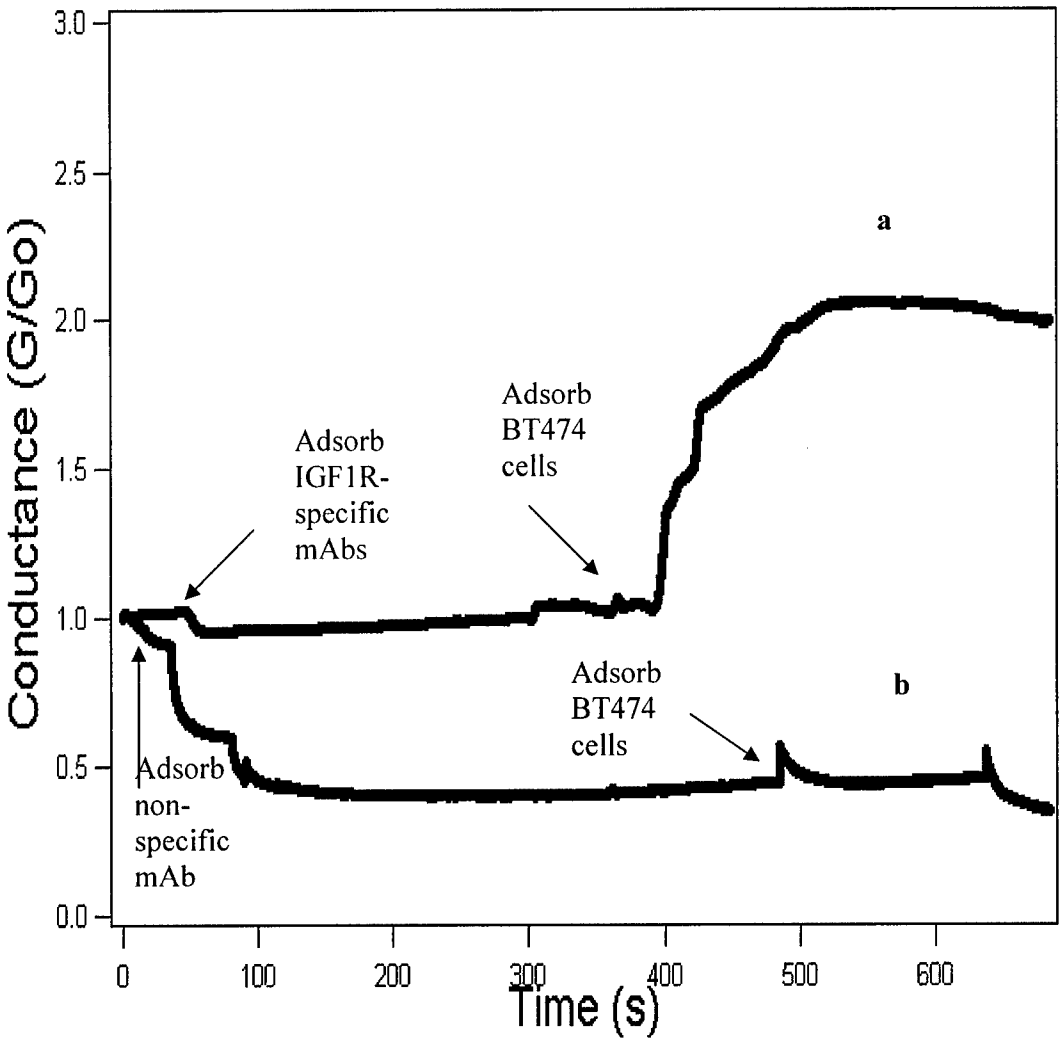

Figure 4: Change in normalized conductance for BT474 breast cancer cells applied to SWCNT devices with adsorbed IGF1R-specific mAb, **a**, or non-specific mAb, **b**, followed by BT474 breast cancer cell application.

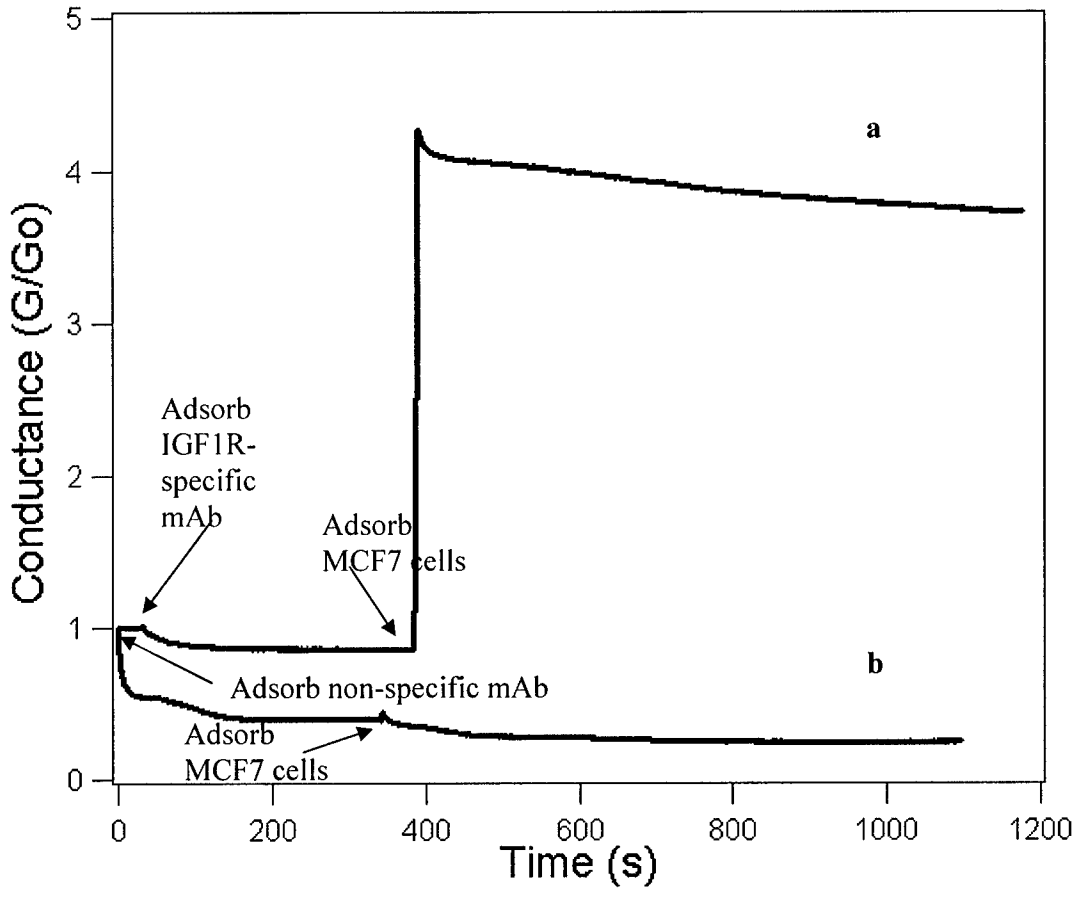

Figure 5: Change in normalized conductance for MCF7 breast cancer cells applied to SWCNT devices with adsorbed IGF1R-specific mAb, **a**, or non-specific mAb, **b**, followed by MCF7 breast cancer cell application.

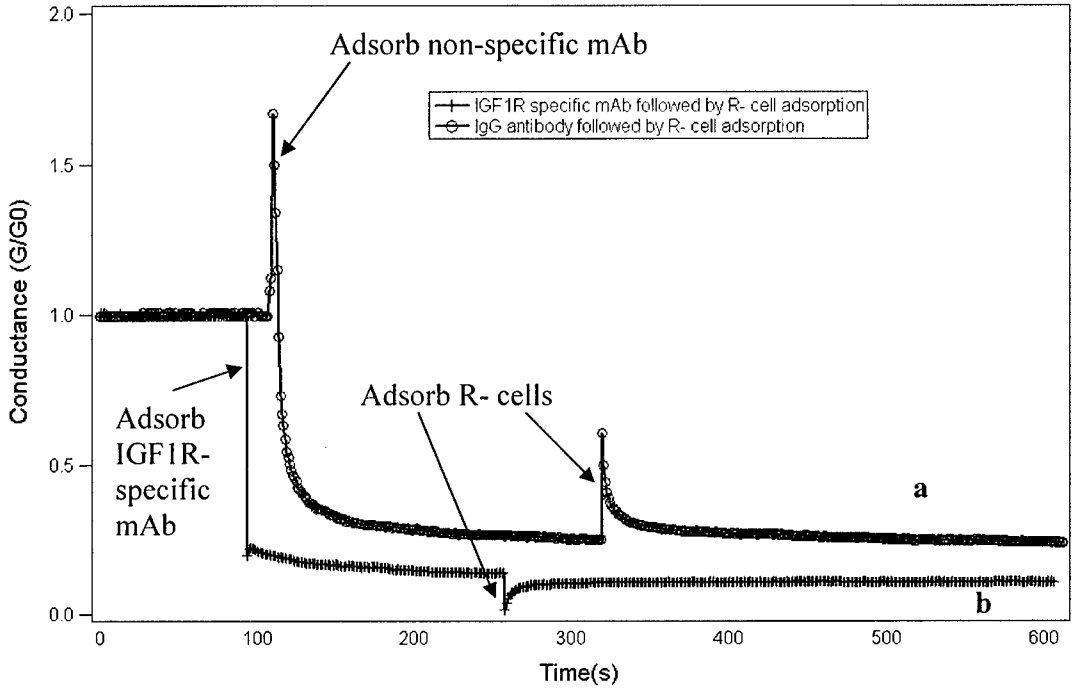

Figure 6: Change in normalized conductance for R- cells applied to SWCNT devices with adsorbed non-specific mAb, **a**, or IGF1R-specific mAb, **b**, followed by R- cell application.